64-10

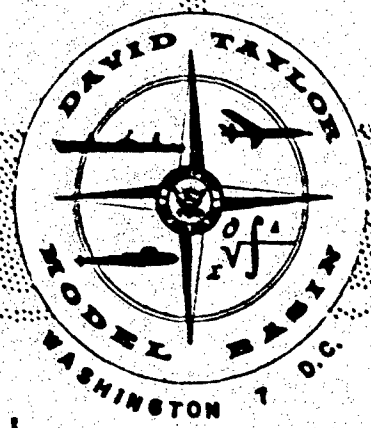

DEPARTMENT OF THE NAVY

HYDROMECHANICS

AERODYNAMICS

STRUCTURAL MECHANICS

APPLIED MATHEMATICS

EXPERIMENTAL INVESTIGATION OF NEAR-SURFACE HYDRODYNAMIC FORCE COEFFICIENTS FOR A SYSTEMATIC SERIES OF TEE HYDROFOILS, DTMB SERIES HF-1

by

Jerome Feldman

HYDROMECHANICS LABORATORY
RESEARCH AND DEVELOPMENT REPORT

DECEMBER 1963 REPORT 1801

EXPERIMENTAL INVESTIGATION OF NEAR-SURFACE HYDRODYNAMIC FORCE COEFFICIENTS FOR A SYSTEMATIC SERIES OF TEE HYDROFOILS, DTMB SERIES HF-1

by

Jerome Feldman

DECEMBER 1963

REPORT 1801
SF013-02-01
Task 1703

TABLE OF CONTENTS

Page

LIST OF FIGURES

Page

LIST OF TABLES

NOTATION

The nomenclature defined in Technical and Research Bulletin No. 1 to 5 of the Society of Naval Architects and Marine Engineers as extended in David Taylor Model Basin Report 1319 is used herein where applicable. The positive direction of axes, angles, forces, moments, and velocities are shown in the accompanying sketch. The coefficients and symbols are defined as follows:

Symbol	Dimensionless Form	Definition
A	$A' = \frac{A}{l^2}$	Projected Area
a	$a = \frac{b}{A}$	Aspect ratio
b	$b' = \frac{b}{l}$	Span
C_{La}		Slope of curve of C_L versus α
c	$c' = 1$	Chord
D	$C_D = \frac{D}{\frac{1}{2}\rho U^2 A}$	Drag component of hydrodynamic force
D_f	$C_f = \frac{D_f}{\frac{1}{2}\rho U^2 S}$	Frictional resistance
D_r	$C_r = \frac{C_r}{\frac{1}{2}\rho U^2 S}$	Residual resistance
F	$F = \frac{U}{\sqrt{gl}}$	Froude number
g		Acceleration of gravity
h	$h' = \frac{h}{l}$	Depth of submergence quarter chord point of mean geometric chord
L	$C_L = \frac{L}{\frac{1}{2}\rho U^2 A}$	Lift component of hydrodynamic force

l	$l' = 1$	Characteristic length or chord, c
R		Reynolds number
S	$S' = \frac{S}{l^2}$	Wetted surface area
U	$U' = 1$	Velocity of origin of body axes relative to fluid in feet per second
u	$u' = \frac{u}{U}$	Component along x axis of velocity of origin of body axes relative to fluid
w	$w' = \frac{w}{U}$	Component along z axis of velocity of origin of body axes relative to fluid
X	$X' = \frac{X}{\frac{1}{2}\rho l^2 U^2}$	Hydrodynamic longitudinal force, positive forward
X_*		Longitudinal force at zero angle of attack
x		The longitudinal axis taken parallel to chord and directed from trailing edge to leading edge of foil with origin taken such that z axis is at quarter chord of foil
Z	$Z' = \frac{Z}{\frac{1}{2}\rho l^2 U^2}$	Hydrodynamic normal force, positive downward
Z_h	$Z_h' = \frac{Z_h}{\frac{1}{2}\rho l U^2}$	Derivative of normal force component with respect to depth of submergence component h

Z_w	$Z_w' = \frac{Z_w}{\frac{1}{2}\rho l^2 U}$	Derivative of normal force component with respect to velocity component w
z		The normal axis, directed perpendicular to chord, with origin taken arbitrarily but such that axis is through quarter chord of foil
α		The angle of attack; the angle to the longitudinal body axis from the projection into the principal plane of symmetry of the velocity of the origin of the body
θ		The angle of pitch; the angle of elevation of the axis, positive in positive sense of rotation
ρ	$\rho' = 2$	Mass density of water

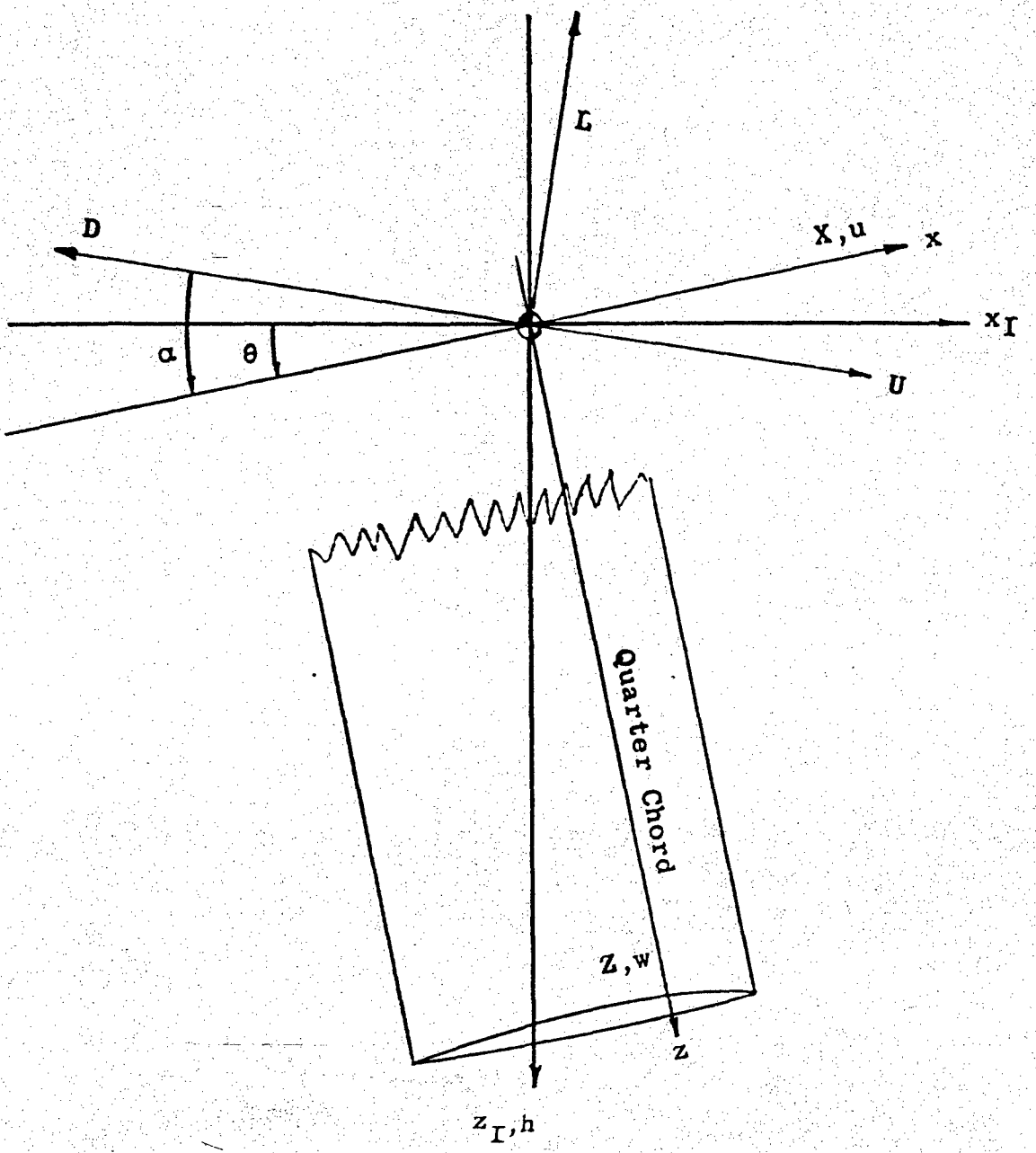

Sketch Showing Positive Directions of Axes, Angles, Forces, Moments, and Velocities

ABSTRACT

Experiments were conducted with the DTMB Planar-Motion-Mechanism System to determine the normal and longitudinal components of force for DTMB Series HF-1, a systematic series of Tee foils designed to operate in the subcavitating regime. The resulting data are presented in a form applicable to the hydrodynamic design of high-speed hydrofoil craft from the standpoint of stability and control. The data are further analyzed to establish the effects of parameters such as Froude Number, depth of submergence, and aspect ratio. Comparisons are made to determine the extent to which existing theories produce agreement with the experimental data.

INTRODUCTION

As part of the Hydrofoil Accelerated Program, the Bureau of Ships authorized the David Taylor Model Basin to undertake research studies pretaining to stability and control of high-speed hydrofoil craft.[1] Accordingly, the Stability and Control Division established a broad research program[2] covering a wide range of parameters which are considered to be pertinent to the design and operation of both subcavitating and supercavitating foil systems. The ultimate objective of the program is to provide fundamental data which can be applied to the design of future hydrofoil craft as well as to gain a full understanding of the behavior of such craft from the standpoint of stability and control.

The experimental investigation which forms the subject of this report lies within the scope of the broad program. It is concerned with the normal and longitudinal hydrodynamic force coefficients for a systematic series of individual foils, designated as DTMB Series HF-1. Each model of the series consists of a horizontal submerged hydrofoil attached to a vertical surface-piercing strut. Both foil and strut are rectangular in planform and have sections designed for operation in the subcavitating regime (fully wetted). The primary geometric parameter varied in the series is the aspect ratio of the hydrofoils. The experiments, which were conducted with the DTMB Planar-Motion-Mechanism System, covered a wide range of parameter variations including speed (Froude Number), depth of submergence, and angle of attack.

This report describes the geometrical characteristics of the hydrofoil series, and the experimental techniques used to obtain the data; presents the data derived from the experiments for each individual model; analyzes the data in terms of the effects of the parameters varied; and compares the experimentally derived coefficients and derivatives with corresponding ones computed from existing theories.

---

[1] References are listed on page 86 .

GEOMETRY OF SERIES

DTMB Series HF-1 is a systematic series of individual hydrofoils consisting of a submerged foil attached to a vertical surface-piercing strut. The parent of this series has a rectangular planform both on the foil and the strut; the aspect ratio of the foil is 4. The section of the foil has the following characteristics: (a) the position of the minimum pressure for the symmetrical section at zero lift is 0.6 of the chord from the leading edge, (b) the amount of camber corresponds to a design lift coefficient of 0.3, and (c) the thickness is 9 percent of the chord corresponding to NACA 16-309. The vertical strut has a symmetrical section with a thickness of 12 percent of the chord corresponding to NACA 16-012. The nondimensional offsets for both the foil and strut are shown in Table 1.

The offspring of the series have the same section and planform of the parent and are derived by varying the aspect ratio (span-to-chord ratio) by changing the span of the foil. The aspect ratios are 1, 2, 3, and 4 with a single strut and 4, 6, and 8 with double struts.

TABLE 1

Nondimensional Offsets of Foils and Struts
(All values are expressed as percentages of chord)

	Foil (NACA 16-309)		Strut (NACA 16-012)
X	Y_1	Y_2	Y
0	0.0	0.0	0.0
5	2.359	1.407	2.509
10	3.369	1.817	3.457
20	4.692	2.304	4.664
30	5.523	2.607	5.417
40	6.000	2.782	5.855
50	6.155	2.845	6.000
60	5.985	2.767	5.835
70	5.412	2.492	5.269
80	4.343	1.955	4.199
90	2.664	1.112	2.517
95	1.536	0.586	1.415
100	0.090	0.090	0.120

DESCRIPTION OF MODELS

The individual models of series HF-1 are constructed of machined aluminum (AL 6061). The dimensions and construction details of a typical model are shown in Figure 1. Each of the models has a chord of 9 inches but the spans differ to give aspect ratios of 1, 2, 3, 4, 6, and 8. The models of aspect ratio 1, 2, and 3 could be mounted with only a single vertical strut at half span whereas those with aspect ratio 4, 6, and 8 could be mounted either with one strut at half span or two struts each positioned six inches from the edges of the chord of the hydrofoil. The dimensional offsets of the foils and struts are given in Table 2 and the geometric characteristics of the series are given in Table 3. The streamline section of the vertical struts extends for a length of 24 inches and merges into a rectangular section for attaching to the test apparatus.

TABLE 2

Dimensional Offsets of Foils and Struts

(All dimensions are in inches)

	Foil (NACA 16-309)		Strut (NACA 16-012)
X	Y_1	Y_2	Y
0.0	0.0	0.0	0.0
0.45	0.212	0.127	0.226
0.90	0.303	0.164	0.311
1.80	0.422	0.207	0.420
2.70	0.497	0.235	0.488
3.60	0.540	0.250	0.527
4.50	0.554	0.256	0.540
5.40	0.539	0.249	0.525
6.30	0.487	0.224	0.474
7.20	0.391	0.176	0.378
8.10	0.240	0.100	0.227
8.55	0.138	0.053	0.127
9.00	0.008	0.008	0.011

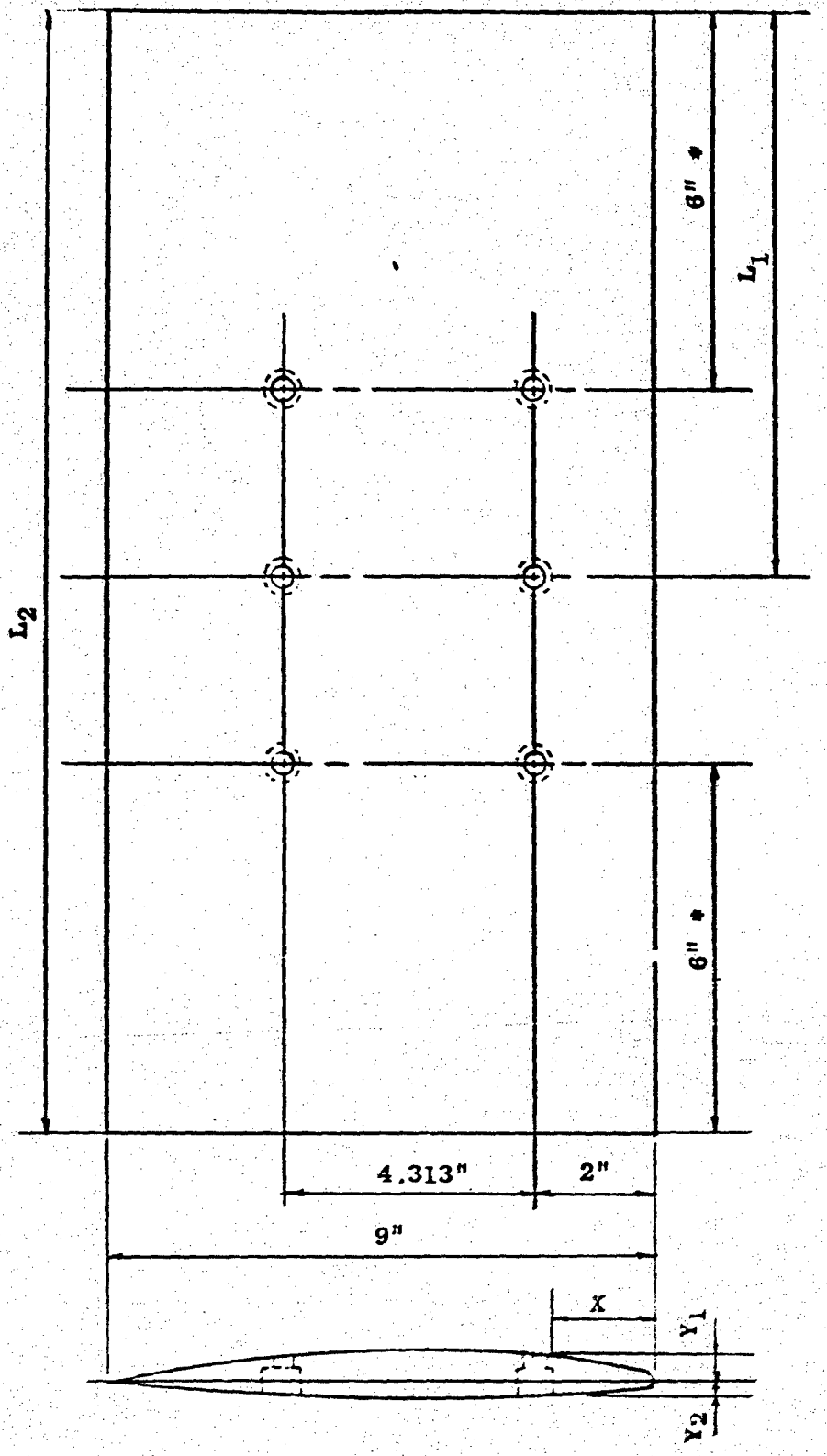

* These holes are used for two-strut configurations and apply only to foils of aspect ratio 4, 6, and 8.

Figure 1 - Sketch of Typical Hydrofoil Model

TABLE 3

Geometric Characteristics of Hydrofoil Series

Aspect Ratio	L_1 in inches	L_2 in inches	Area in squared inches
1	4.5	9	81
2	9	18	162
3	13.5	27	243
4	18	36	324
6	27	54	486
8	36	72	648

TEST APPARATUS AND PROCEDURE

The bulk of the experimental work was conducted in the deep water basin on Towing Carriage 2 using the DTMB Planar-Motion-Mechanism System Mark I described in Reference 2. Additional tests were run on the high speed basin on Towing Carriage 5 using the DTMB Planar-Motion-Mechanism System Mark II.

The test arrangements used with Mark I and Mark II are shown in Figures 2 and 3, respectively. In both cases, the vertical strut(s) are attached to a lateral box beam which in turn is fastened to the underside of a longitudinal box beam. The gages are attached to the upperside of the longitudinal box beam and then to each of the two struts going to the pistons in a manner similar to that described in Reference 3.

The only tests conducted in this program were the so-called static stability tests. These were carried out with the various foils using the standard procedures described in Reference 4. The angle of attack was varied by rotating the tilt table about its own trunnion. The change in depth of submergence at the quarter chord of the foil introduced by this rotation was corrected to maintain the same depth as that for zero pitch angle.

The models with aspect ratios of 1, 2, and 3 were tested with a single strut only and those with aspect ratios of 6 and 8 were tested with two struts. The model with aspect ratio of 4 was tested with both one and two struts.

All of the models were tested over a range of speeds of 6 to 16 knots on Mark I. One model was tested on Mark II over a range of speeds of 10 to 28 knots. A range of angles of attack of -4 to 10 degrees and a range of depth of submergences of 2 to 20 inches were covered.

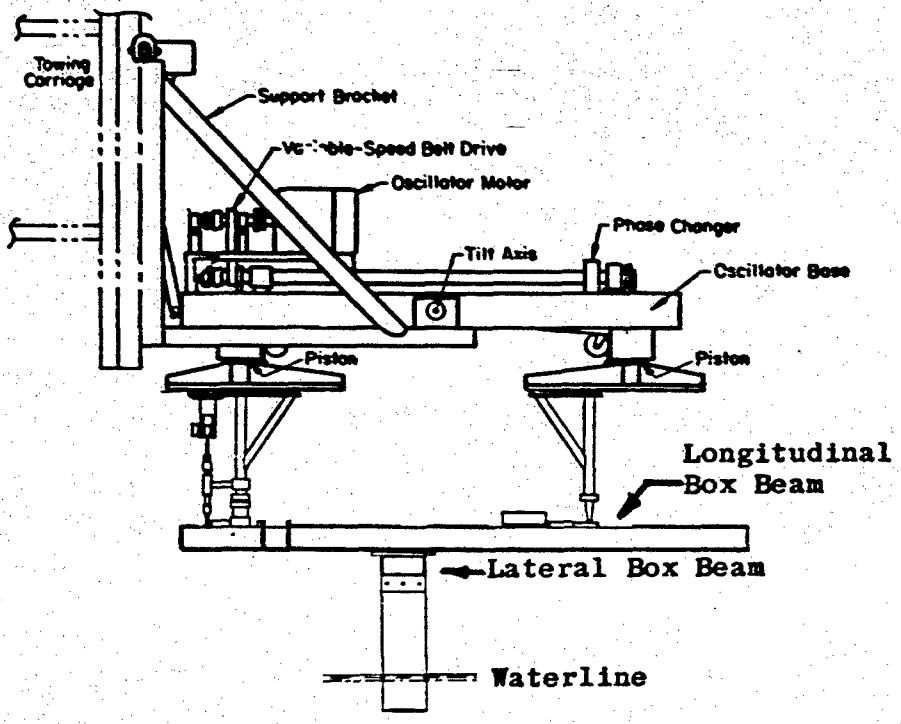

Figure 2 - Schematic Sketch of DTMB Planar-Motion-Mechanism System Mark I with Hydrofoil Model Attached

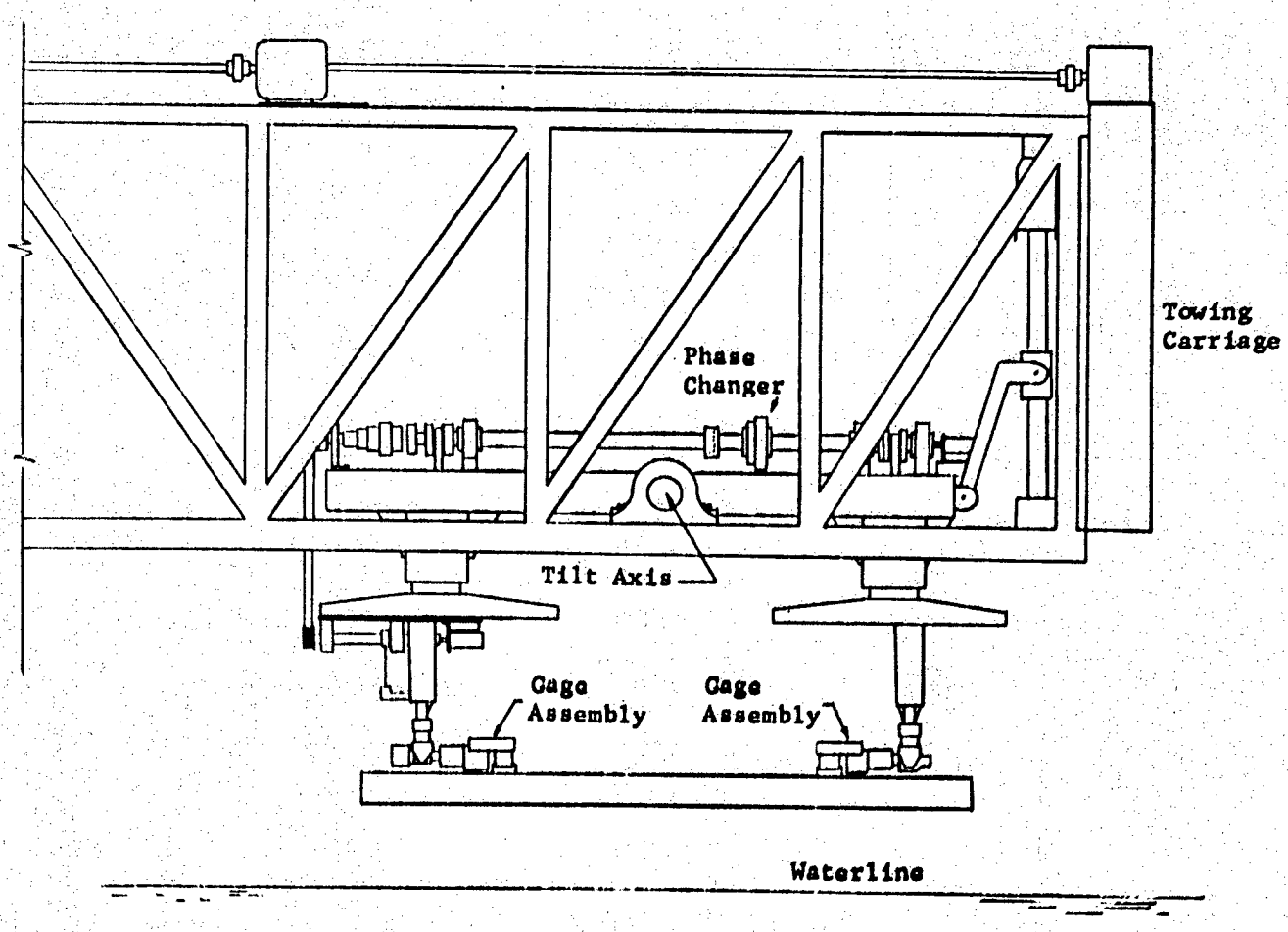

Figure 3 - Sketch of DTMB Planar-Motion-Mechanism System Mark II

Since two different facilities were used in the test program, exploratory tests were conducted to determine if both methods would give the same results. The normal force data obtained from these tests are presented in Figures 4 and 5. It may be noted that the results of the test with aspect ratio of 4 model (Figure 4) are in excellent agreement. However, the results with aspect ratio of 6 model (Figure 5) are in agreement in so far as slope is concerned but are somewhat displaced. This is believed to be due to faulty alignment during the Mark II tests amounting to an angle of attack of about one degree. It may be reasonably concluded that both techniques provide the same results as far as normal force is concerned. The longitudinal force data for the comparative tests are shown in Figure 6. Here again, the agreement is excellent for aspect ratio of 4 model but the curve is offset for aspect ratio of 6 model by an amount equivalent to about one degree angle of attack.

REDUCTION AND PRESENTATION OF DATA

The results of the tests have been reduced to nondimensional form and are plotted in the appendices as curves of force coefficient versus either angle of attack or nondimensional depth of submergence. Unless stated otherwise, the characteristic length used to normalize the coefficients is the chord of the hydrofoils. All derivatives with respect to angular quantities are given as "per radian."

Appendix A contains the curves of normal force coefficient as a function of angle of attack for Froude Number 5.50. Appendix B contain similar curves as a function of depth of submergence. Both of these appendices include data for single and double strut configurations. Appendix C contains curves of normal force coefficient as a function of angle of attack for aspect ratio of 4 model with single strut for five additional Froude Numbers (2.06, 2.75, 3.44, 4.13, 4.81). Appendix D is similar to Appendix C except that the curves are functions of depth of submergence. Appendices E and F contain curves of longitudinal force coefficient versus angle of attack and submergence, respectively, for a Froude Number of 5.50.

The curves in the appendices have not only been cross-faired for each individual model but they have been cross-faired on the geometric parameter of the series (aspect ratio). Therefore, these curves can be interpolated for conditions not covered in the test program. The slopes of the curves of normal force coefficient versus angle of attack (Z_w') were computed for zero angle of attack and the slopes of the curves of normal force coefficient versus depth of submergence (Z_h') were computed for a depth of submergence coefficient of unity. The derivatives so obtained were cross-faired against certain parameters in addition to aspect ratio. The resulting curves appear as summary figures later in the text.

Since the forces obtained from the tests are components referred to body axes (normal and longitudinal forces) the lift-to-drag ratios were computed using the following relationship:

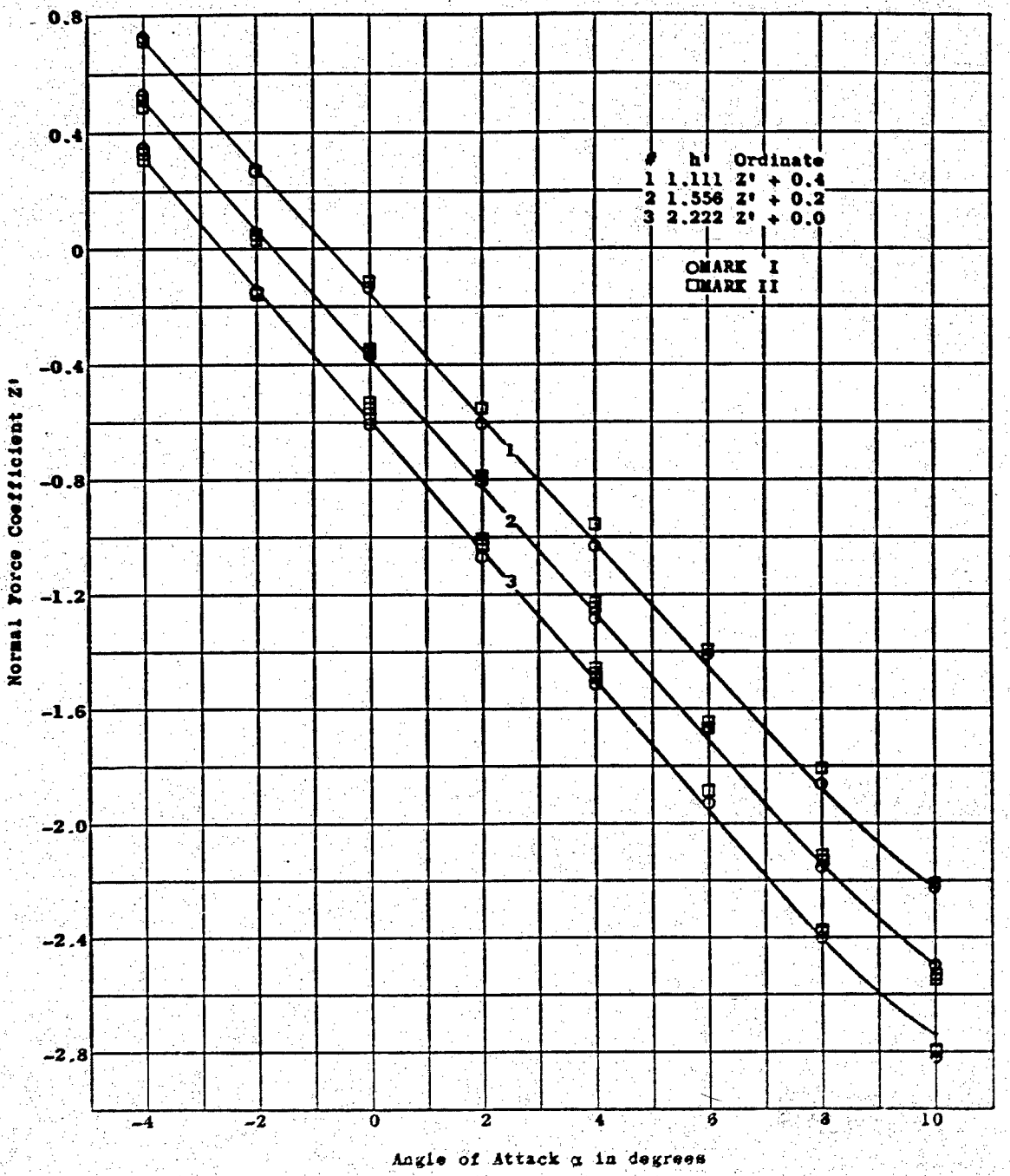

Figure 4 - Comparison of Mark I and II Data for Normal Force Coefficient with Angle of Attack for Various Submergences for one Hydrofoil Configuration (a = 4) and Fixed Froude Number (5.50)

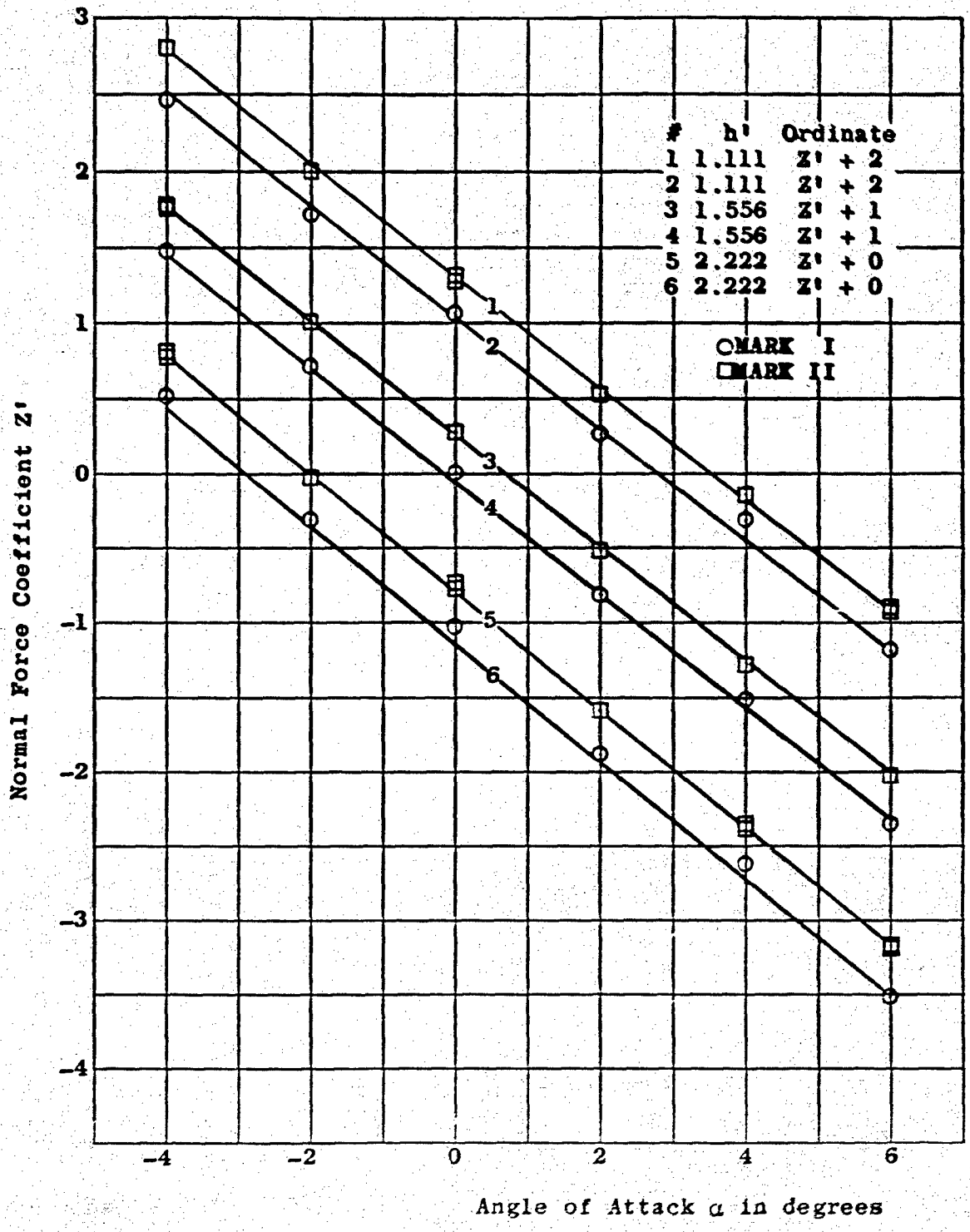

Figure 5 - Comparison of Mark I and II Data for Normal Force Coefficient with Angle of Attack for Various Submergences for One Hydrofoil Configuration (A = 6) and Fixed Froude Number (5.50)

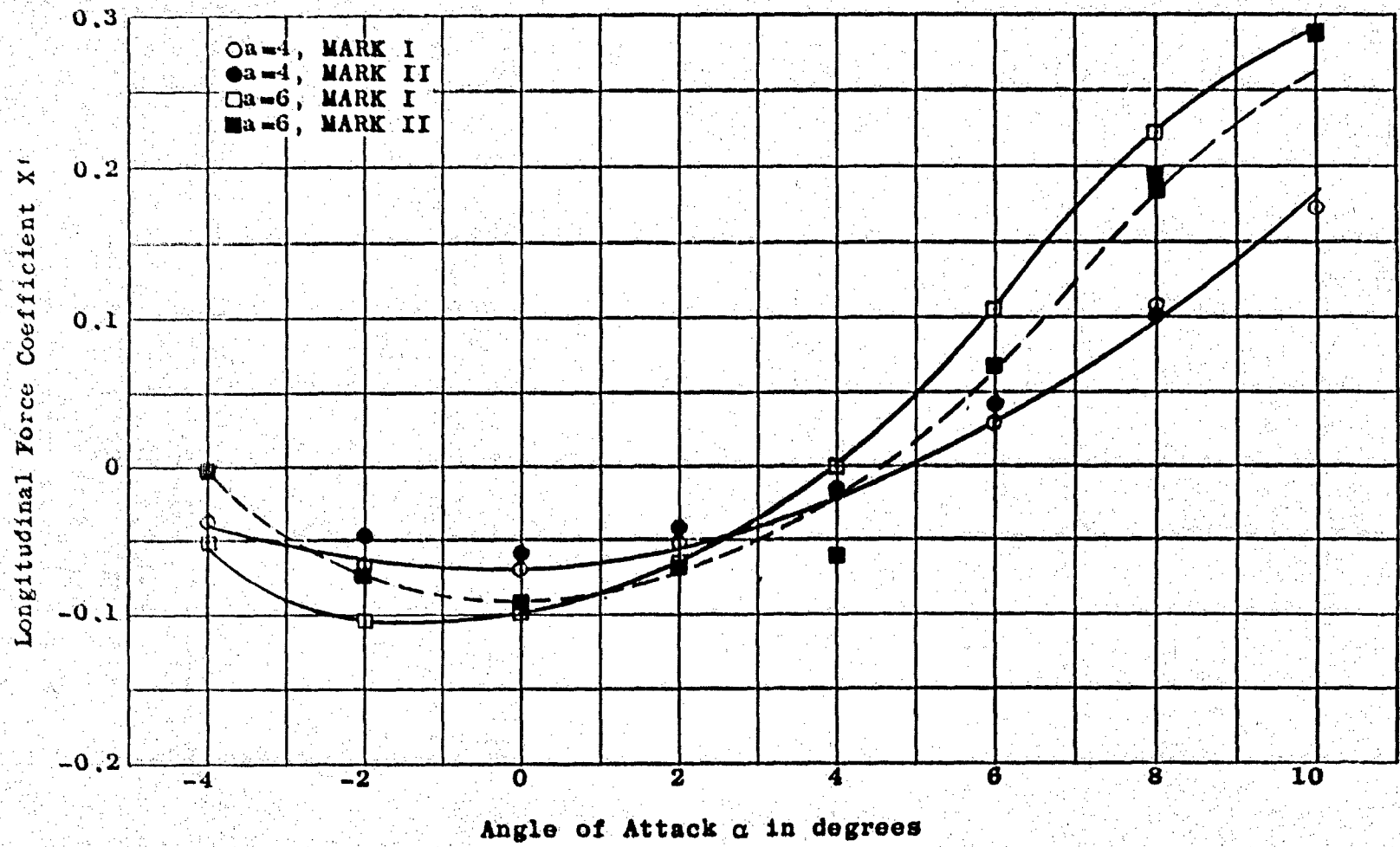

Figure 6 - Comparison of Mark I and II Data for Longitudinal Force Coefficient with Angle of Attack for Fixed Froude Number (5.50) and Submergence (h' = 2.222)

$$\frac{L}{D} = \frac{Z'\cos\alpha - X'\sin\alpha}{Z'\sin\alpha + X'\cos\alpha} \qquad [1]$$

ANALYSIS OF NORMAL FORCE COEFFICIENTS

The effect on normal force coefficient of each of the investigated parameters is discussed herein.

EFFECT OF FROUDE NUMBER

Figure 7 shows the effect of Froude Number on normal force coefficient for various aspect ratios with a large fixed angle of attack (α = 10) and a shallow fixed submergence (h' = 0.222). Normal force coefficient is less sensitive to Froude Number as the Froude Number is increased and as the aspect ratio is decreased.

Figure 8 shows the effect of Froude Number on normal force coefficient for various depth of submergences with a large fixed aspect ratio (a = 8) and angle of attack (α = 10). The normal force coefficient is less sensitive to Froude Number for deeper submergences and higher Froude Numbers.

Figure 9 shows the effect of Froude Number on normal force coefficient for various angles of attack for a large fixed aspect ratio (a = 8) and a shallow submergence (h' = 0.222). The normal force coefficient is less sensitive to Froude Number for smaller angles of attack and higher Froude Numbers.

Figures 7, 8, and 9 show, in combination, that normal force coefficient is least sensitive to Froude Number for small aspect ratio, small angles of attack, deep submergence, and high Froude Numbers. The practical operating range of most hydrofoil craft lie within this domain.

Figure 10 shows that the normal force coefficients of most hydrofoil craft are relatively insensitive to Froude Number at all Froude Number within the operating range. Therefore, data for the parent foil at lower Froude Numbers and Figures 7, 8, and 9 are sufficient to determine the normal force coefficients for other aspect ratios at these Froude Numbers.

EFFECT OF DEPTH OF SUBMERGENCE

Figure 11 shows the effect of submergence on normal force coefficient for a typical set of conditions (a = 6, α = 0, Froude Number = 6.88). The normal force coefficient decreases as the submergence decreases. The rate of this decrease increases as the foil approaches the surface. These exponential curves approach, asymptotically, the infinite submergence condition. From the standpoint of stability and control, the shallow submergences require the automatic control system to overcome the greater wave induced excitations and steep

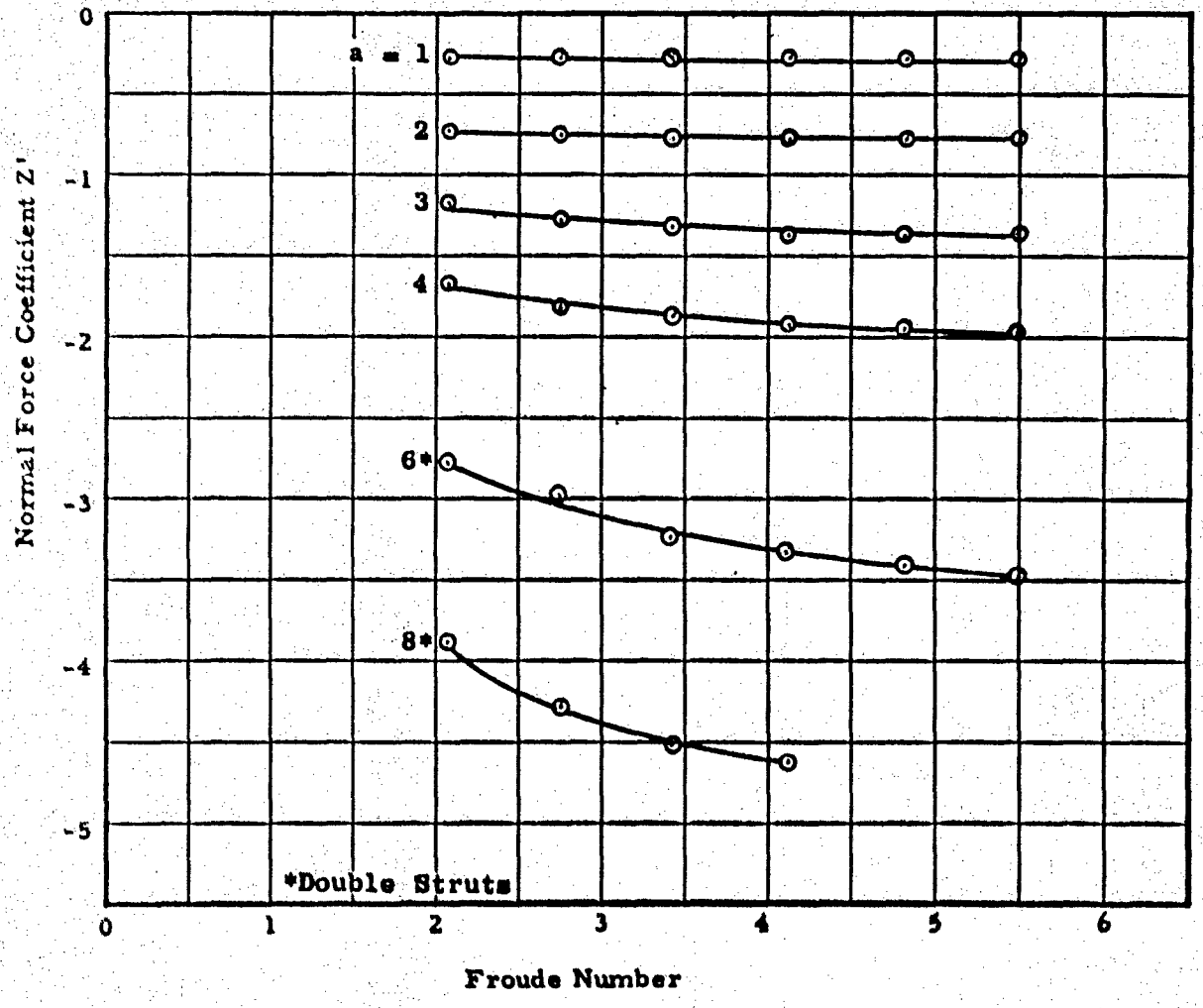

Figure 7 - Effect of Froude Number on Normal Force Coefficient of Various Hydrofoil Configurations at Fixed Submergence ($h' = 0.222$) and Angle of Attack ($\alpha = 10$)

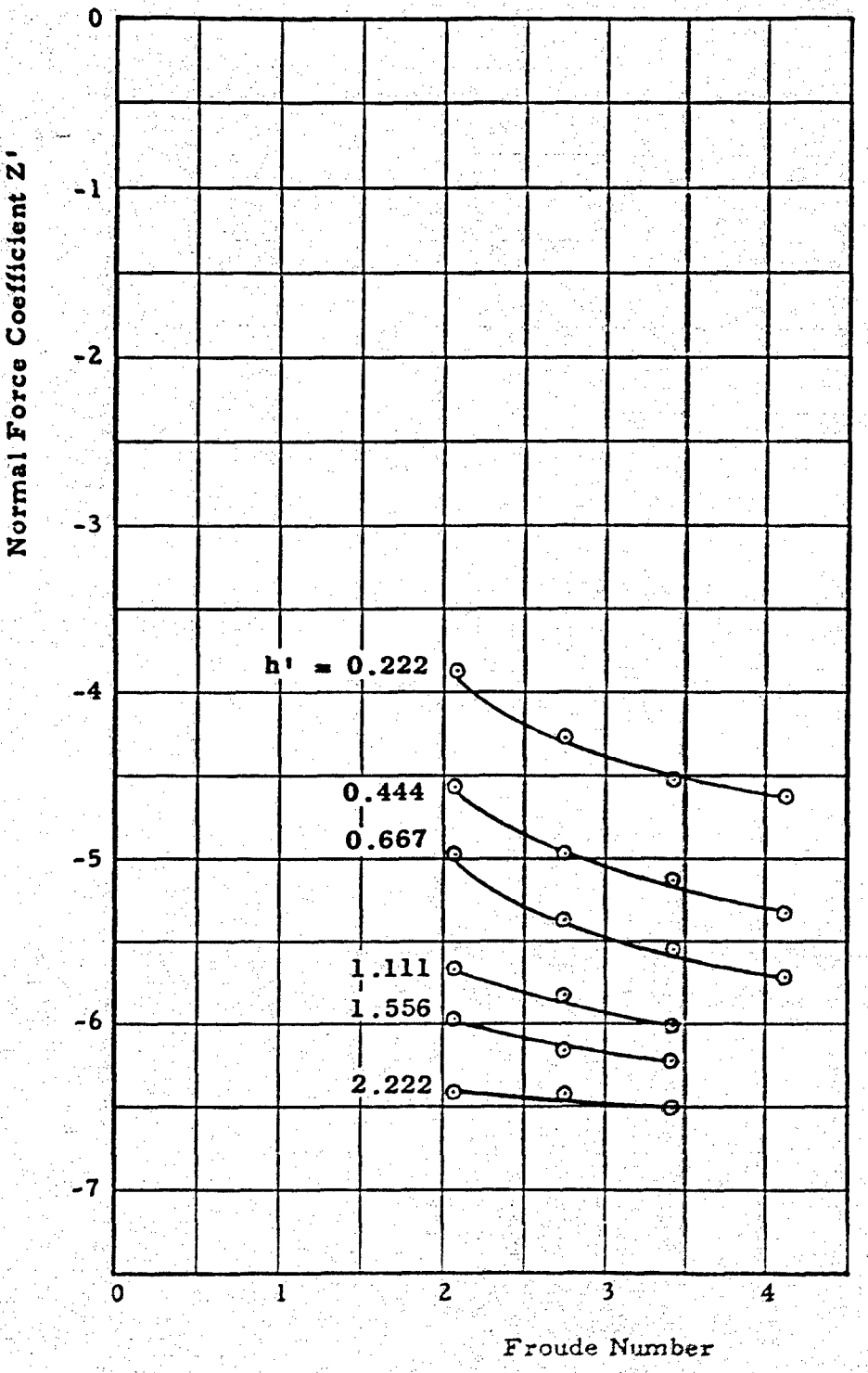

Figure 8 - Effect of Froude Number on Normal Force Coefficient for Various Submergences with One Hydrofoil Configuration (a = 8) at Fixed Angle of Attack (α = 10)

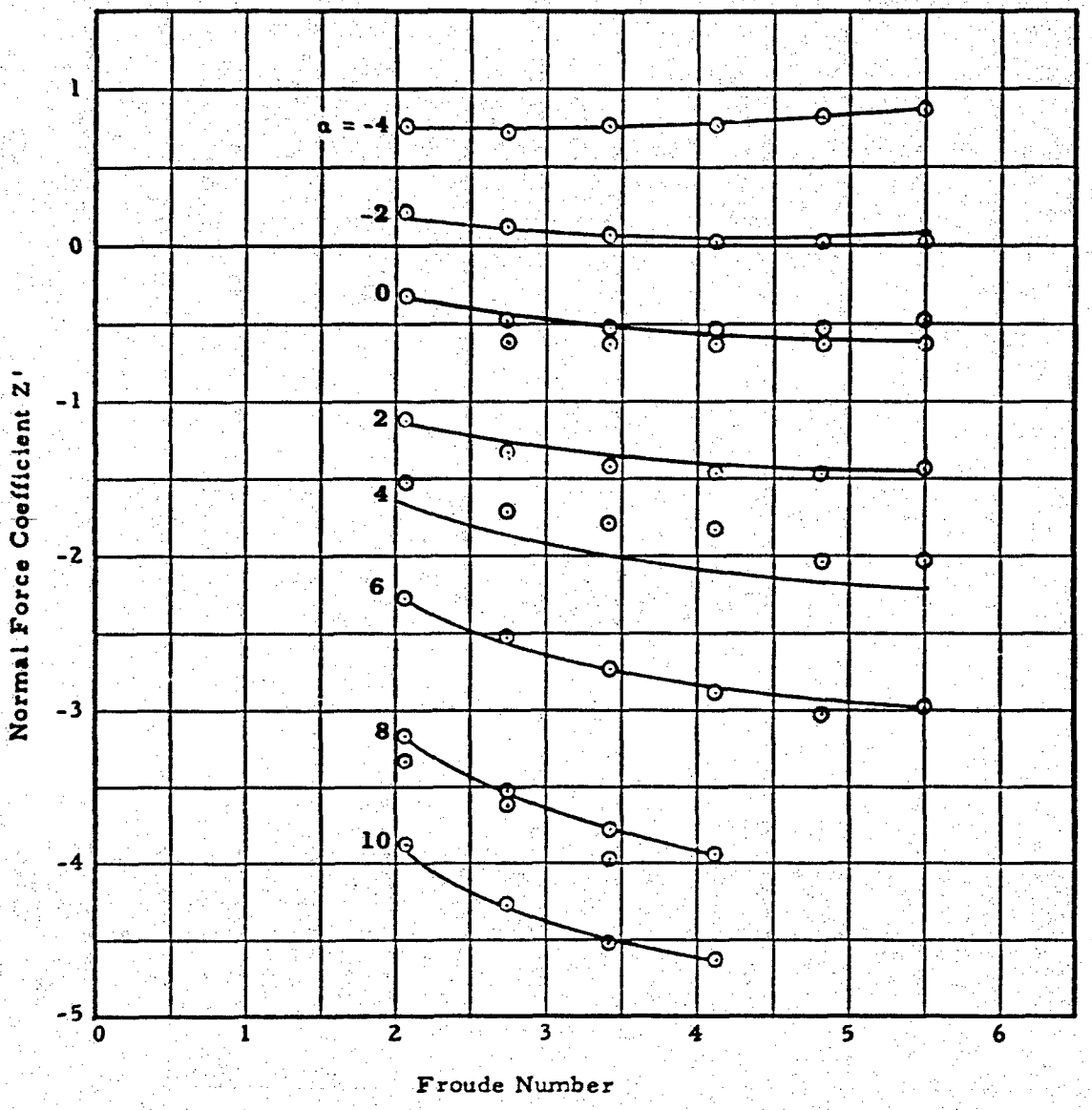

Figure 9 - Effect of Froude Number on Normal Force Coefficient for Various Angles of Attack with One Hydrofoil Configuration (a = 8) at Fixed Submergence (h' = 0.222)

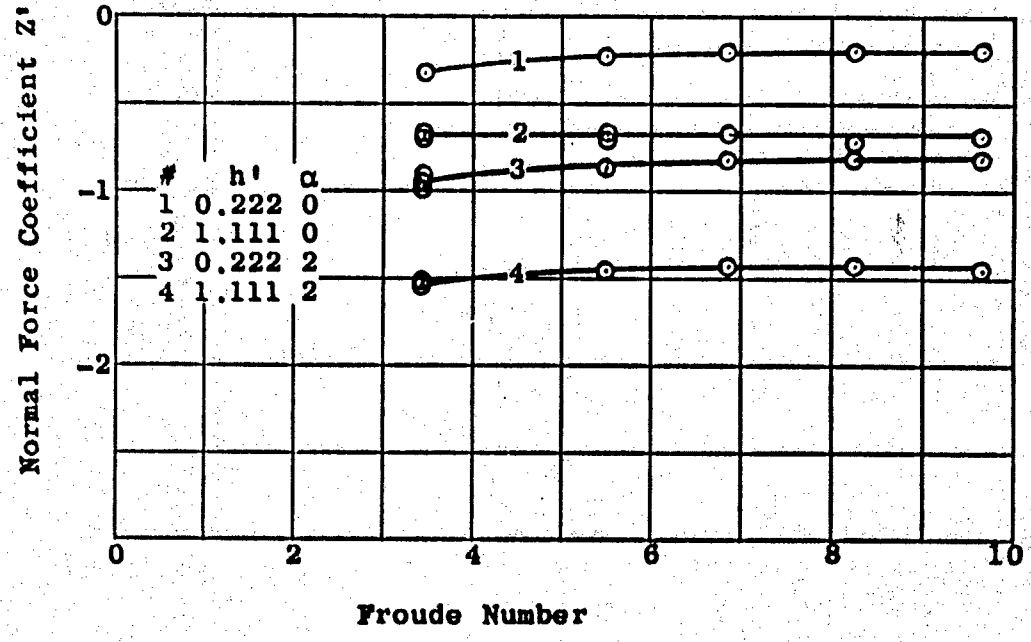

Figure 10 - Effect of High Froude Numbers on Normal Force Coefficient for Typical Hydrofoil Configuration (a = 6) for Various Submergences and Angles of Attack

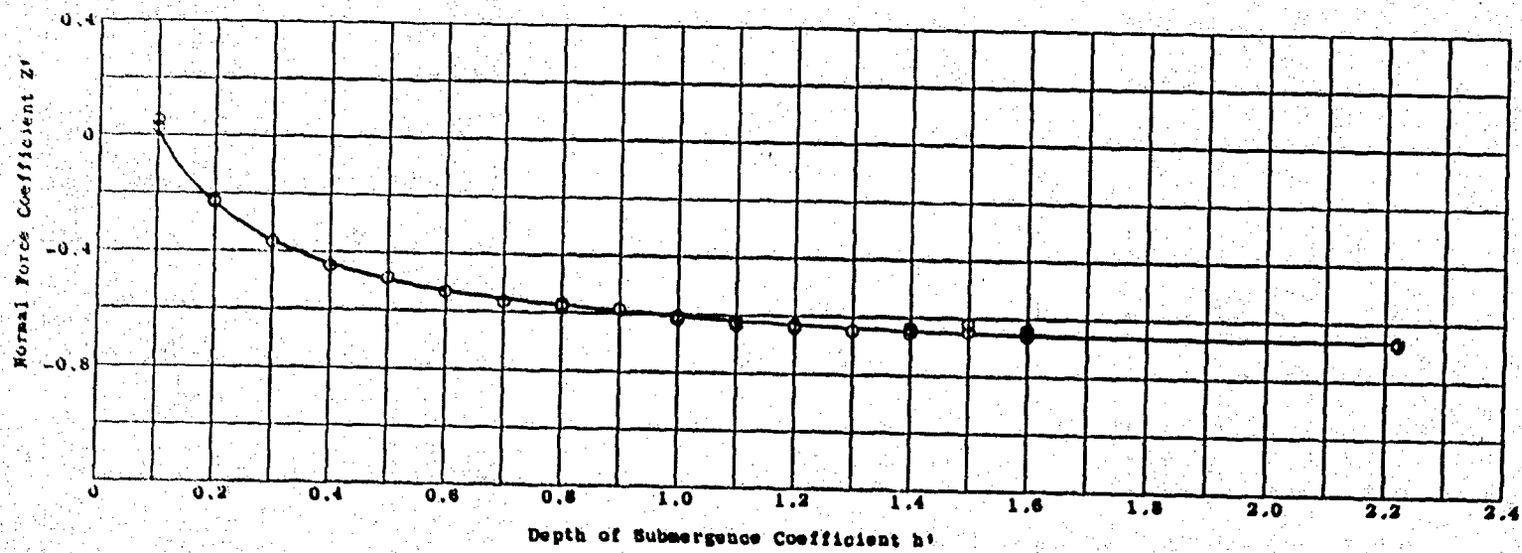

Figure 11 - Effect of Submergence on Normal Force Coefficient with One Hydrofoil Configuration (a = 6) at a Fixed Froude Number (6.88) and Zero Angle of Attack

changes in lift for small perturbations in submergence. Hence, a submergence of greater than one chord is desirable. From the standpoint of resistance and propulsion, however, a compromise is required which is discussed.

Figure 12 shows the effect of submergence on the stability derivative Z_w'. This derivative decreases as the submergence decreases. The rate of this decrease is increased with decreasing submergence. In addition, Z_w' is more sensitive to submergence for the larger aspect ratios. These exponential curves approach, asymptotically, the infinite submergence condition.

EFFECT OF ASPECT RATIO

Figures 13 and 14 show the effect of aspect ratio on the stability derivative Z_w'. The value of this derivative for the aspect ratio of 4 is the average of the single and double strut values. Increasing the aspect ratio is shown to increase Z_w'; the greatest increase is obtained at the deepest submergence. Figure 14 gives the following empirical relationship:

$$Z_w' = -1.68(h')^{0.14}(a)^{1.43} \qquad [2]$$

for aspect ratios less than 6.

Figure 15 shows the effect of angle of attack and aspect ratio on the stability derivative Z_h'. Increasing the aspect ratio is shown to increase Z_h' with the greatest increase for the largest angle of attack. Figure 16 gives the following empirical relationship for a submergence of one chord:

$$Z_h' = -(0.150\alpha + 0.012)(a)^{1.5} \qquad [3]$$

EFFECT OF STRUTS

The effect of the number of struts on normal force coefficient is shown in Figure 17. Double struts decrease the normal force coefficient for small or negative angles of attack and shallow submergences. At higher angles of attack, the normal force coefficient is greater for the double strut configurations. Figures 12 and 14 show that the double strut configurations give slightly higher values of Z_w' and Z_h', respectively, for all submergences and angles of attack.

ANALYSIS OF LONGITUDINAL FORCE COEFFICIENTS

The effect on longitudinal force coefficient of each of the investigated parameters is discussed herein.

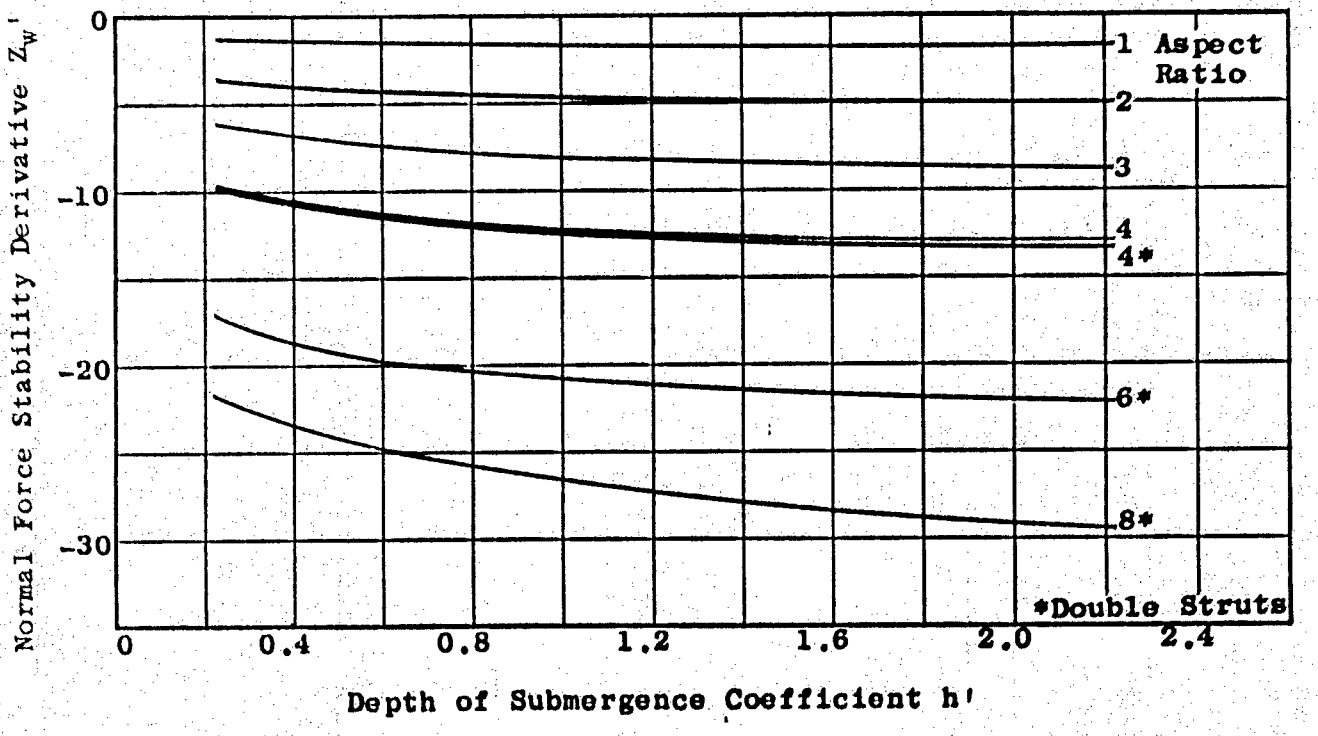

Figure 12 - Effect of Submergence on Normal Force Stability Derivative Z_w' for Various Hydrofoil Configuration and Fixed Froude Number (5.50)

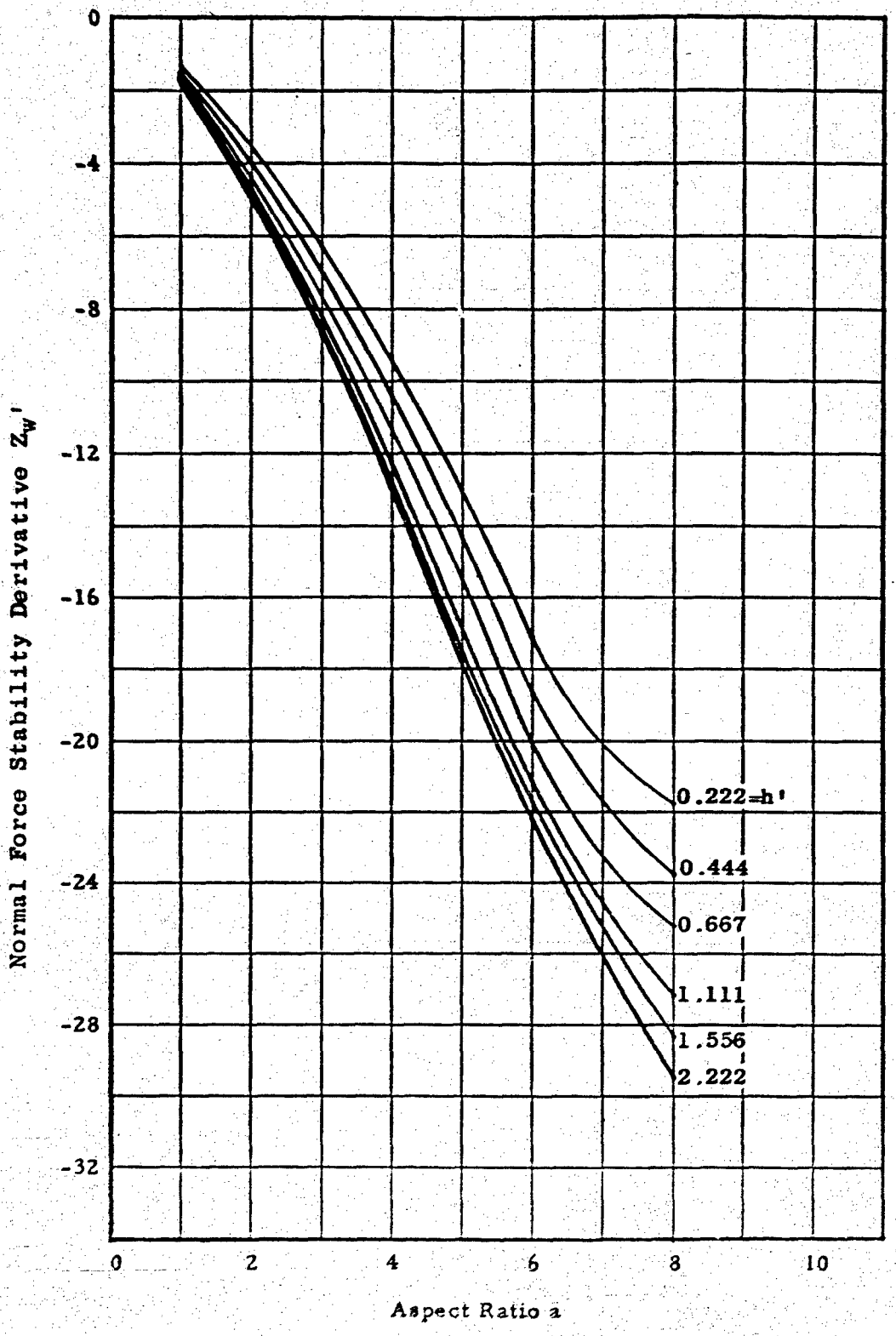

Figure 13 - Effect of Aspect Ratio on Normal Force Stability Derivative Z_w' for Various Submergences and Fixed Froude Number (5.50)

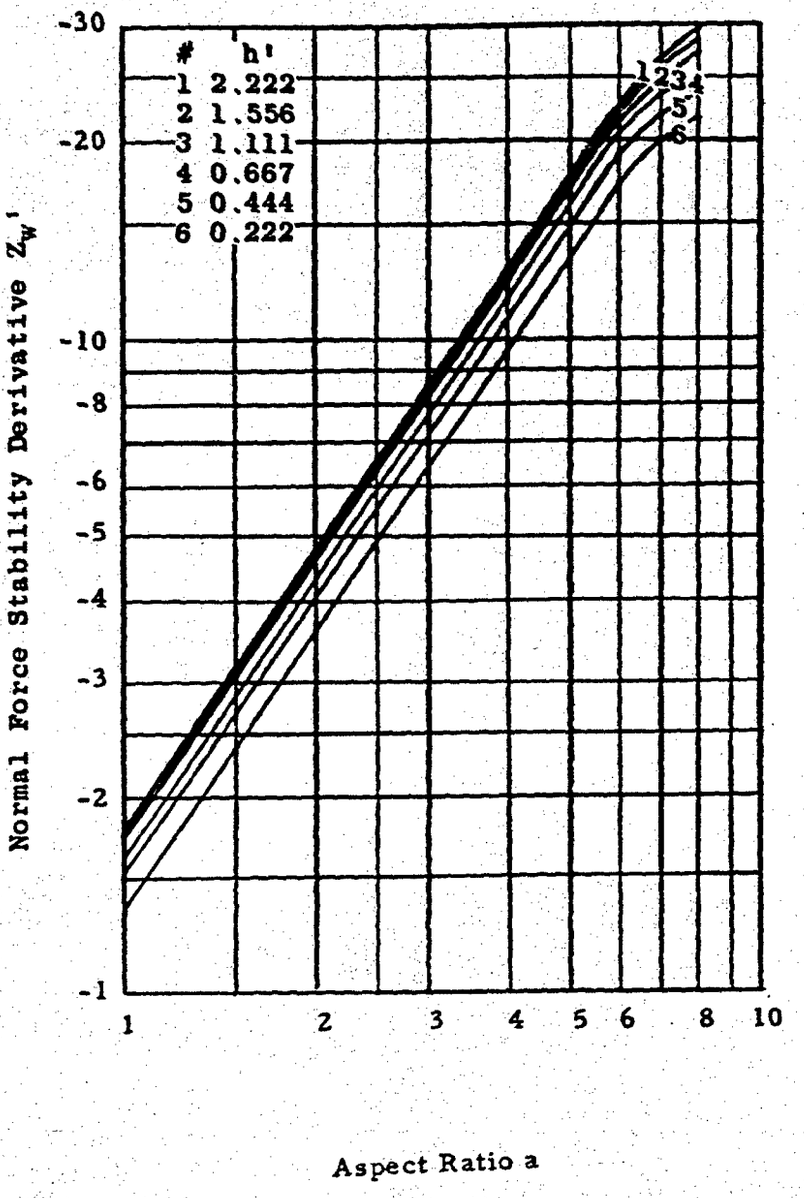

Figure 14 - Logarithmic Variation of Normal Force Stability Derivative Z_w' with Aspect Ratio for Various Submergences and Fixed Froude Number (5, 50)

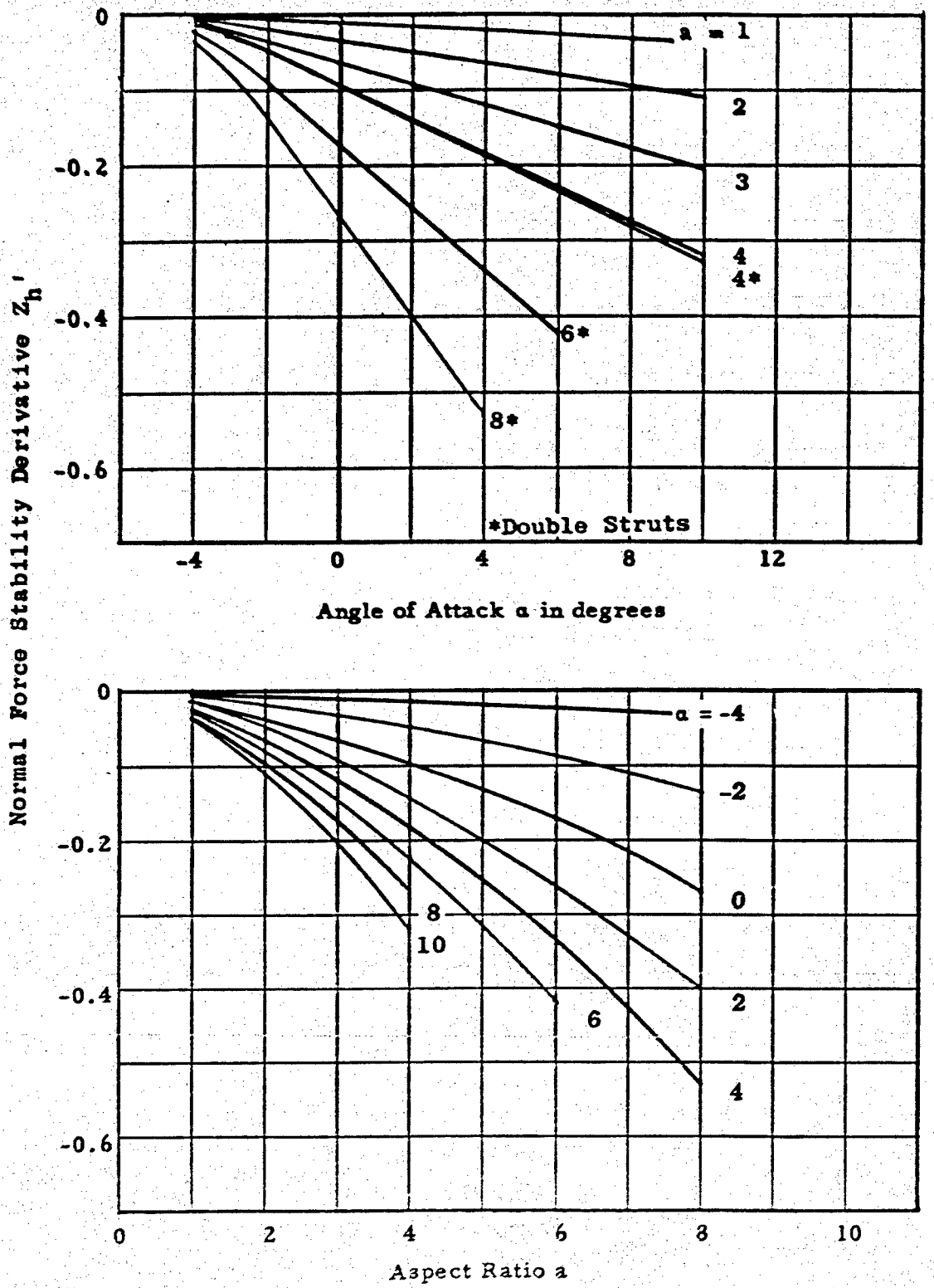

Figure 15 - Effect of Angle of Attack and Aspect Ratio on Normal Force Stability Derivative $Z_{h'}$ for Fixed Froude Number (5.50) and Submergence ($h' \geq 1$)

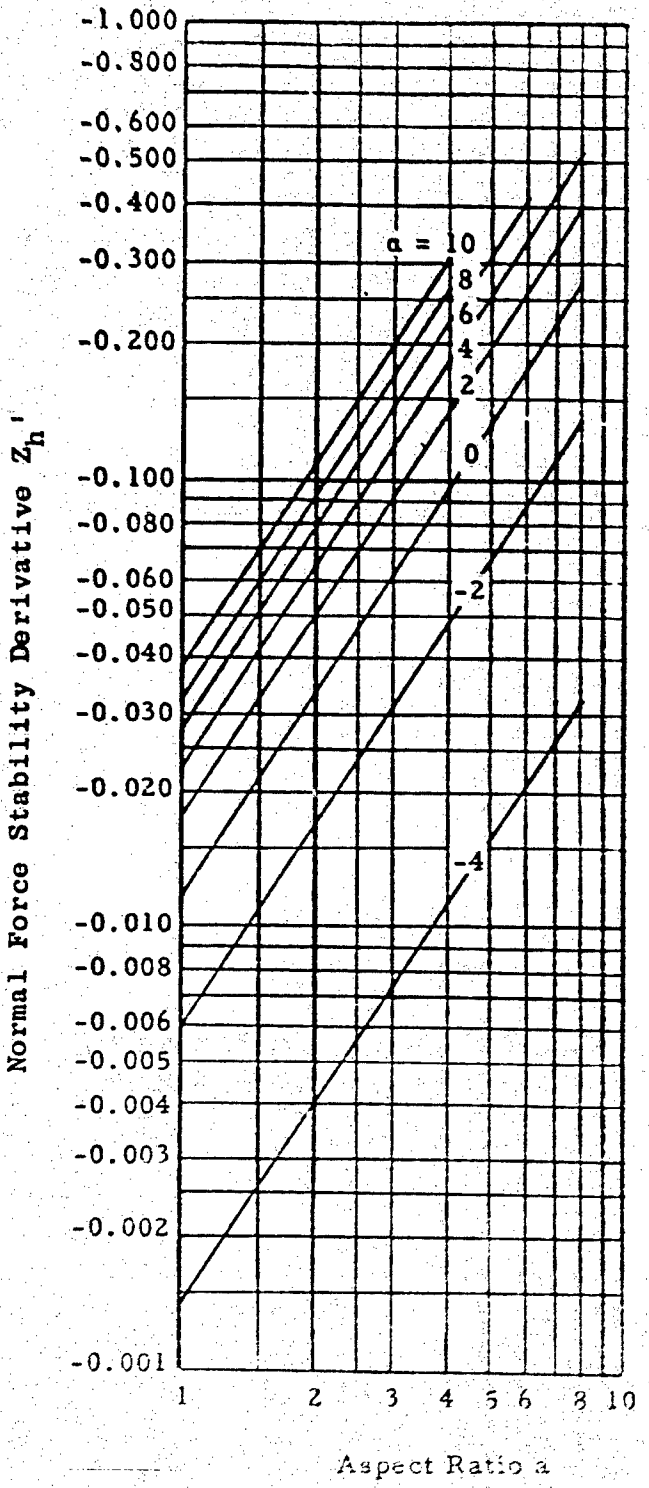

Figure 16 - Logarithmic Variation of Normal Force Stability Derivative Z_h' with Aspect Ratio for Various Angle of Attack for Fixed Froud Number (6.30) and Submergence ($h' = 1$)

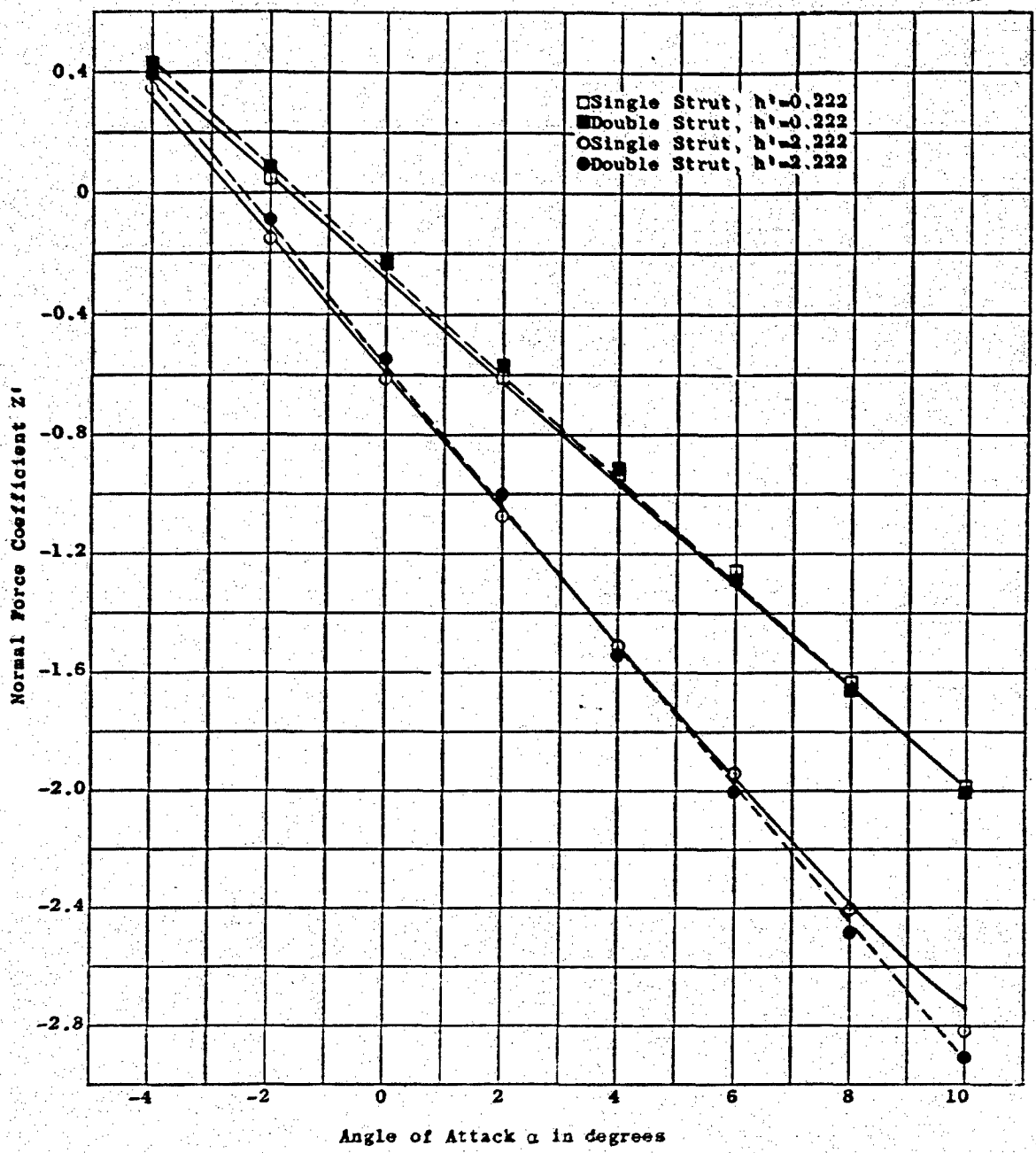

Figure 17 - Effect of Number of Struts on Normal Force Coefficient with Angle of Attack for Various Submergences for One Hydrofoil Configuration (a = 4) and for Fixed Froude Number (5.50)

EFFECT OF REYNOLDS NUMBER

The longitudinal forces developed at zero angle of attack and at large Froude Numbers are due essentially to the viscous drag of the foil and the strut. Consequently, it is to be expected that these forces will vary with Reynolds Number. One method of reflecting the dependency with Reynolds Number is by the use of the residual resistance coefficient. The residual resistance coefficient is related to the longitudinal force at zero angle of attack as follows:

$$C_r = -\frac{X}{\frac{1}{2}\rho S U^2} - C_f \qquad [4]$$

where C_f is the frictional resistance coefficient tabulated in Reference 8.

Figures 18, 19, and 20 show the residual resistance coefficient for various series models as a function of Reynolds Number. It may be noted that the C_r curves are in most cases nearly horizontal for Reynolds Numbers above about 18×10^5 but drop off and/or hump for lower Reynolds Numbers. Laminar flow over the hydrofoils decreases the C_r and free surface wavemaking tends to hump the C_r curve. Since the humps in the C_r curves are not affected by either aspect ratio or submergence, they must be caused mainly by the struts and not the foils. Although laminar flow sections were used for the hydrofoils, it is clear that the full scale hydrofoil craft will be operating in a fully developed turbulent regime.

Judging from this trend, it is resonable to assume for extrapolation purposes that C_r will be constant at all high Reynolds Numbers experienced in the full scale case. Consequently, in making predictions of the longitudinal force coefficient, the values given in Appendices E and F should be amended as follows:

(1) Determine the total drag coefficient for the model from

$$C_{tm} = -\frac{c^2}{S}\,(X' \cos\alpha + Z' \sin\alpha) \qquad [5]$$

(2) Determine the total drag coefficient for the full scale from

$$C_t = C_{tm} + (C_f - 3.92 \times 10^{-3}) \qquad [6]$$

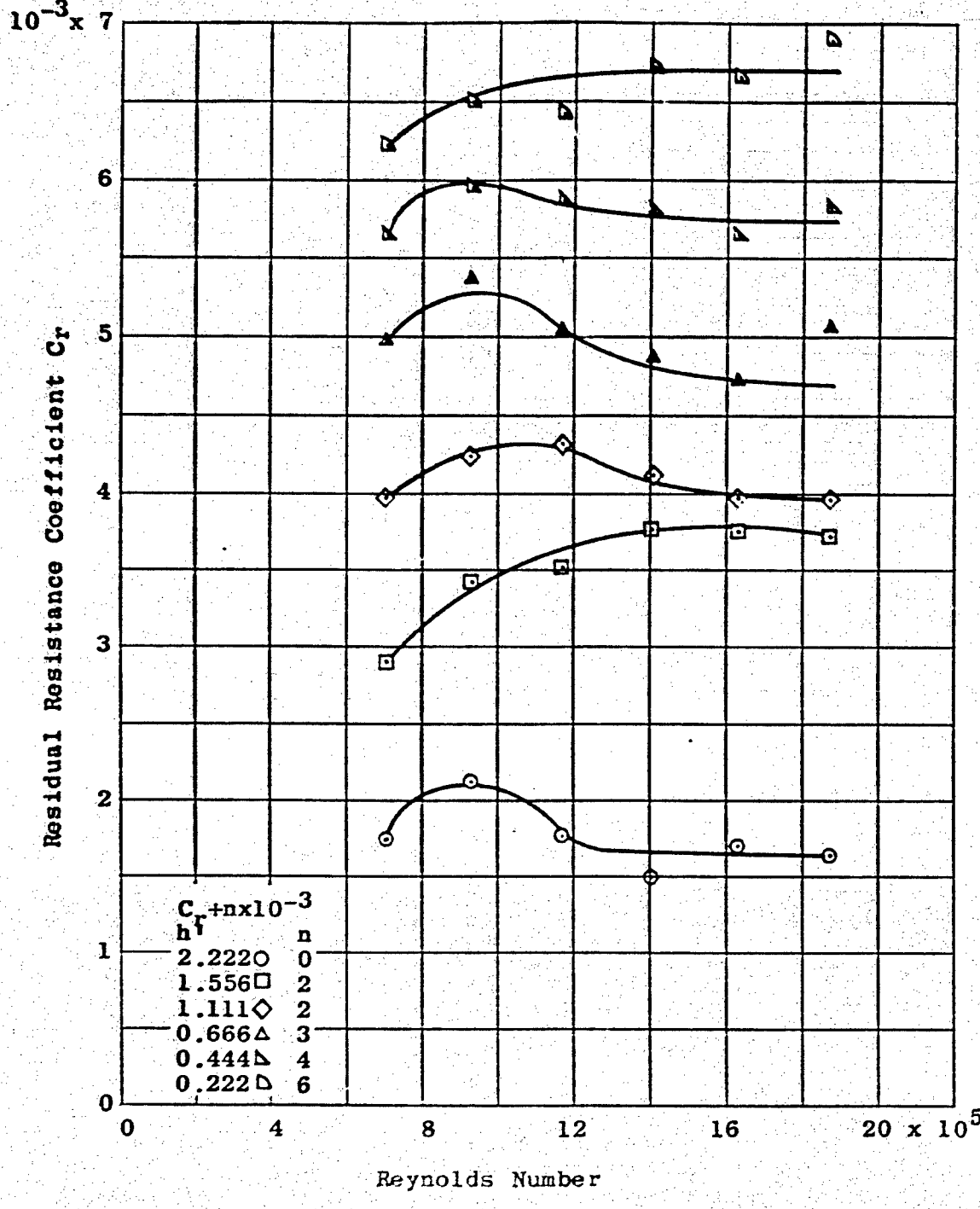

Figure 18 - Variation of Residual Coefficient with Reynolds Number for One Hydrofoil Configuration (a = 4) at Zero Angle of Attack

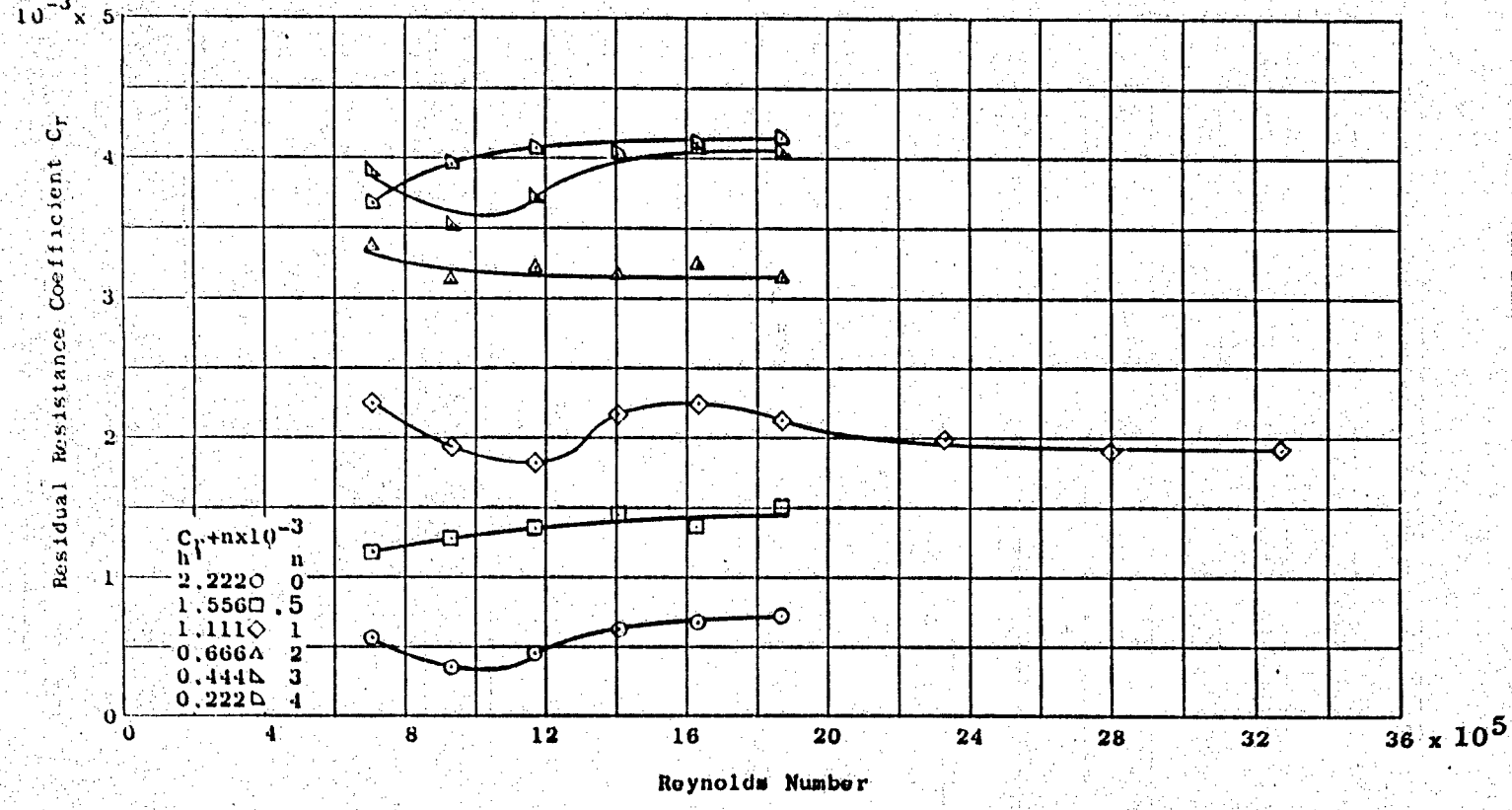

Figure 19 - Variation of Residual Coefficient with Reynolds Number for One Hydrofoil Configuration (a = 6) at Zero Angle of Attack

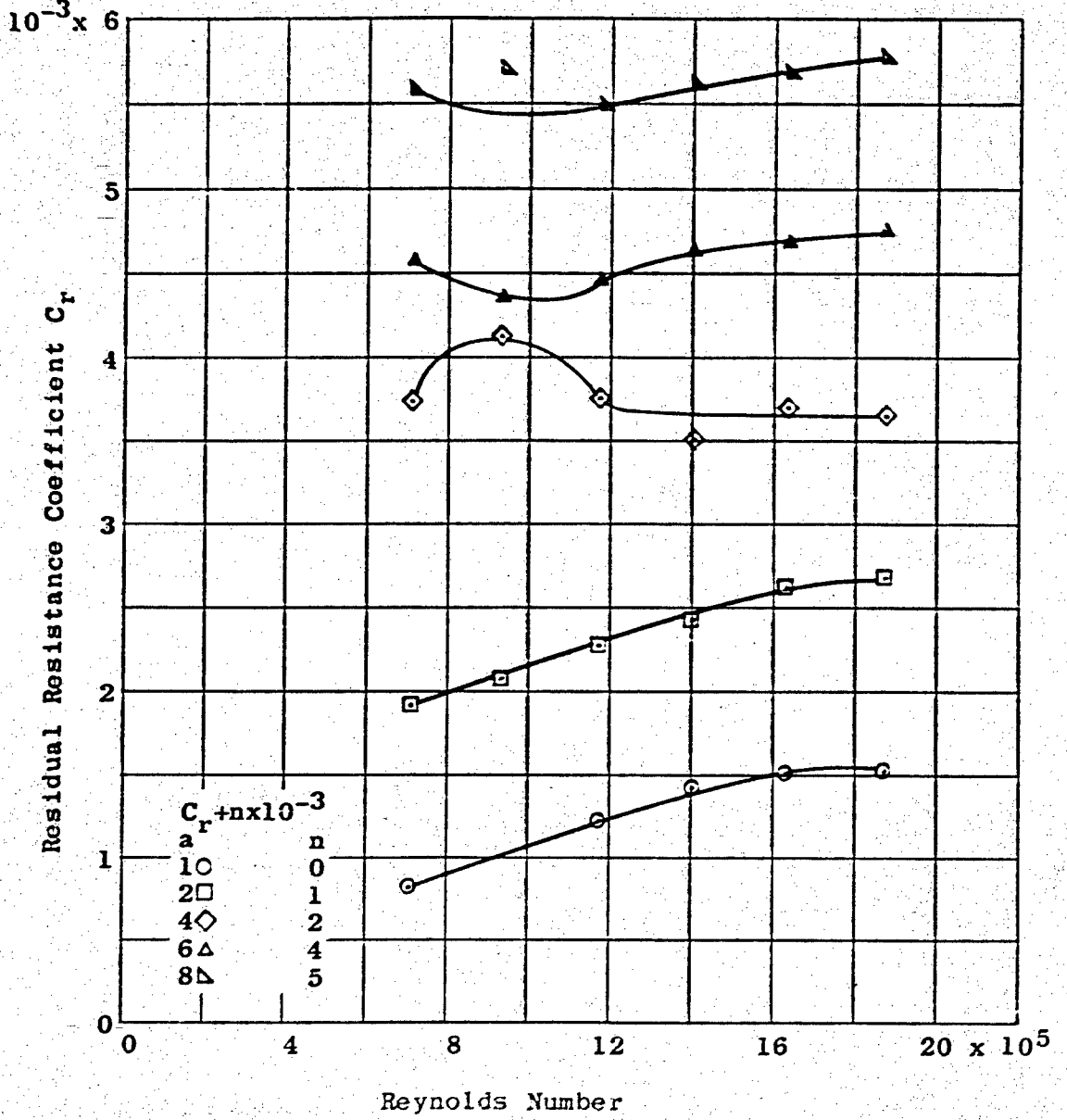

Figure 20 - Variation of Residual Coefficient with Reynolds Number for Various Aspect Ratios at Fixed Submergence (h' = 2.222) and Zero Angle of Attack

EFFECT OF DEPTH OF SUBMERGENCE

Figure 21 shows the effect of submergence on the longitudinal force coefficient for the case where the angle of attack is zero. The longitudinal force coefficient decreases as the submergence decreases. The rate of this decrease becomes more pronounced as the foil approaches the surface. The figures in Appendix E show the longitudinal force coefficient to be equal at a certain angle of attack at all submergences. This angle of attack decreases with increasing aspect ratio. The positive values of the longitudinal force coefficient are due to the lift component at high angles of attack. The increase of longitudinal force coefficient with submergence is due to the additional strut wetted surface.

EFFECT OF STRUTS

Figure 22 shows the effect of number of struts on the longitudinal force coefficient. For zero angle of attack, the longitudinal force coefficient is higher for the double strut configurations. This occurs for both shallow and deep submergence. However, the increase due to the additional strut is more pronounced at the deeper submergence.

LIFT-DRAG RATIO

The lift-drag ratio, computed from Equation [1], is presented as a function of the significant test parameters in Figures 23, 24, and 25. The trends for any intermediate condition are similar.

Figure 23 shows the effect of aspect ratio and angle of attack on the lift-drag ratio for single strut configurations at deep submergence ($h' = 2.222$). The lift-drag ratio reaches a maximum value at an angle of attack between 2 and 7 degrees depending on the aspect ratio. Increasing the aspect ratio decreases the angle of attack at which the peak occurs.

Figure 24 shows the effect of aspect ratio and angle of attack on the lift-drag ratio for double strut configurations at deep submergence ($h' = 2.222$). The lift-drag ratio reaches a maximum value at an angle of attack which decreases as the aspect ratio is increased. The increase in peak lift-drag ratio is greater in going from an aspect ratio of 4 to an aspect ratio of 6 than in going from an aspect ratio of 6 to an aspect ratio of 8.

Figure 25 shows the effect of depth of submergence on the lift-drag ratio. The maximum lift-drag ratio for a fixed aspect ratio ($a = 6$) is relatively insensitive to depth of submergence.

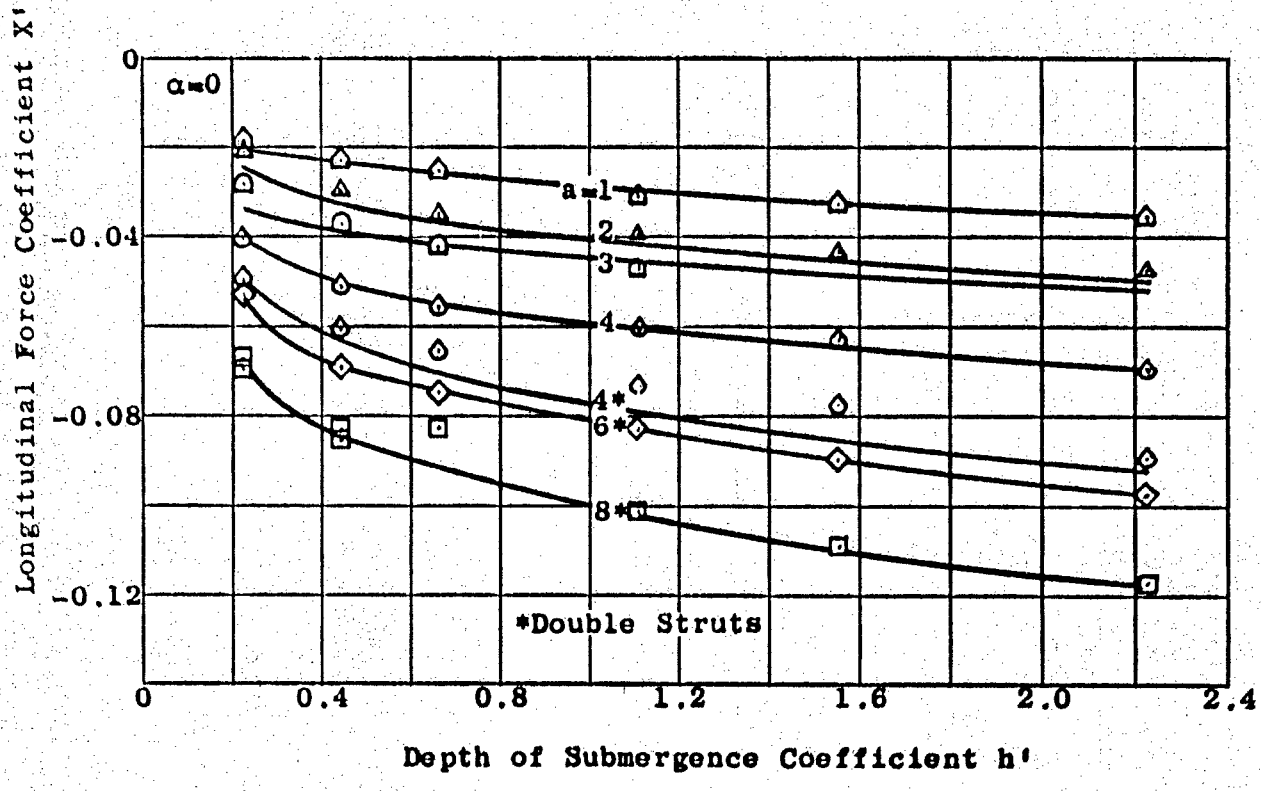

Figure 21 - Variation of Longitudinal Force Coefficient with Submergence for Various Hydrofoil Configurations, Fixed Froude Number (5.50), and Zero Angle of Attack

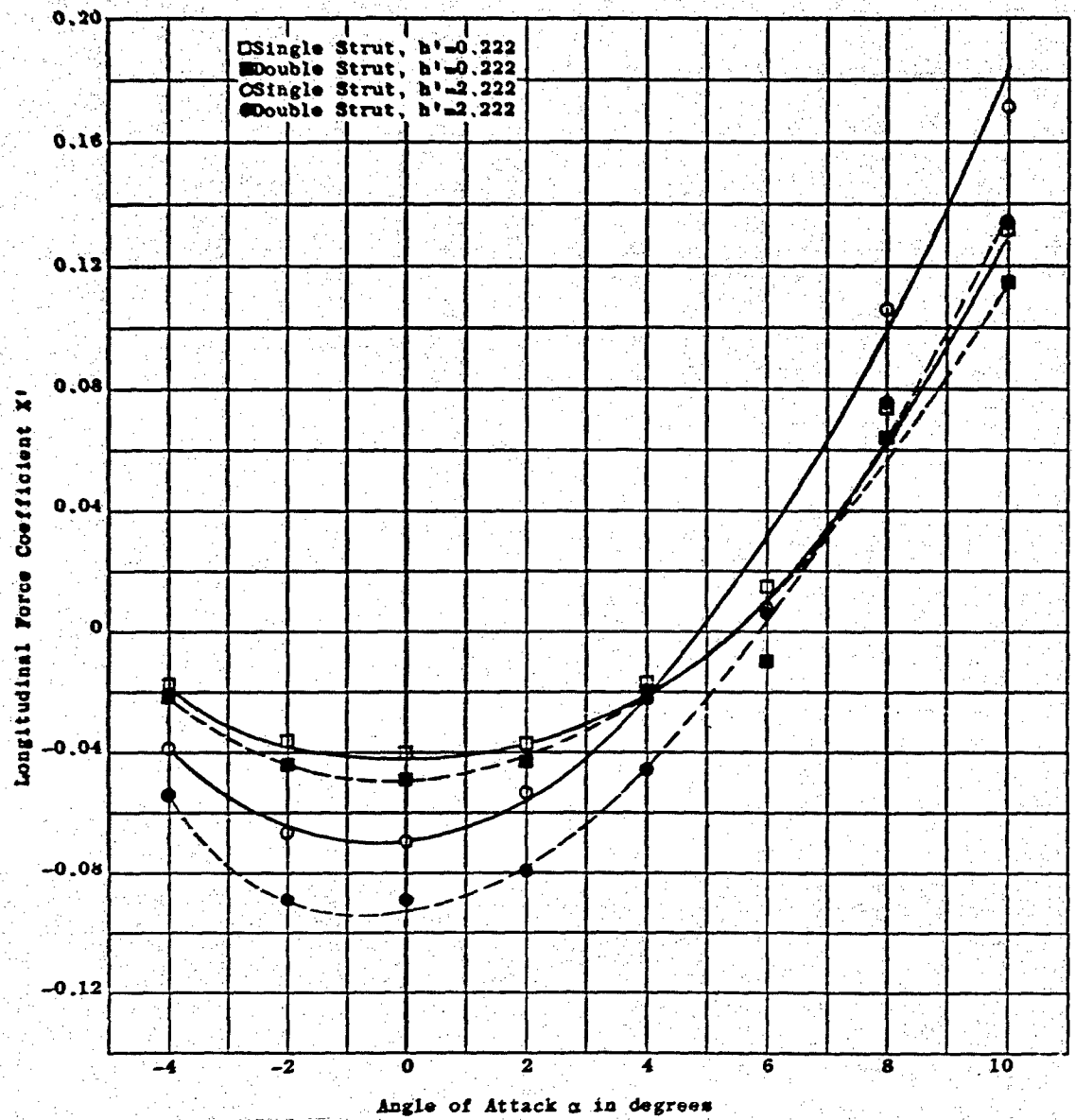

Figure 22 - Effect of Number of Struts on Longitudinal Force Coefficient with Angle of Attack for Various Submergences for One Hydrofoil Configuration and Fixed Froude Number (5.50)

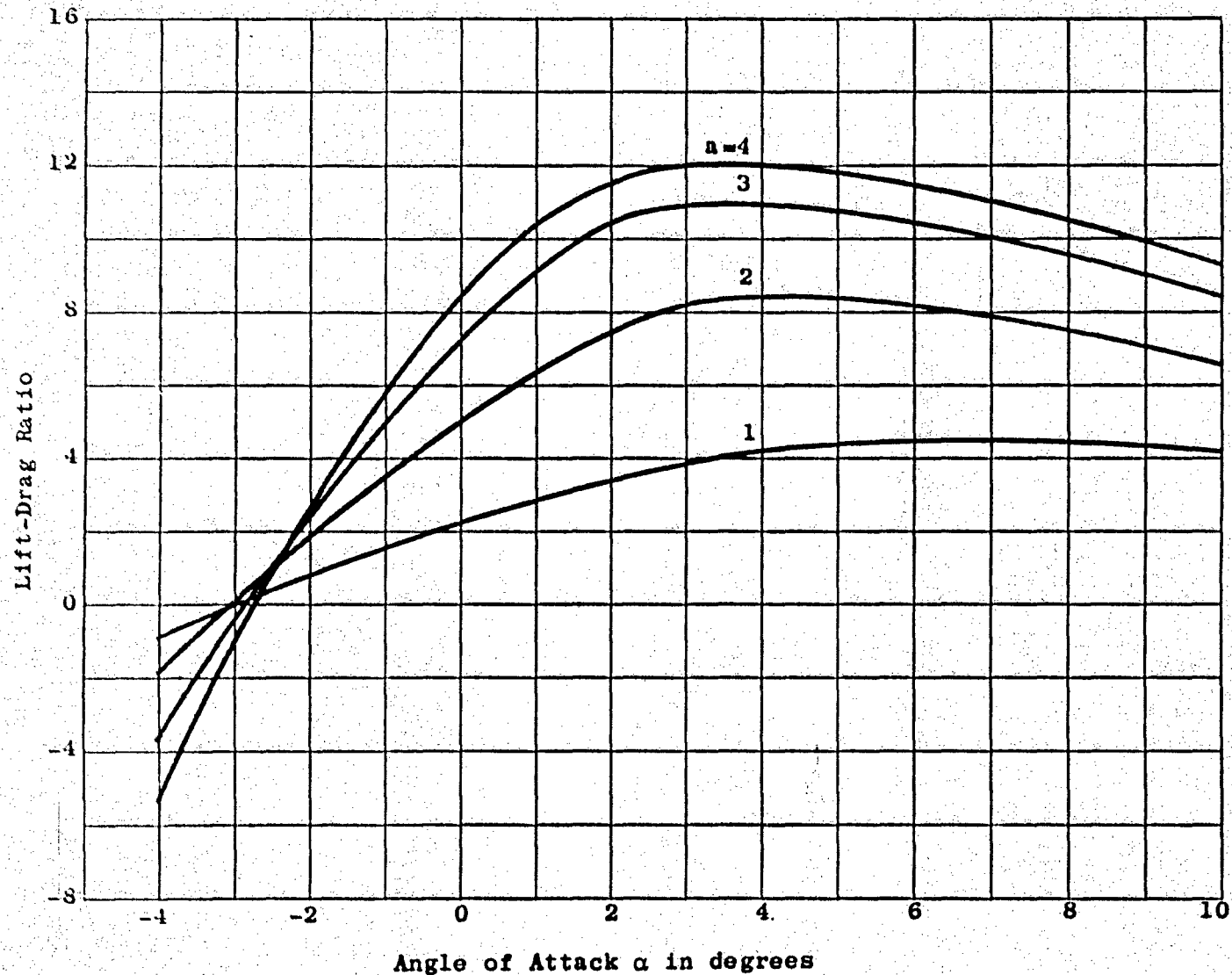

Figure 23 - Variation of Lift-Drag Ratios of Various Single-Strut Hydrofoil Configurations at Fixed Submergence (h' = 2.222) and Froude Number (5.50)

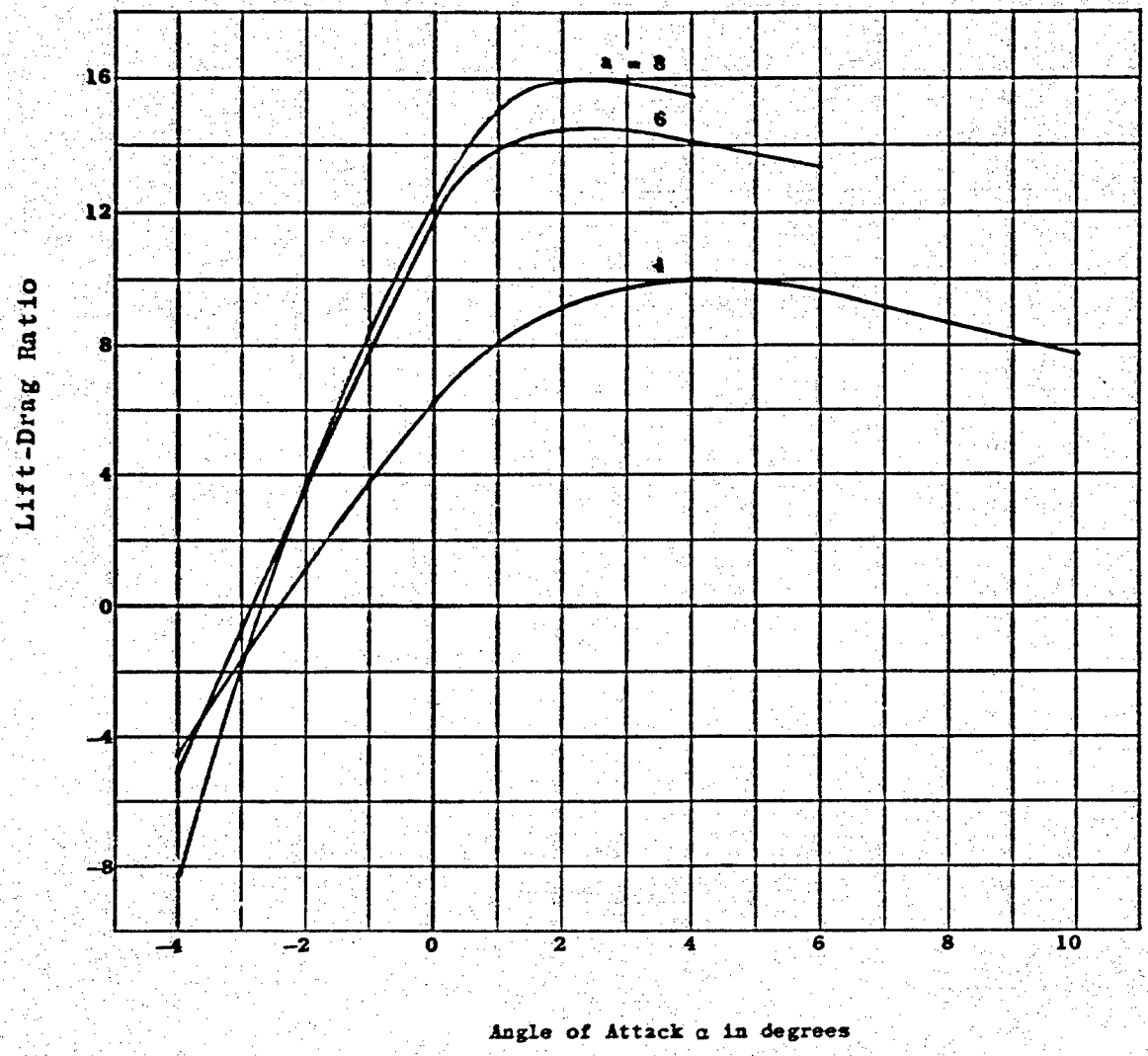

Figure 24 - Variation of Lift-Drag Ratios of Various Double-Strut Hydrofoil Configurations at Fixed Submergence (h' = 2.222) and Froude Number (5.50)

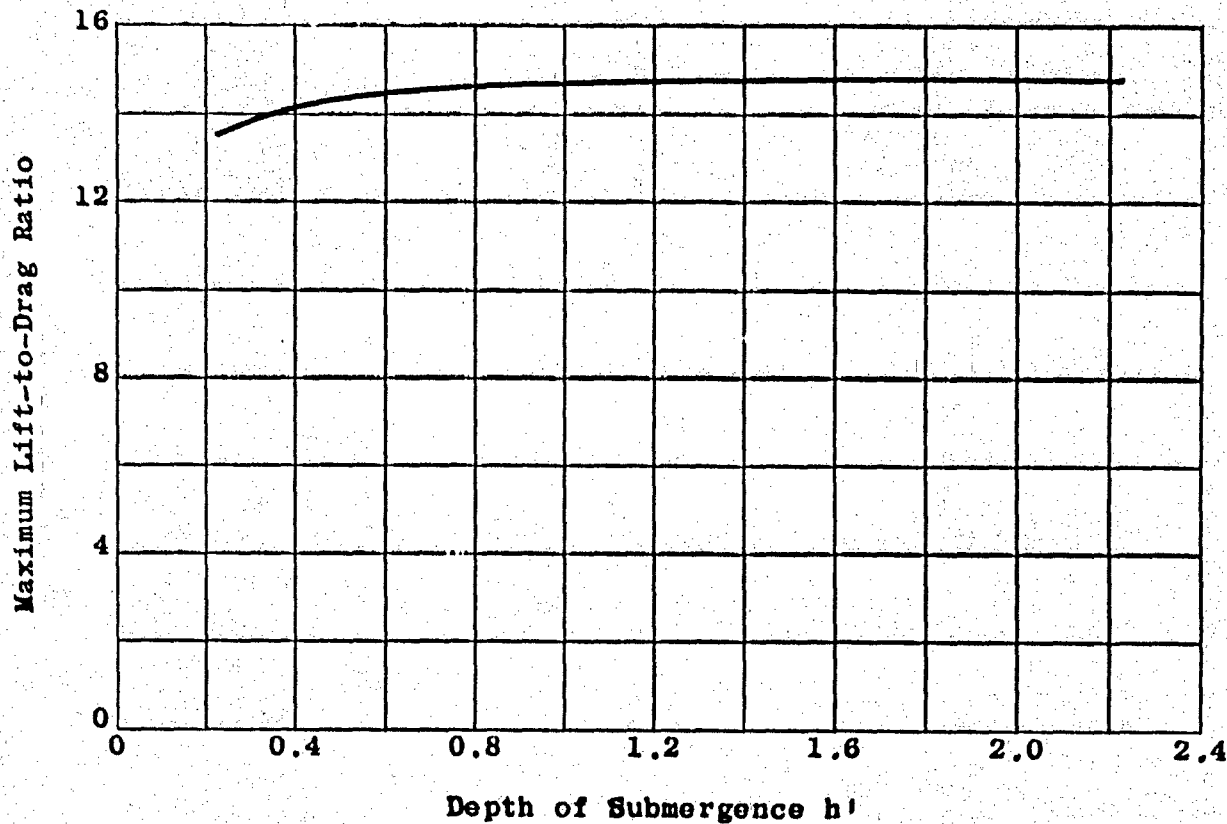

Figure 25 - Effect of Submergence on Maximum Lift-Drag Ratio for One Hydrofoil Configuration (a = 6) and Fixed Froude Number (5.50)

Figures 23 and 24 suggest that the larger the aspect ratio chosen for a hydrofoil craft the better the chances of flying the boat at its maximum lift-drag ratio. From the standpoint of lift-drag ratio, Figure 25 shows a submergence of greater than 0.6 chord to be desirable. However, the combination of high aspect ratio foils deeply submerged presents the designer with structural problems which require a compromise in selecting a configuration.

COMPARISONS WITH EXISTING THEORY

A review of the literature has revealed that a number of theories exist for predicting lift coefficient for hydrofoils. Several of these theories make allowances for the effect of the free surface. The theories [5,8] used herein as a basis for comparison were selected as those which gave the best agreement with the experimental results on DTMB Series HF-1. In addition, the results of another experimental investigation[7] are included in the comparison.

The coefficients reported for this series are referred to a normal-longitudinal force axis system. Consequently, the theoretical expressions which are referred to the lift-drag axis system have been transformed as follows:

$$C_L = \frac{c^2}{A} (-Z'\cos\alpha + X'\sin\alpha) \qquad [7]$$

$$C_{L\alpha} = \frac{c^2}{A}(-Z_w' + X_{\dot{\alpha}}') \qquad [8]$$

The comparisons which follow are based on the slopes of the data curves and not on the data curves themselves. For all the models tested, Z_w' is greater than $X_{\dot{\alpha}}'$. In addition,

$$A = bc \qquad [9]$$

$$\ell = c \qquad [10]$$

These relationships simplify Equation [3] to

$$Z_{w'} = -aC_{L\alpha} \qquad [11]$$

The theories of References 5 and 6 are restated in terms of the normal force stability derivative for the deep submergence case in the following formulas:

$$Z_w' = -\frac{2\pi a^2}{\frac{4}{\pi}a + 2} \quad \text{(Based on Reference 5)} \qquad [12]$$

$$Z_w' = -\frac{2\pi a^2}{a + 3} \quad \text{(Based on Reference 6)} \qquad [13]$$

For the near surface case, the theory of Reference 5 leads to a complex formulation and is therefore not restated. The theory of Reference 6 utilizes an empirical correction for the near-surface effect which results in modifying Equation [13] as follows:

$$Z_w' = -\frac{2\pi K_s a^2}{a + 2K_s + 1} \qquad [13a]$$

where

$$K_s = \frac{(4h')^2 + 1}{(4h')^2 + 2}$$

Figure 26 compares the experimental values with those obtained from the two theories for the deep submergence case. It may be noted that the theory of Reference 5 gives the closest agreement with the experimental results of the series. The extent of this agreement is shown by the ratio curve in Figure 27. The theory apparently overpredicts the lift coefficient by about 7% over aspect ratios of 3 to 7 and by over 10% for both lower and higher aspect ratios.

No apparent reason can be advanced for the discrepancy between the theory and experiment. It is true that the theory, in an absolute sense, represents the case of a hydrofoil configuration without vertical struts. However, the absence of a single strut would have only a negligible effect on lift[9]. The absence of double struts would tend to decrease the lift (as shown by the experiments) and thus increase the discrepancy between theory and experiment.

Figure 28 compares the experimental and theoretical values for the near-surface case. The experimental values for the series and values computed from both theories indicate that the near surface effect above a submergence of 0.8 chord is very small. The experimental results of Reference 7, however, indicate a strong near-surface effect as deep as 1.4 chords. It may be noted that curves 1 and 3 are displaced by a constant amount at all submergences deeper than 0.4 chord. Thus, if the displacement is attributed to a discrepancy in the prediction of the deep submergence case, it appears that the formulation

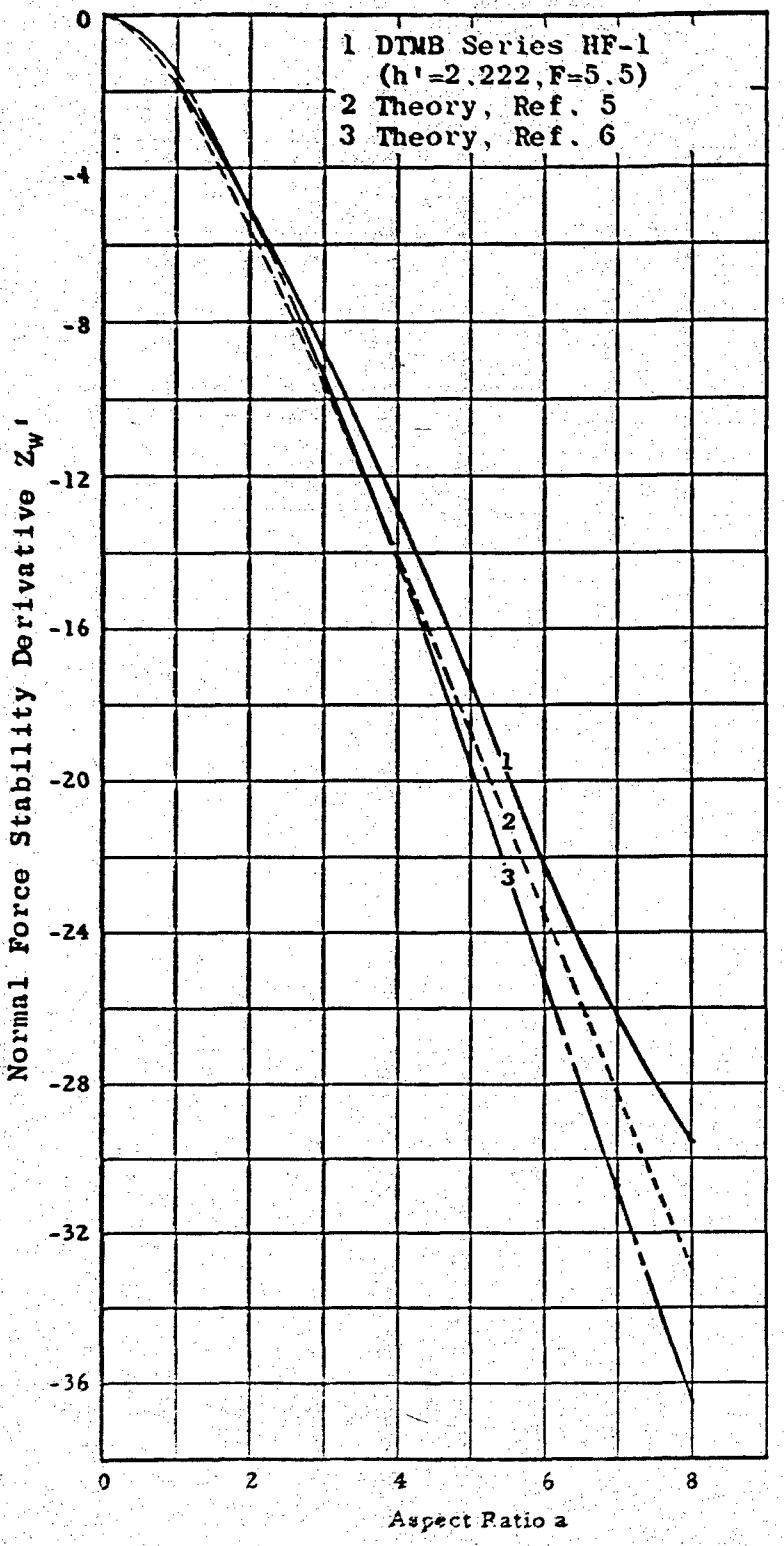

Figure 26 - Comparison Between Experiment and Theory for Normal Force Stability Derivative Z_w' with Aspect Ratio for Fixed Submergence ($h' = 2.222$)

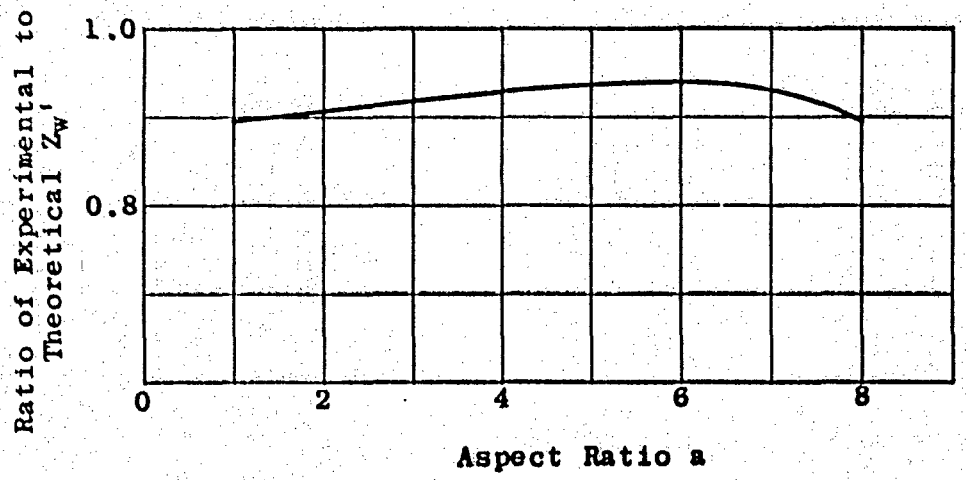

Figure 27 - Ratio of Experimental to Theoretical Values of Normal Force Stability Derivative Z_w' with Aspect Ratio for Fixed Submergence ($h' = 2.222$)

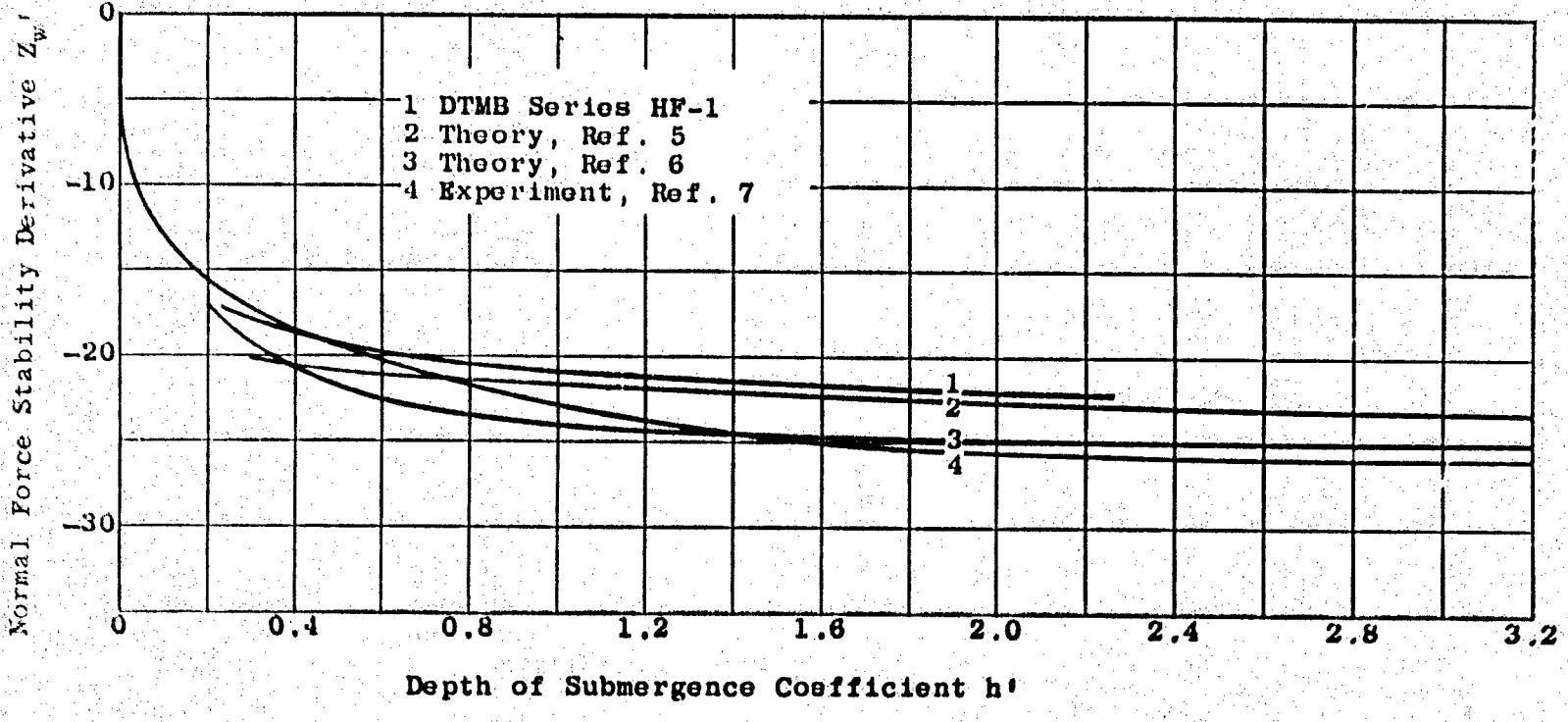

Figure 28 - Comparison Between Experiment and Theory for Normal Force Stability Derivative Z_w' with Submergence for One Hydrofoil Configuration (a = 6)

of Reference 6 can be used to predict reliably the incremental contribution due to the near-surface effect. Between submergences of 0.3 and 0.4 chord, the method of Reference 6 appears to predict a greater decrease in Z_w' than the series. Applying similar reasoning, curves 1 and 2 tend to diverge progressively as the submergence decreases. It appears, therefore, that if the theory of Reference 5 is used to compute the near-surface effect that it would result in an insufficient decrease in Z_w'.

CONCLUSIONS

Based on the experimental results for a systematic series of Tee hydrofoils, DTMB Series HF-1, the following conclusions are drawn:

1. Normal force coefficient is essentially independent of Froude Number for Froude Numbers above 5.50 for the range of aspect ratios and submergences covered by the series.

2. The normal force coefficient is progressively reduced as the submergence of the foils is decreased. At submergences deeper than 0.7 chord, the near-surface effect for the entire series is negligible. For higher aspect ratios a deeper submergence is required to minimize the near-surface effect.

3. The use of two vertical struts instead of a single central strut results in a small increase in the normal force coefficient.

4. The normal force stability derivative Z_w' increases with aspect ratio approximately to the power of 1.43 for all submergences covered by the investigation.

5. The best available theory predicts the normal force stability derivative Z_w' which are from 7% to 10% greater than the corresponding experimental values at deep submergence. In general, both theories studied are in agreement with the experiments conducted in so far as the depth of submergence at which the near-surface effect becomes negligible. However, neither theory accurately predicts the change of normal force stability derivative due to submergences of less than 0.3 chord.

6. The various foils of the series operate in a fully turbulent flow regime at Reynolds Numbers above 1.87×10^7 as shown by a constant residual resistance coefficient. The longitudinal force coefficient at zero angle of attack decreases with increased Reynolds Number. This suggests that the longitudinal force coefficient should be corrected to account for differences in frictional resistance in making predictions for the full scale hydrofoil craft.

7. The longitudinal force coefficient is progressively reduced as the submergence of the foils is decreased. At submergences deeper than 0.7 chord, the near-surface effect for the entire series is negligible. For higher aspect ratios a deeper submergence is required to minimize the near-surface effect.

8. The double struts increase the longitudinal force coefficient, particularly at small angles of attack.

9. For any given configuration, the maximum lift-drag ratio is essentially constant for submergences greater than 0.6 chord. Consequently, the choice of operating depth should take into account structural considerations.

10. The angle of attack for which the maximum lift-drag ratio achieved decreases from about 7 degrees for an aspect ratio of 1 to about 2 degrees for an aspect ratio of 8. This suggests that large aspect ratios should be used for hydrofoil craft, if feasible, from a standpoint of structural considerations.

ACKNOWLEDGMENTS

The author wishes to express his appreciation to Mr. Harvey Blauvelt who assisted in the experimental work, and for the contributions and guidance by Messrs. M. Gertler, A. Goodman, and G. Hagen all of whom are members of the Stability and Control Division of the David Taylor Model Basin.

APPENDIX A

NORMAL FORCE COEFFICIENTS FOR INDIVIDUAL CONFIGURATIONS OF TMB SERIES HF-1 AT A FROUDE NUMBER OF 5.50 AS A FUNCTION OF ANGLE OF ATTACK

The coefficients in this appendix apply strictly to a Reynolds Number of 1.87×10^6 and a Froude Number of 5.50 but can be considered to be independent of both of these parameters at higher values.

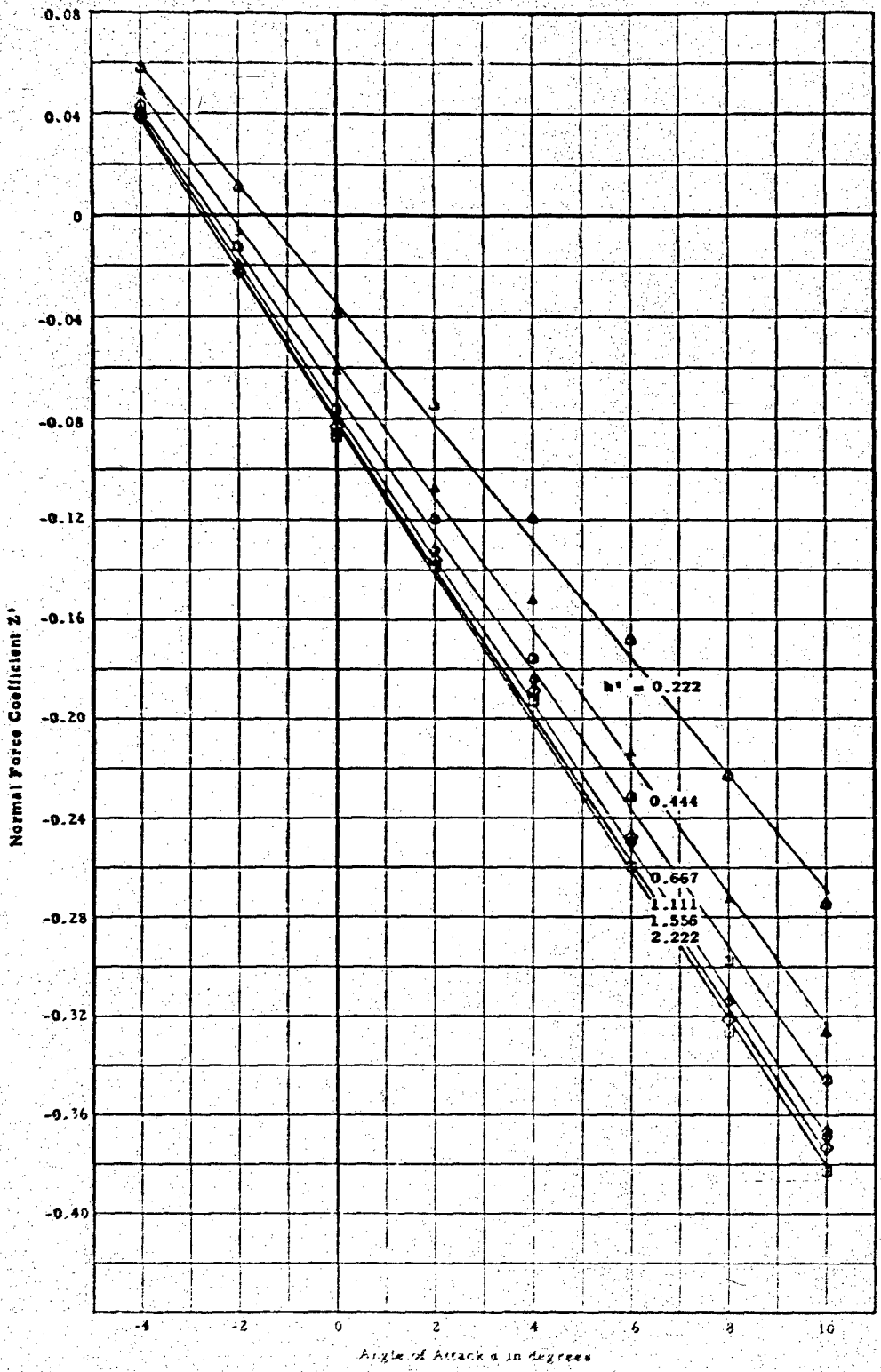

Figure 29 - Foil with Aspect Ratio of 1 Supported by Single Strut

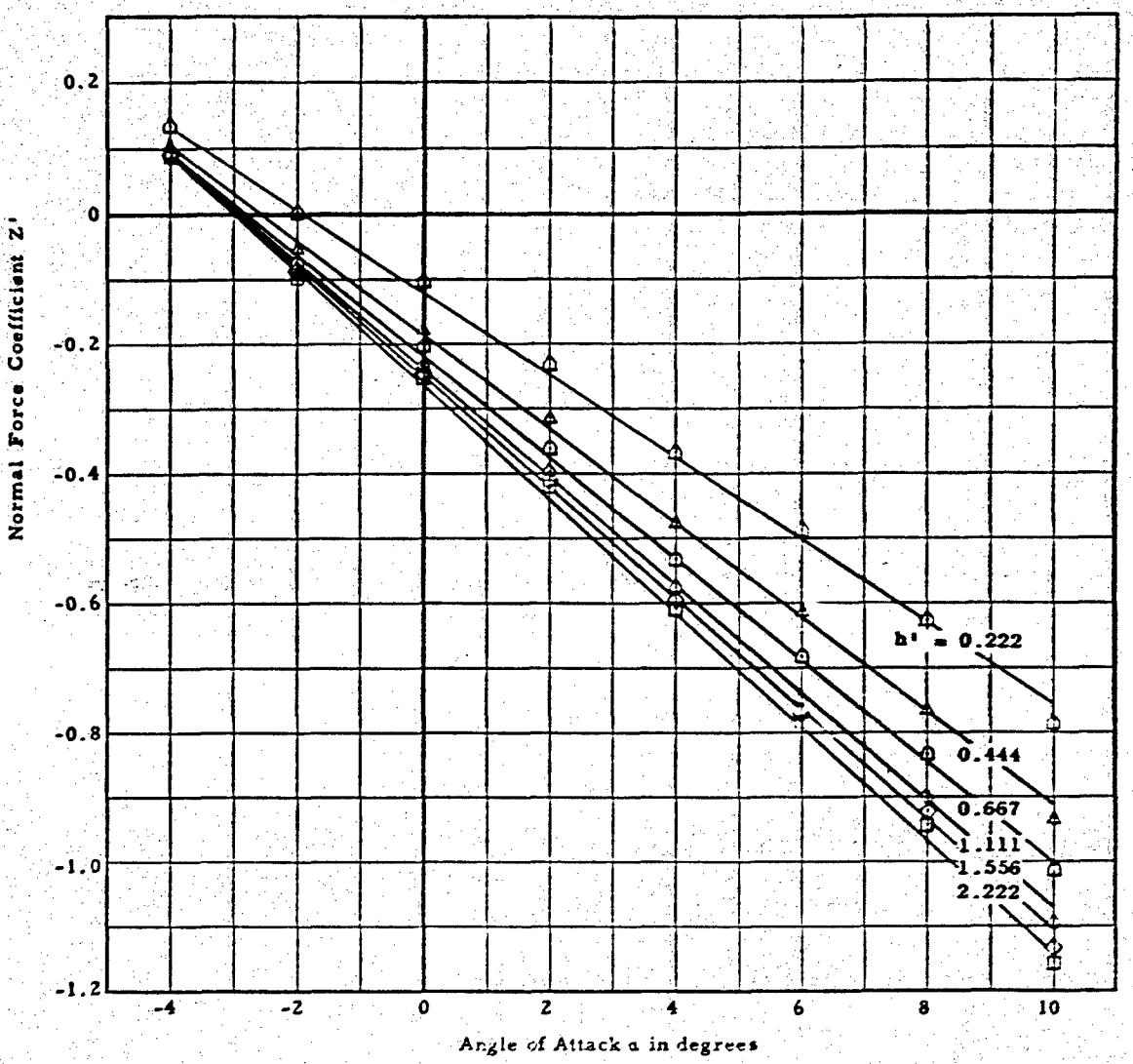

Figure 30 - Foil with Aspect Ratio of 2 Supported by Single Strut

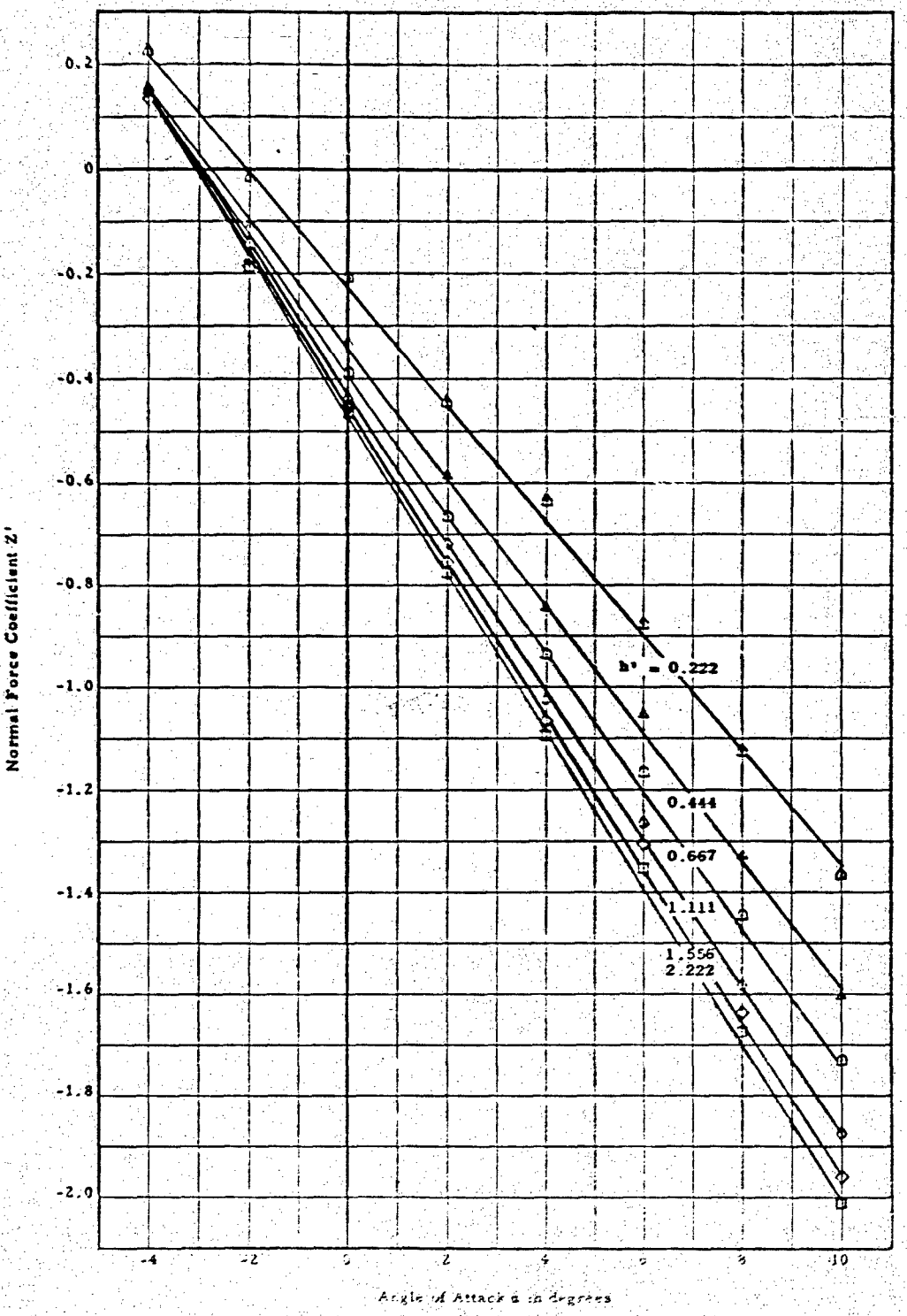

Figure 31 - Foil with Aspect Ratio of 3 Supported by Single Strut

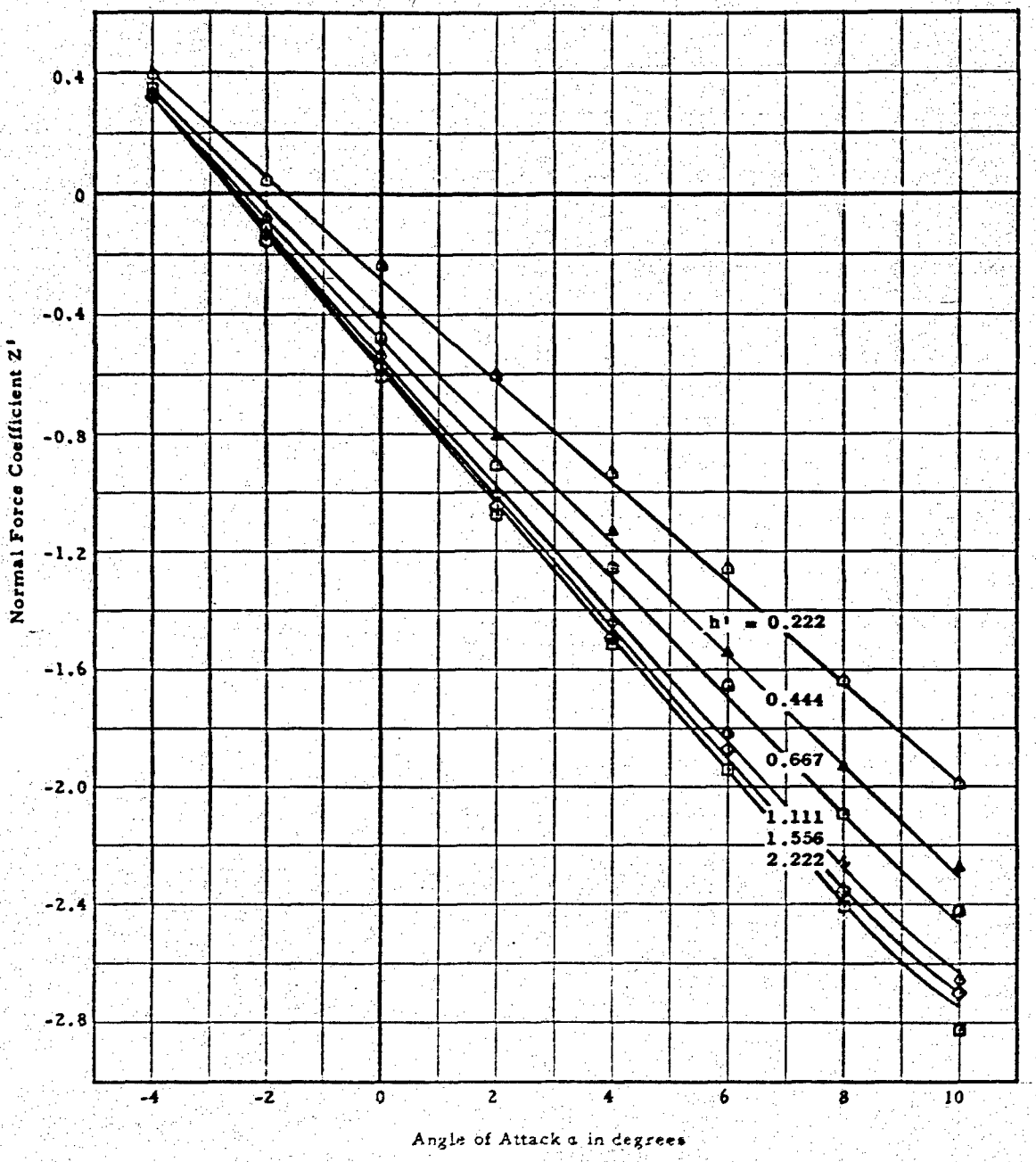

Figure 32 - Foil with Aspect Ratio of 4 Supported by Single Strut

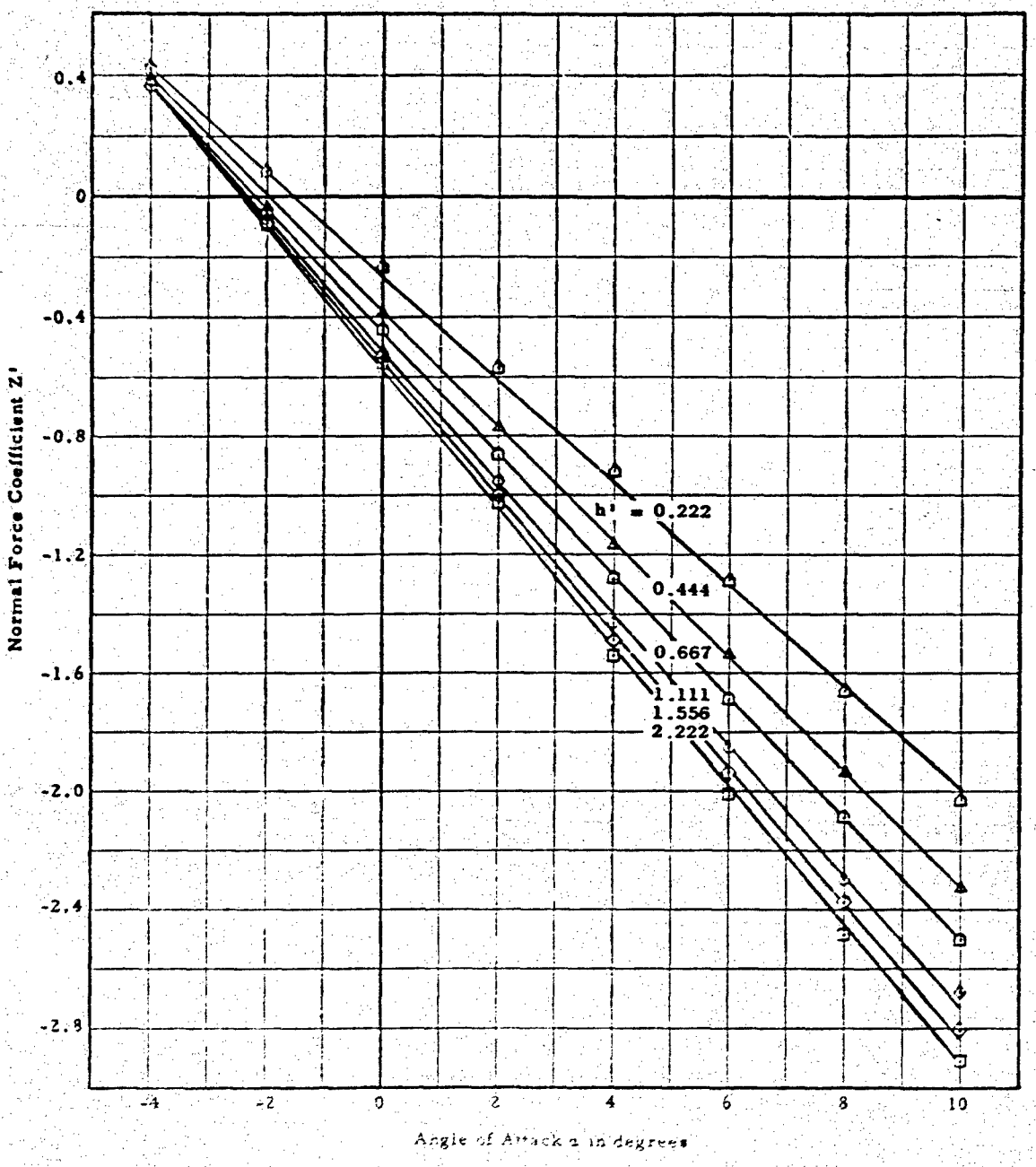

Figure 33 - Foil with Aspect Ratio of 4 Supported by Double Strut

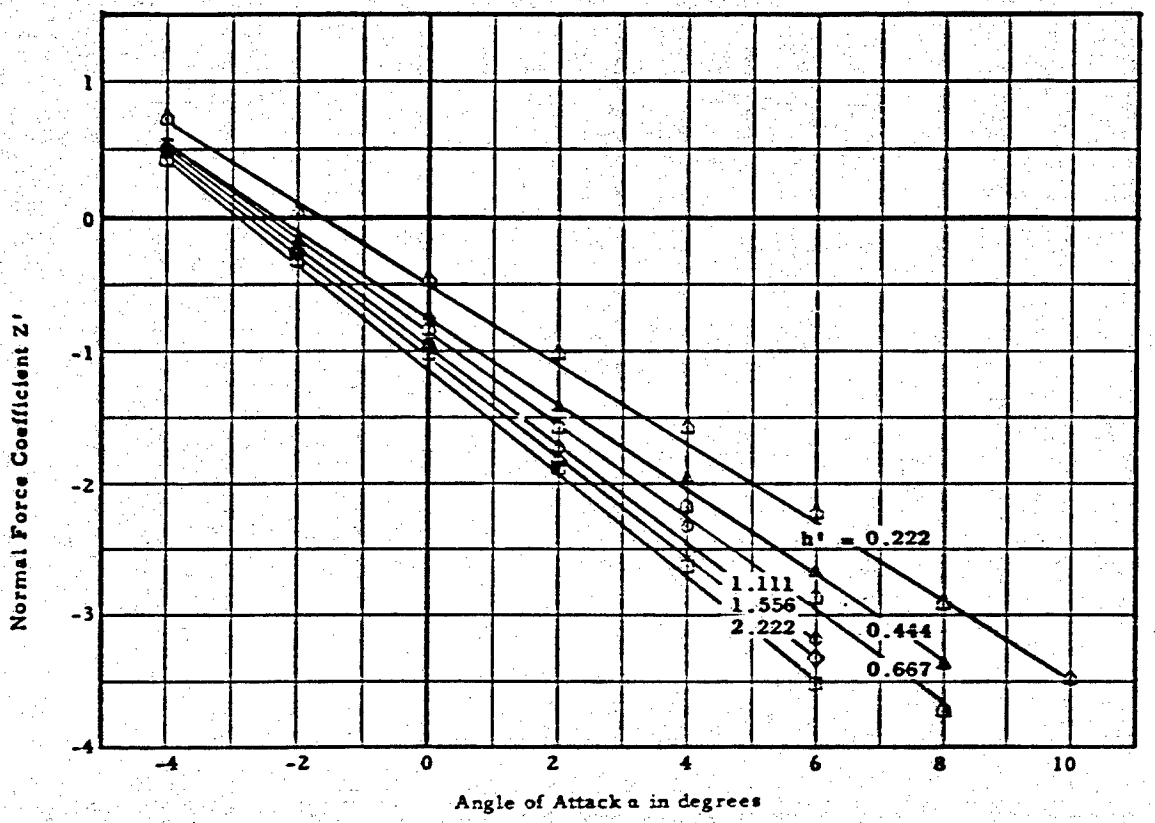

Figure 34 - Foil with Aspect Ratio of 6 Supported by Double Strut

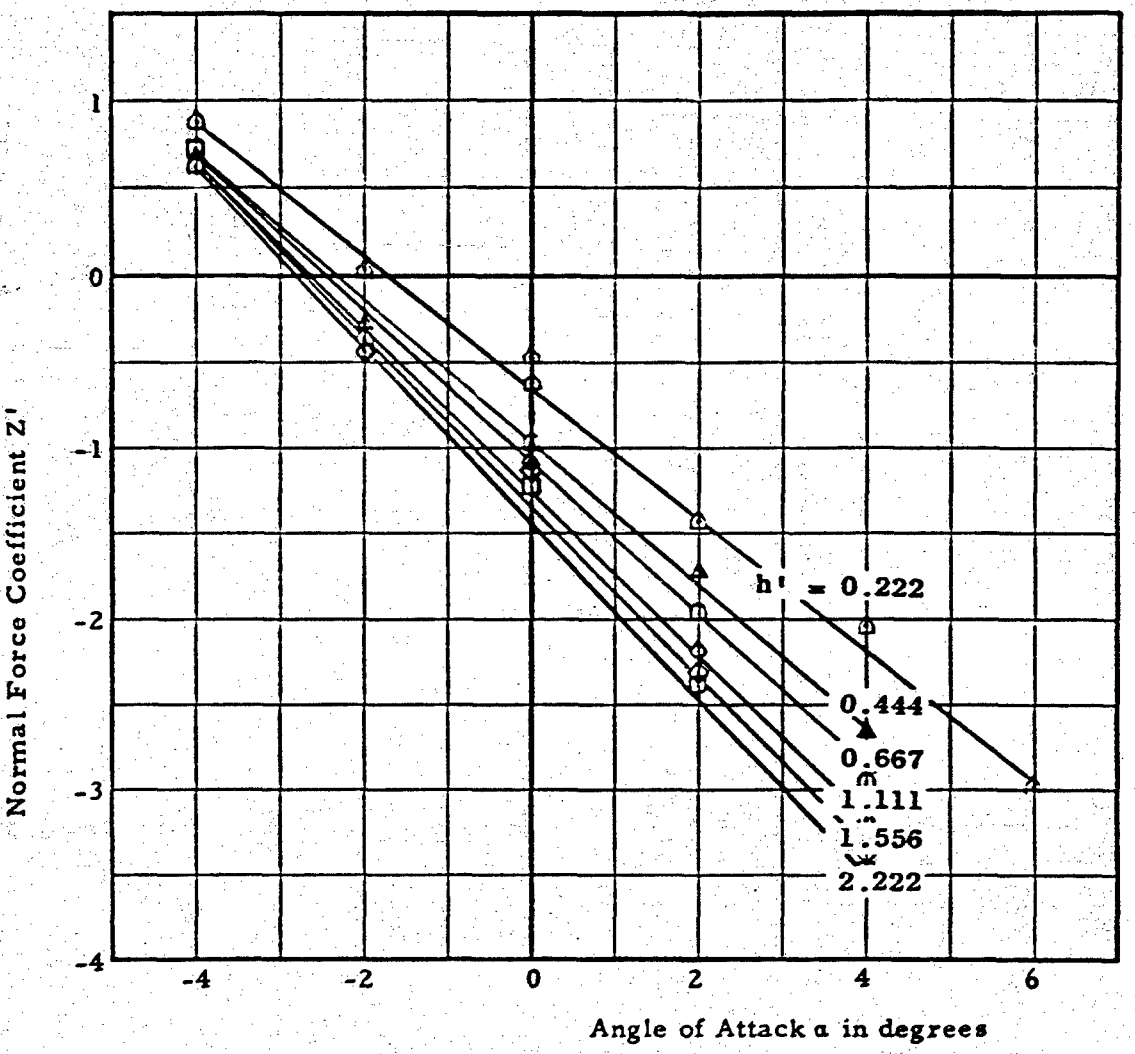

Figure 35 - Foil with Aspect Ratio of 8 Supported by Double Strut

APPENDIX B

NORMAL FORCE COEFFICIENTS FOR INDIVIDUAL CONFIGURATIONS OF TMB SERIES HF-1 AT A FROUDE NUMBER OF 5.50 AS A FUNCTION OF SUBMERGENCE

The coefficients in this appendix apply strictly to a Reynolds Number of 1.87×10^6 and a Froude Number of 5.50 but can be considered to be independent of both of these parameters at higher values.

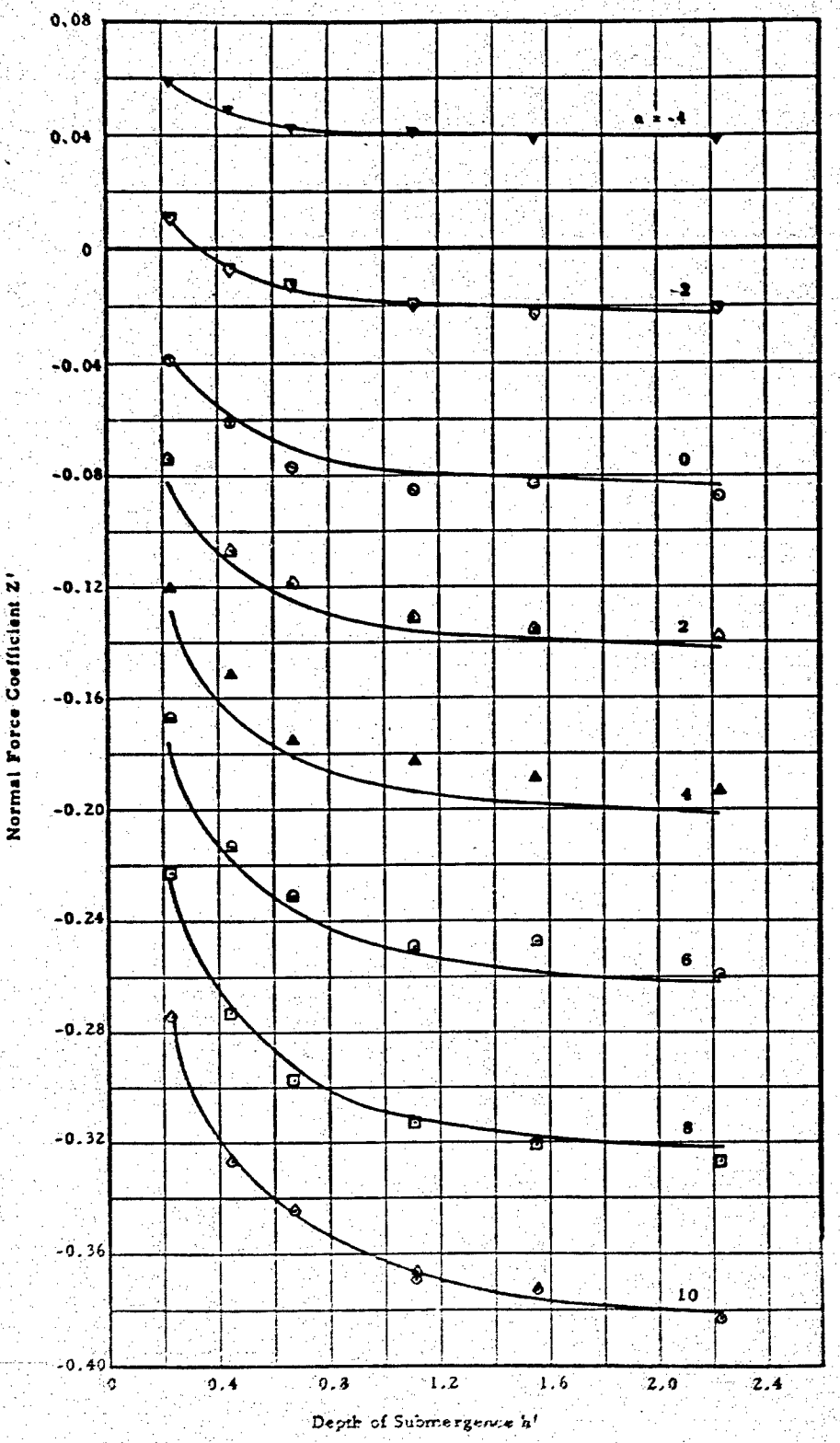

Figure 36 - Foil with Aspect Ratio of 1 Supported by Single Strut

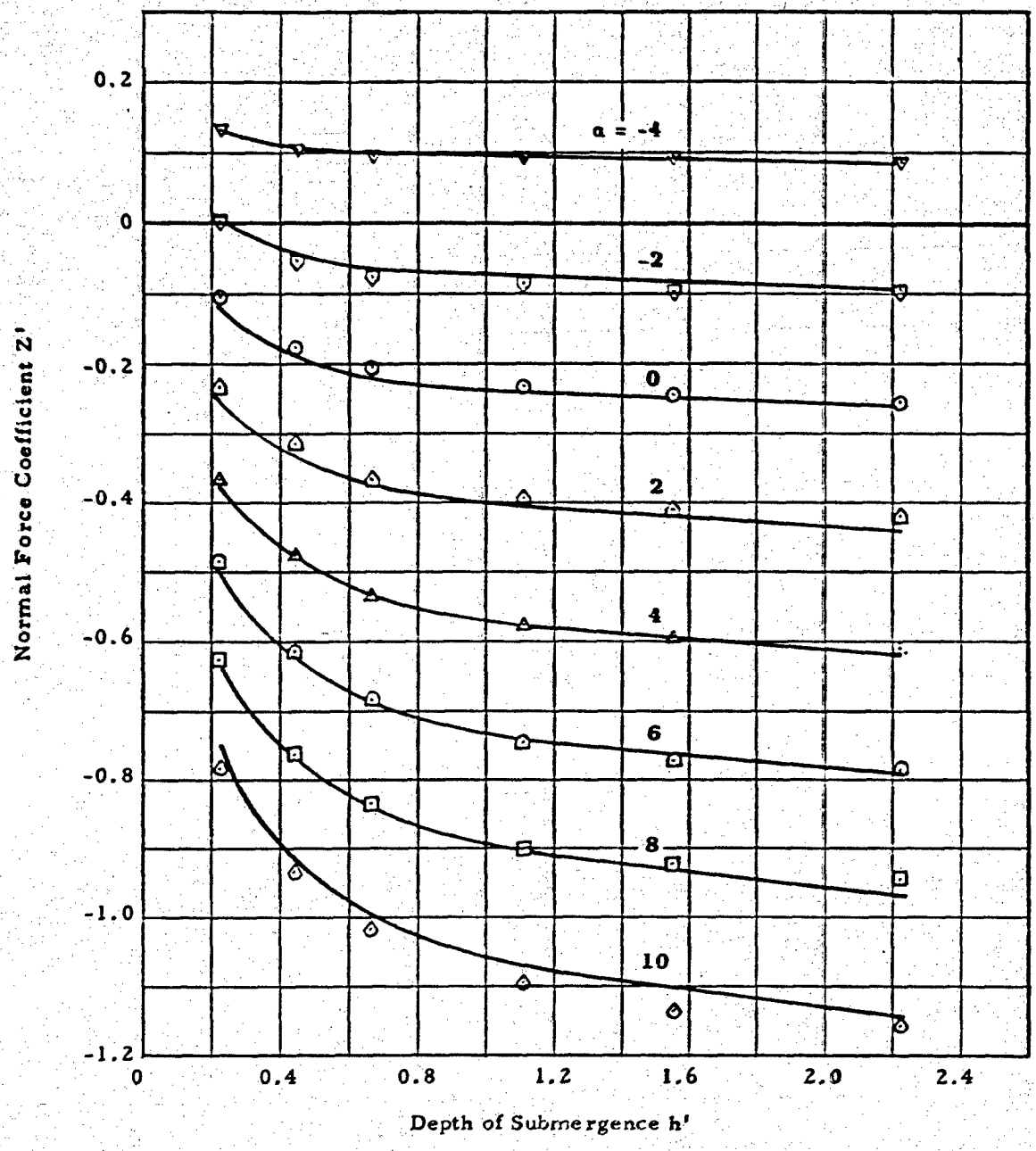

Figure 37 - Foil with Aspect Ratio of 2 Supported by Single Strut

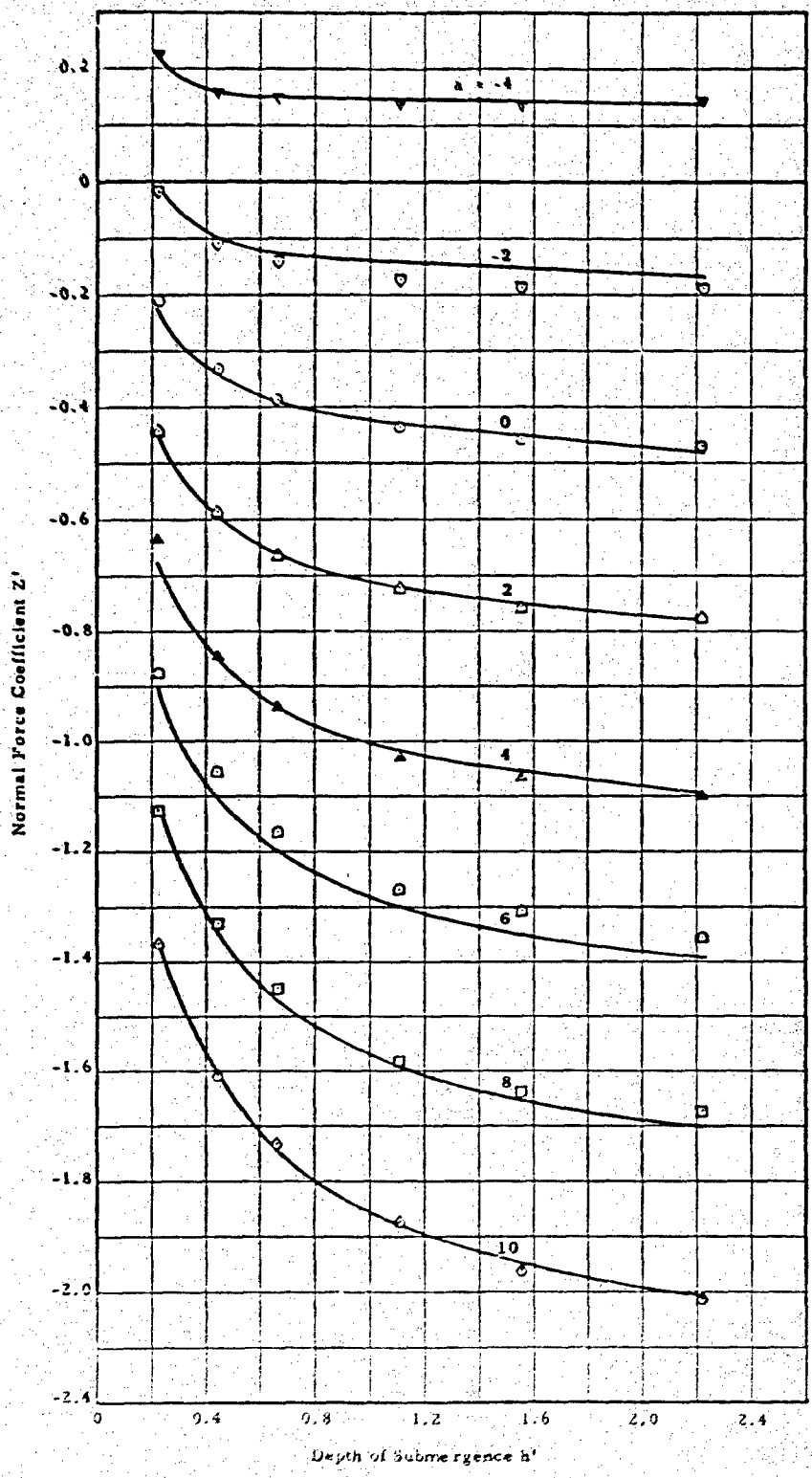

Figure 38 - Foil with Aspect Ratio of 3 Supported by Single Strut

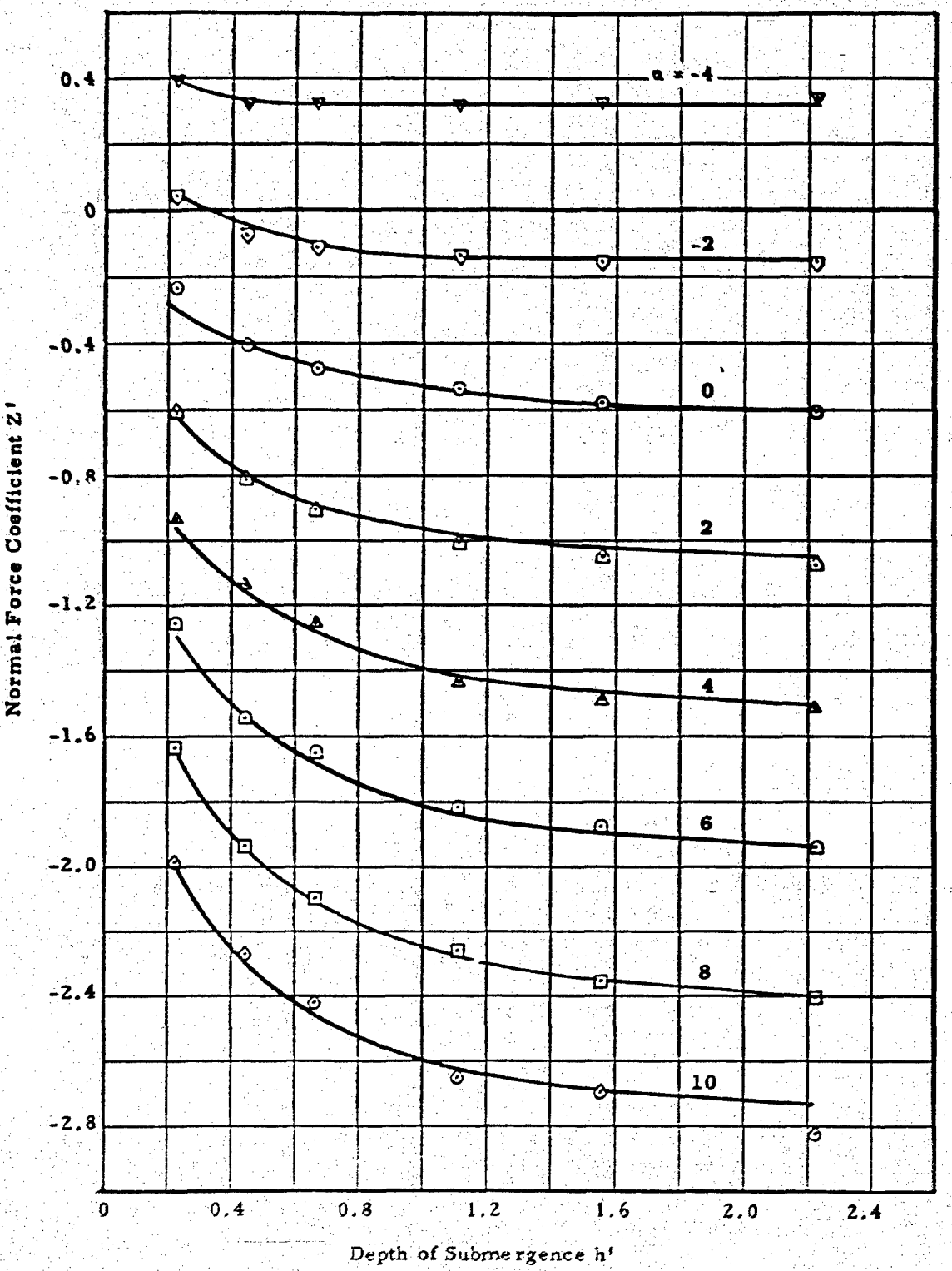

Figure 39 - Foil with Aspect Ratio of 4 Supported by Single Strut

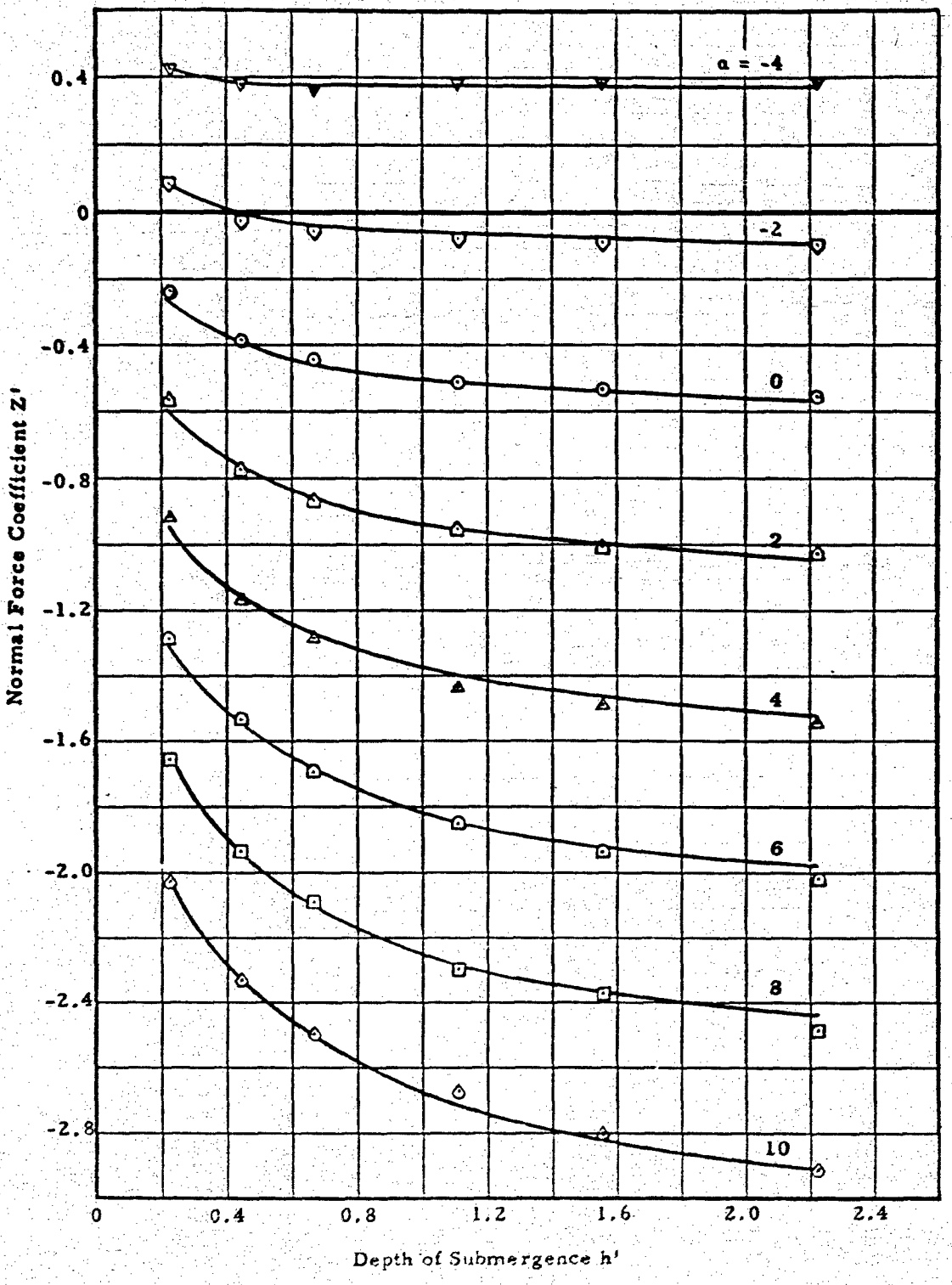

Figure 40 - Foil with Aspect Ratio of 4 Supported by Double Strut

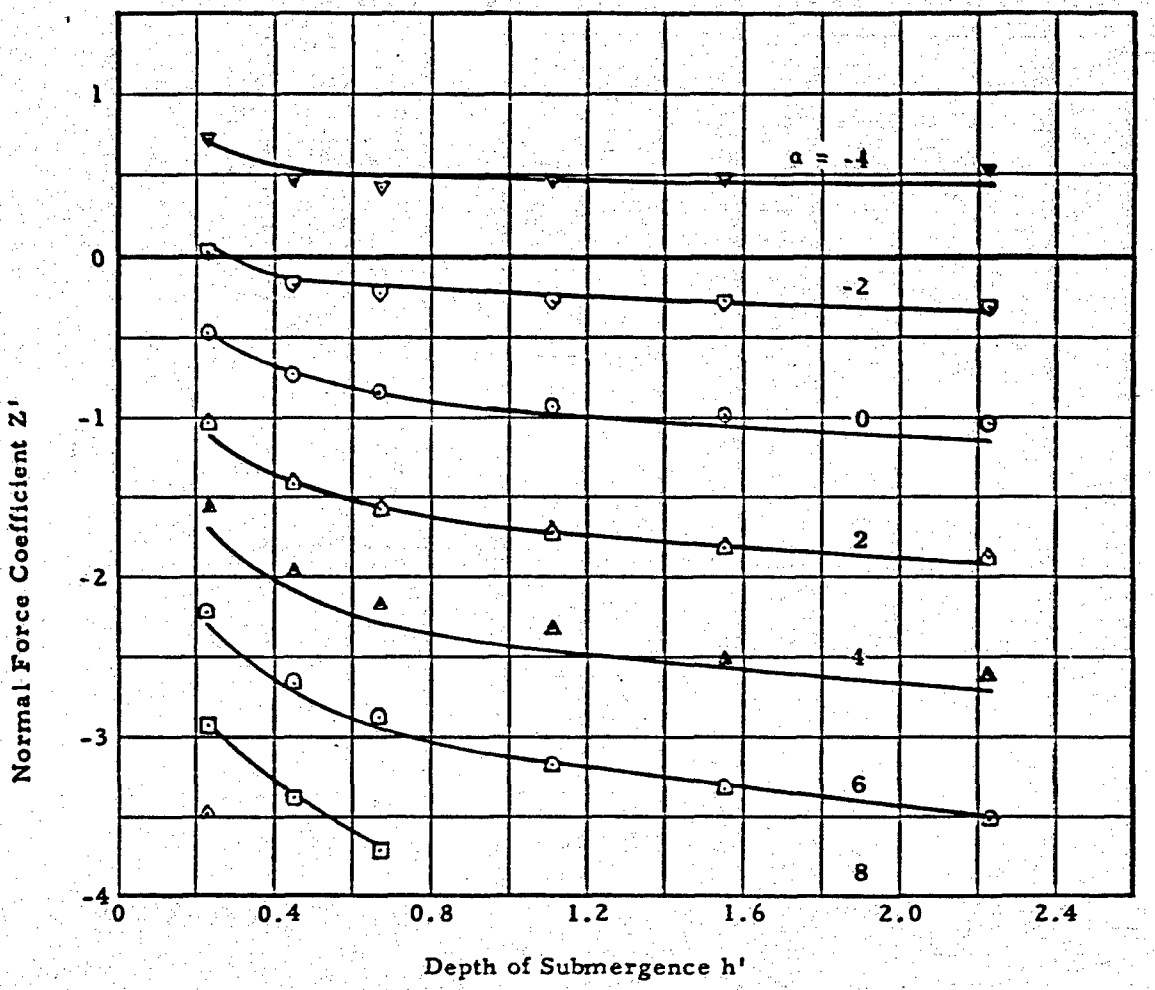

Figure 41 - Foil with Aspect Ratio of 6 Supported by Double Strut

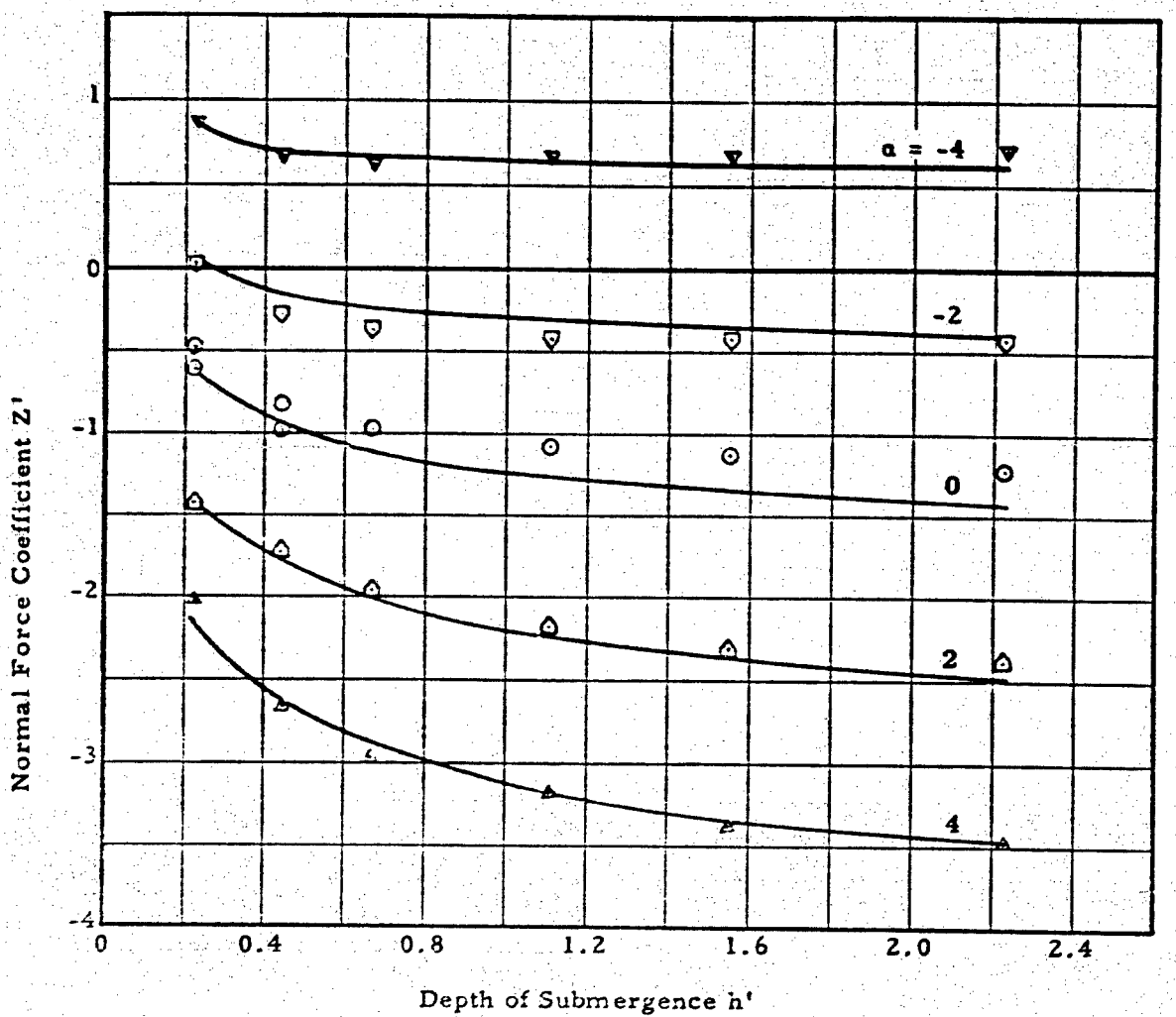

Figure 42 - Foil with Aspect Ratio of 3 Supported by Double Strut

APPENDIX C

NORMAL FORCE COEFFICIENTS FOR HYDROFOIL CONFIGURATION HAVING AN ASPECT RATIO OF 4 AT VARIOUS FROUDE NUMBERS AS A FUNCTION OF ANGLE OF ATTACK

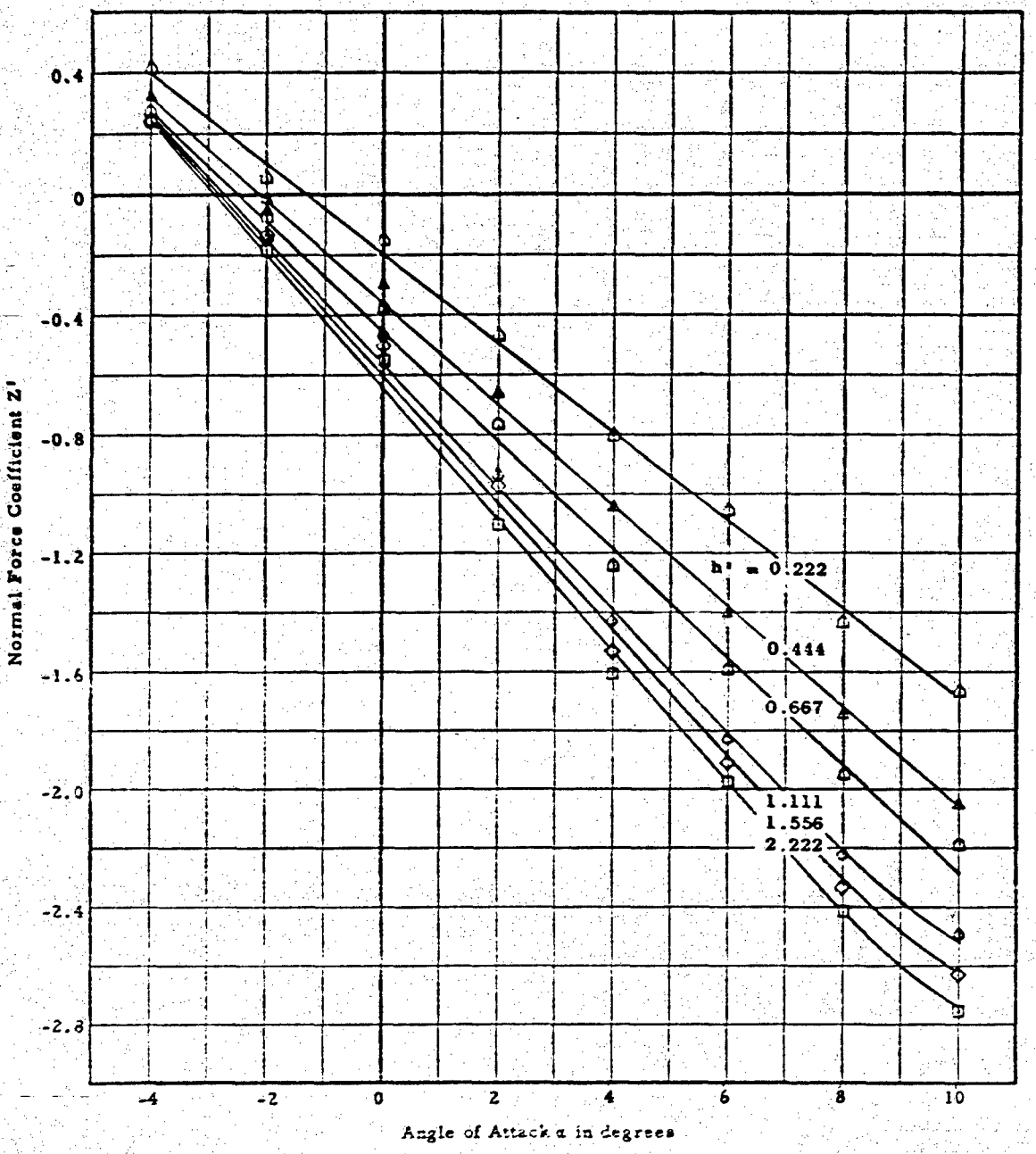

Figure 43 - Foil at Froude Number of 2.06 Supported by Single Strut

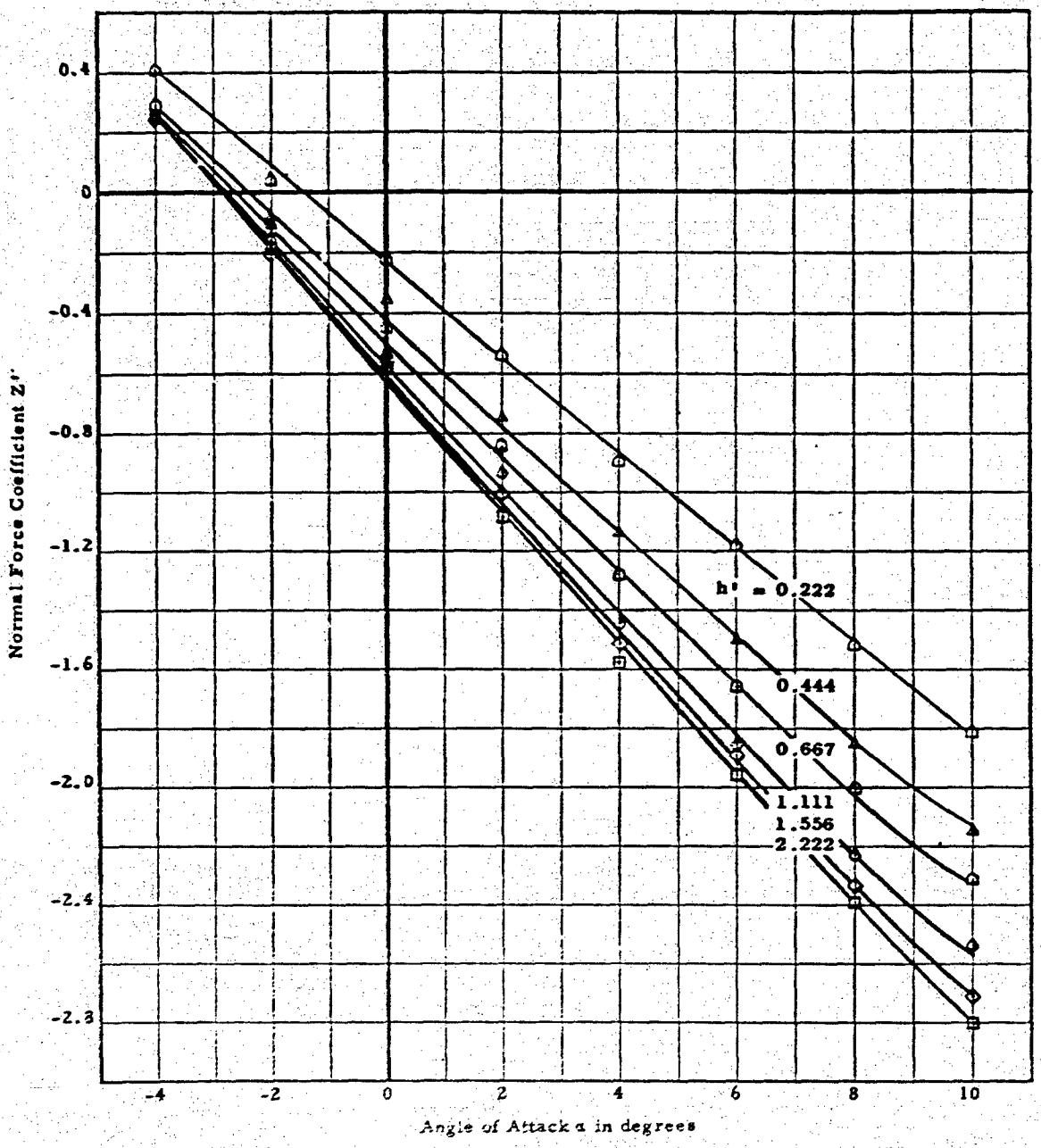

Figure 44 - Foil at Froude Number of 2.75 Supported by Single Strut

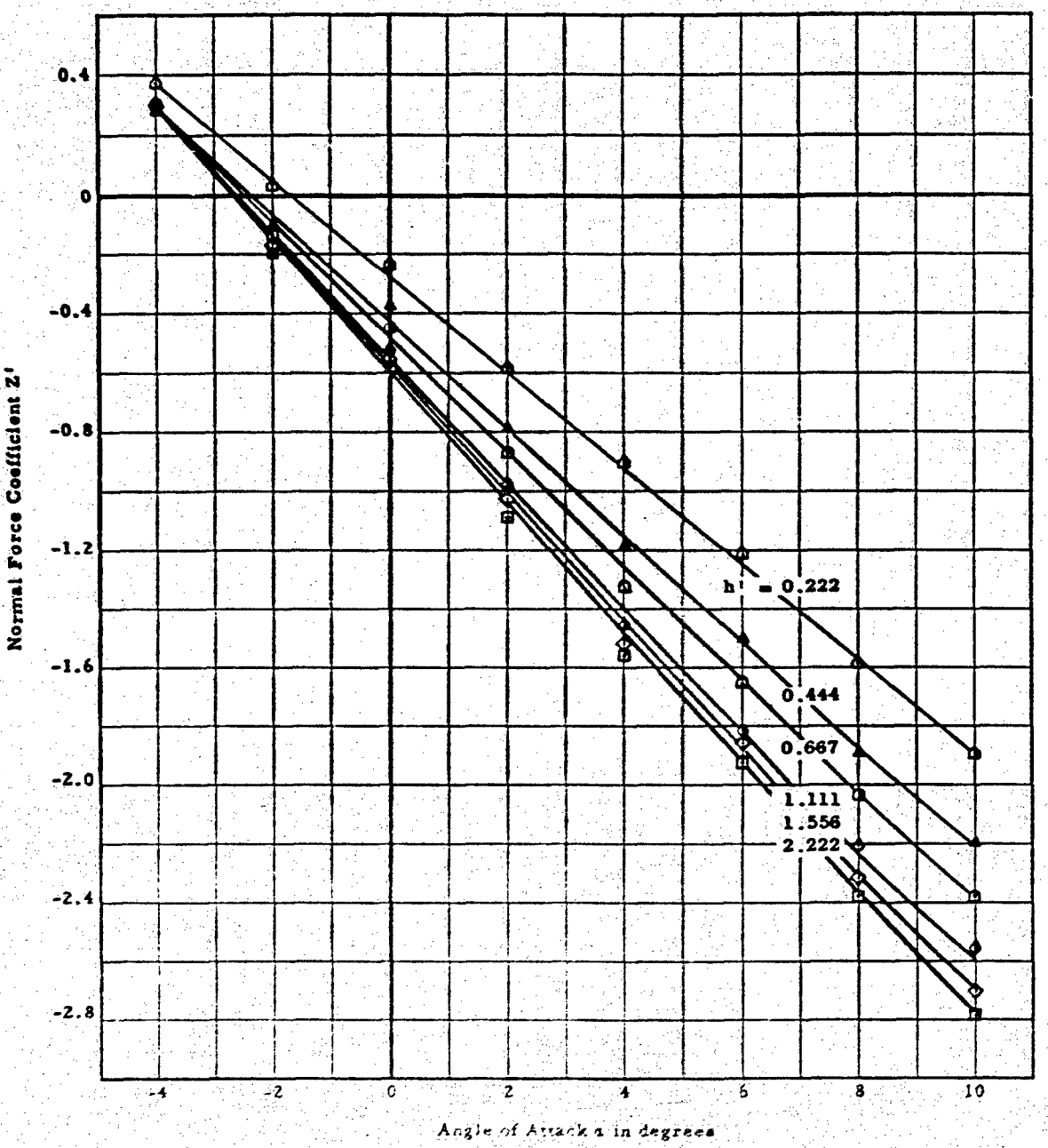

Figure 45 - Foil at Froude Number of 3.44 Supported by Single Strut

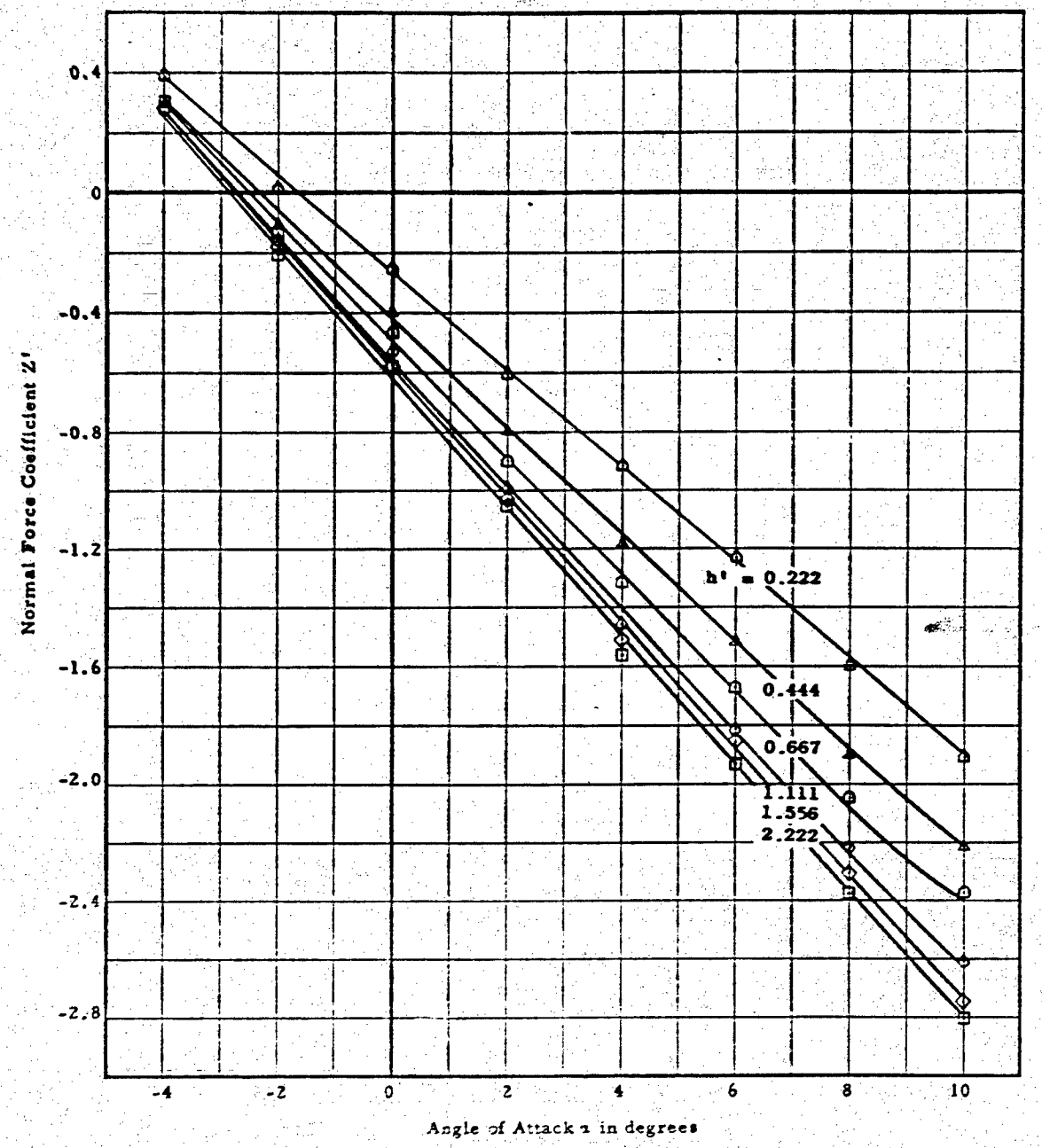

Figure 46 - Foil at Froude Number of 4.13 Supported by Single Strut

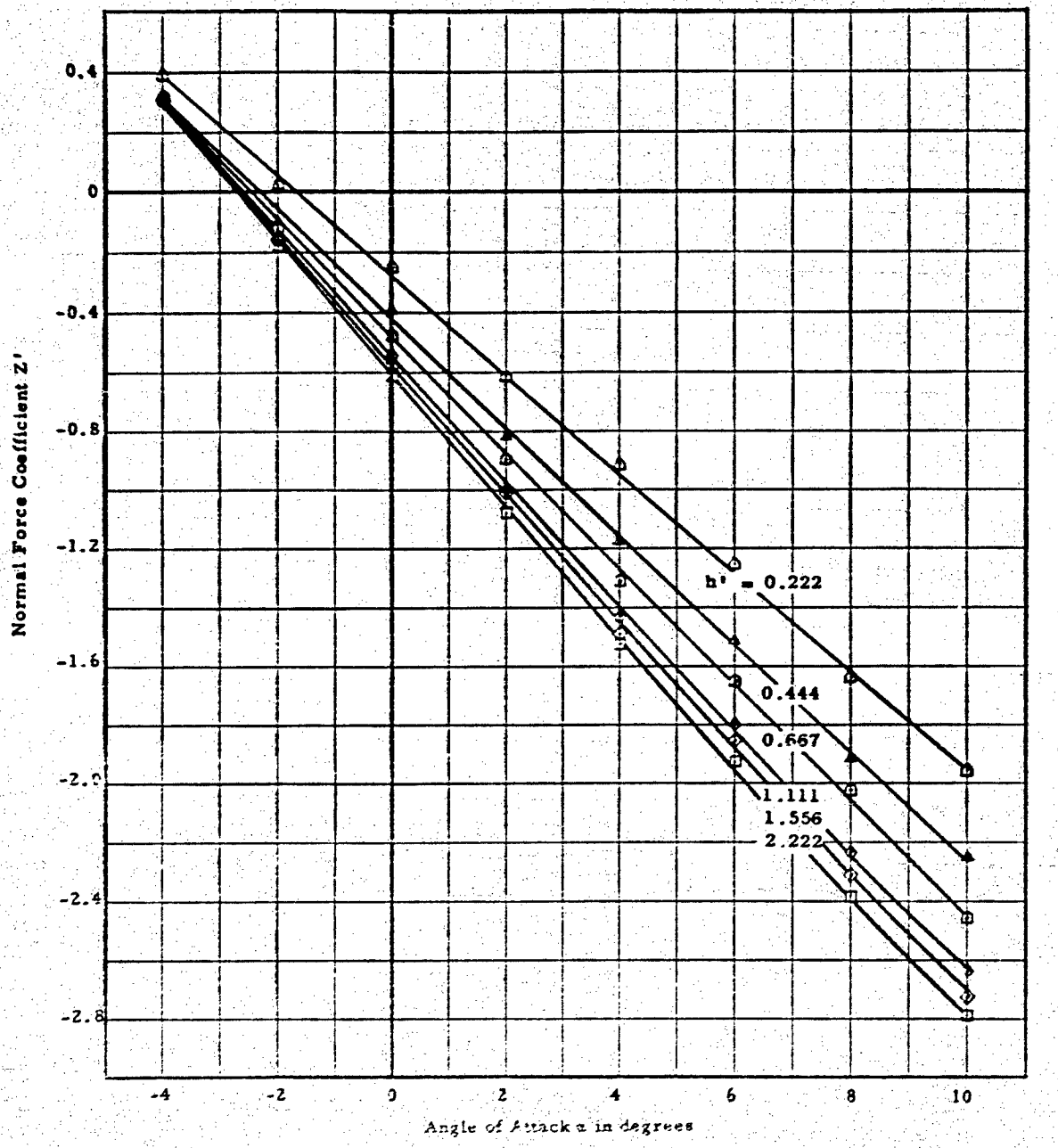

Figure 47 - Foil at Froude Number of 4.81 Supported by Single Strut

APPENDIX D

NORMAL FORCE COEFFICIENTS FOR HYDROFOIL CONFIGURATION HAVING AN ASPECT RATIO OF 4 AT VARIOUS FROUDE NUMBERS AS A FUNCTION OF SUBMERGENCE

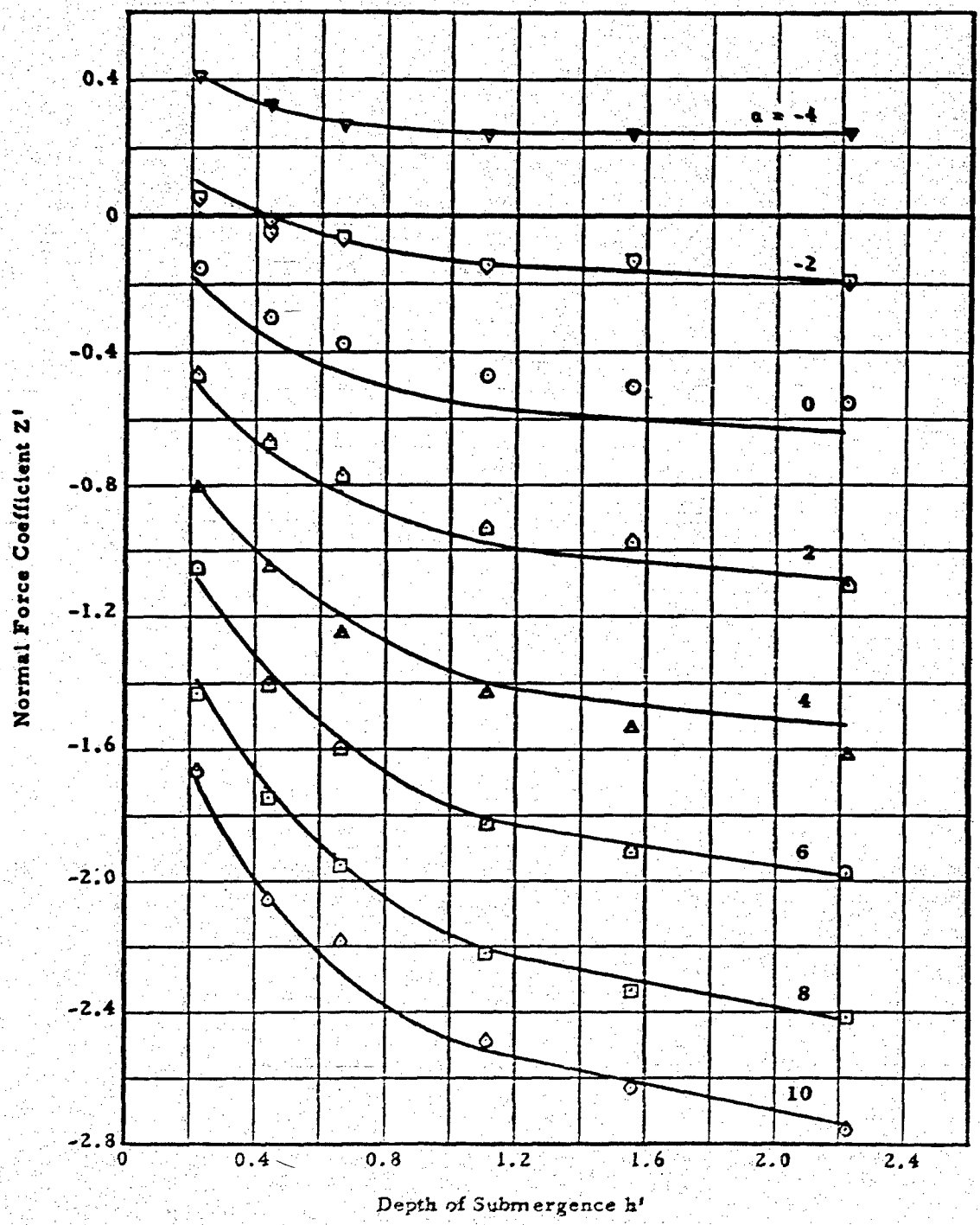

Figure 48 - Foil at Froude Number of 2.06 Supported by Single Strut

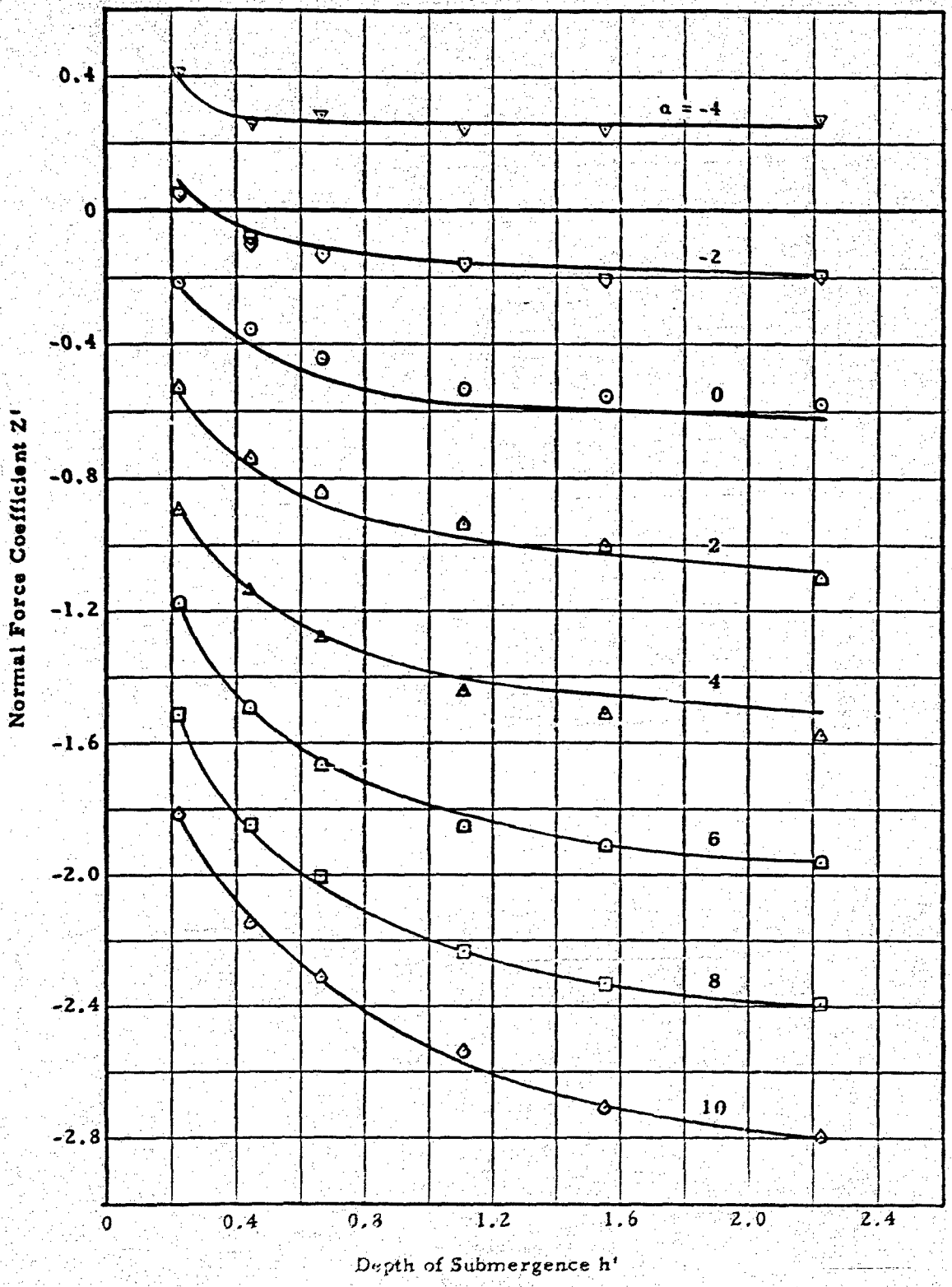

Figure 49 - Foil at Froude Number of 2.75 Supported by Single Strut

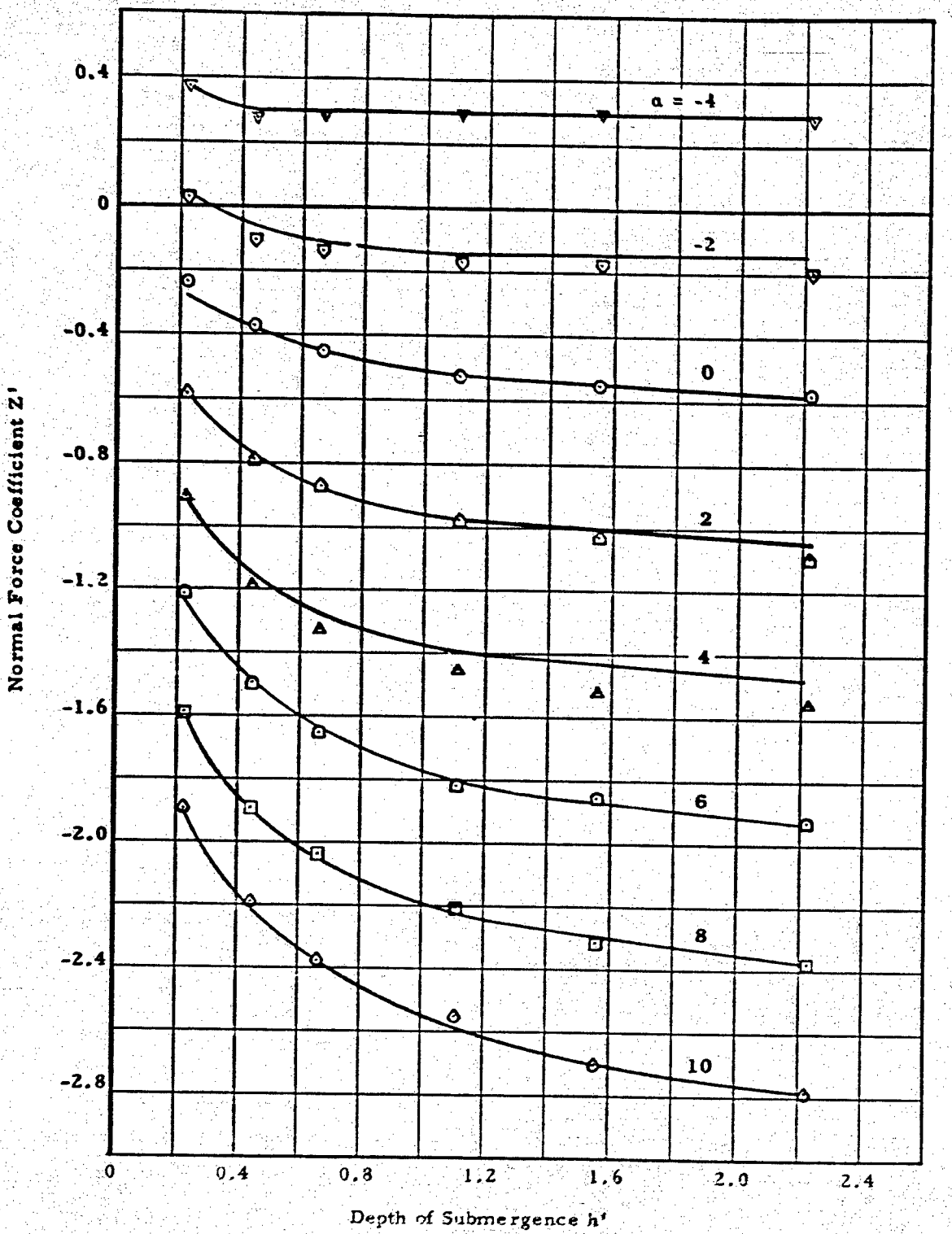

Figure 50 - Foil at Froude Number of 3.44 Supported by Single Strut

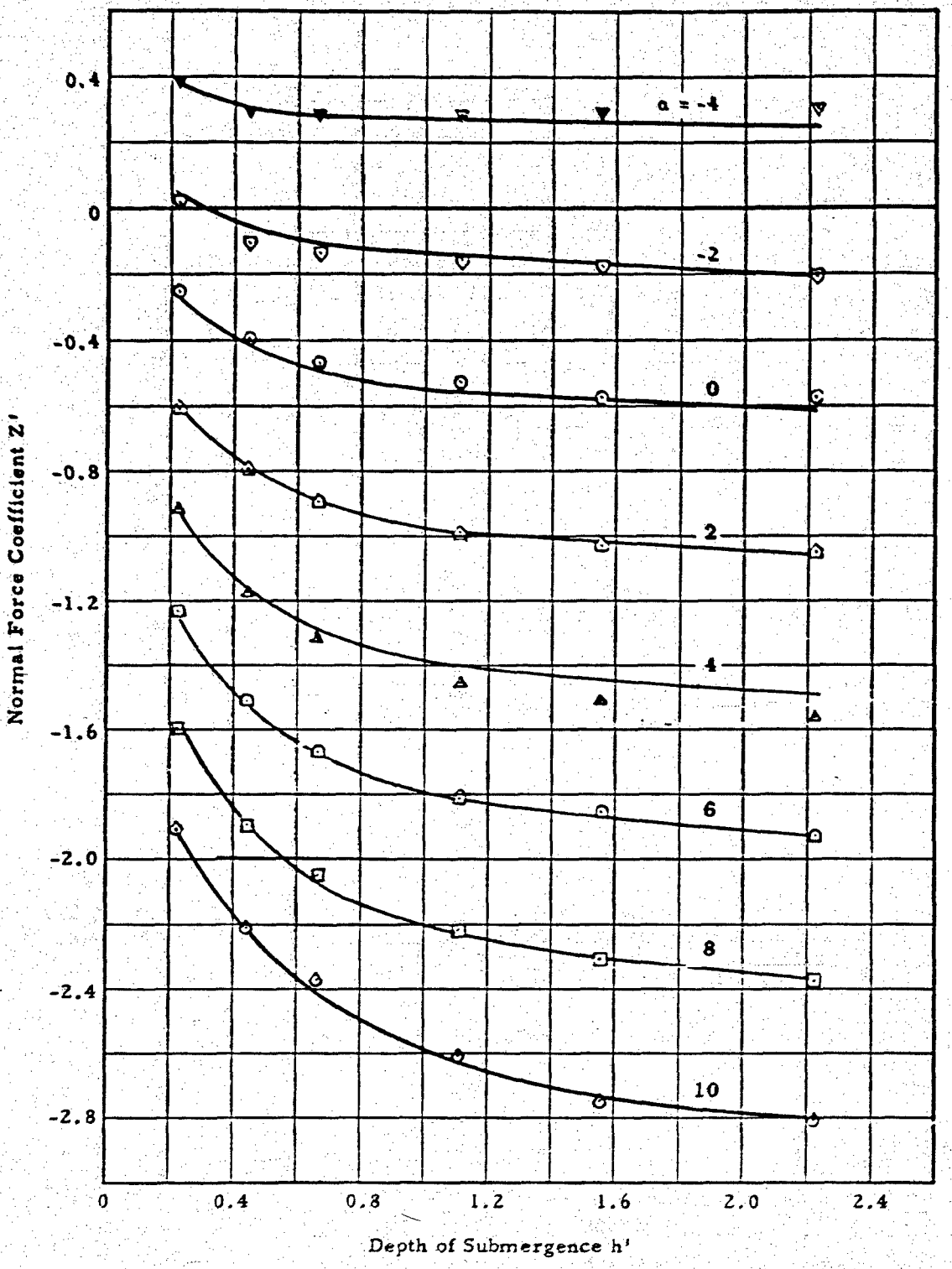

Figure 51 - Foil at Froude Number of 4.13 Supported by Single Strut

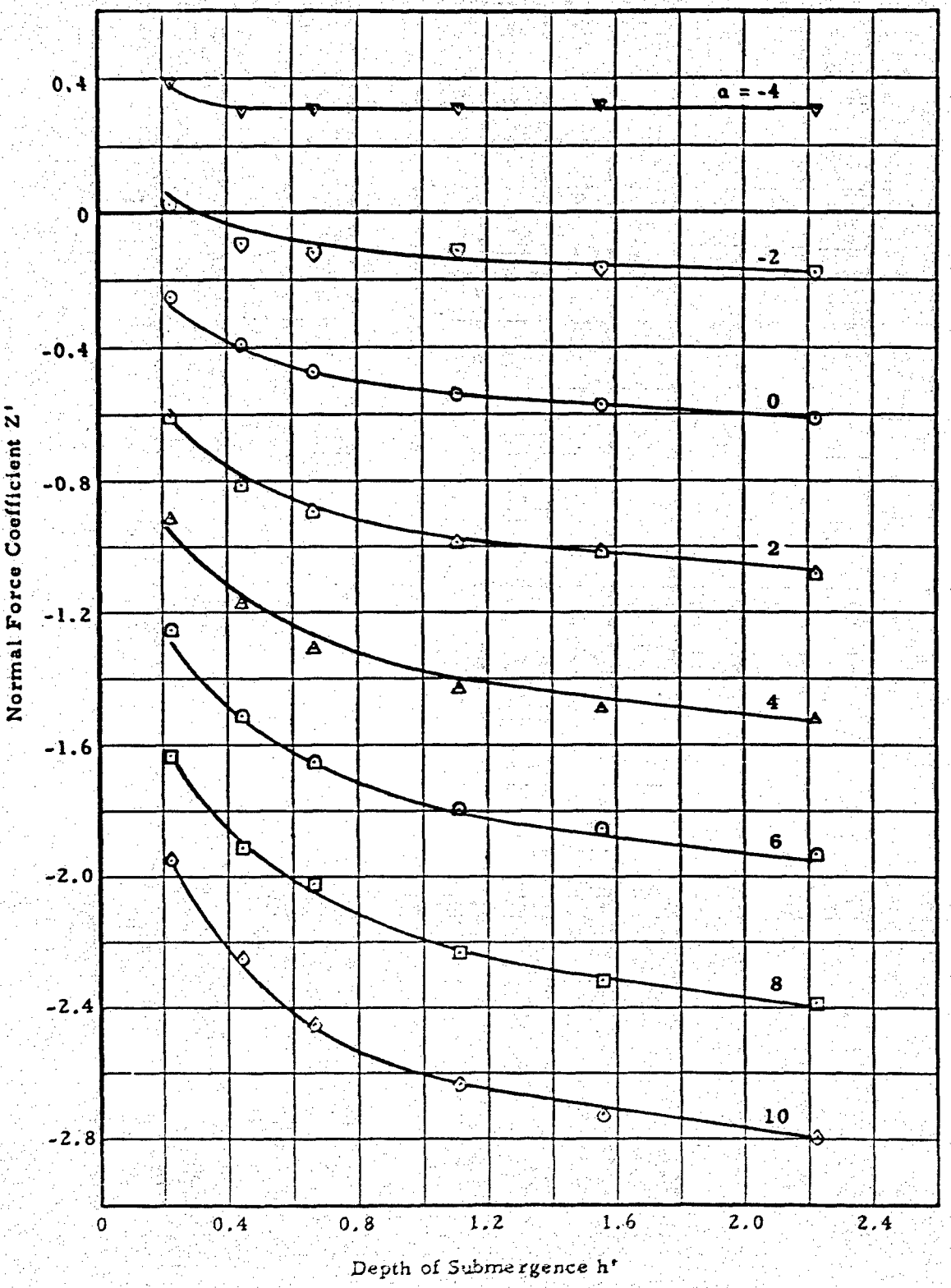

Figure 32 - Foil at Froude Number of 4.81 Supported by Single Strut

APPENDIX E

LONGITUDINAL FORCE COEFFICIENTS FOR INDIVIDUAL CONFIGURATONS OF TMB SERIES HF-1 AT A FROUDE NUMBER OF 5.50 AS A FUNCTION OF ANGLE OF ATTACK

The coefficients in this appendix apply strictly to a Reynolds Number of 1.87×10^6 and a Froude Number of 5.50 but can be amended for higher values of these parameters using the method outlined in the text.

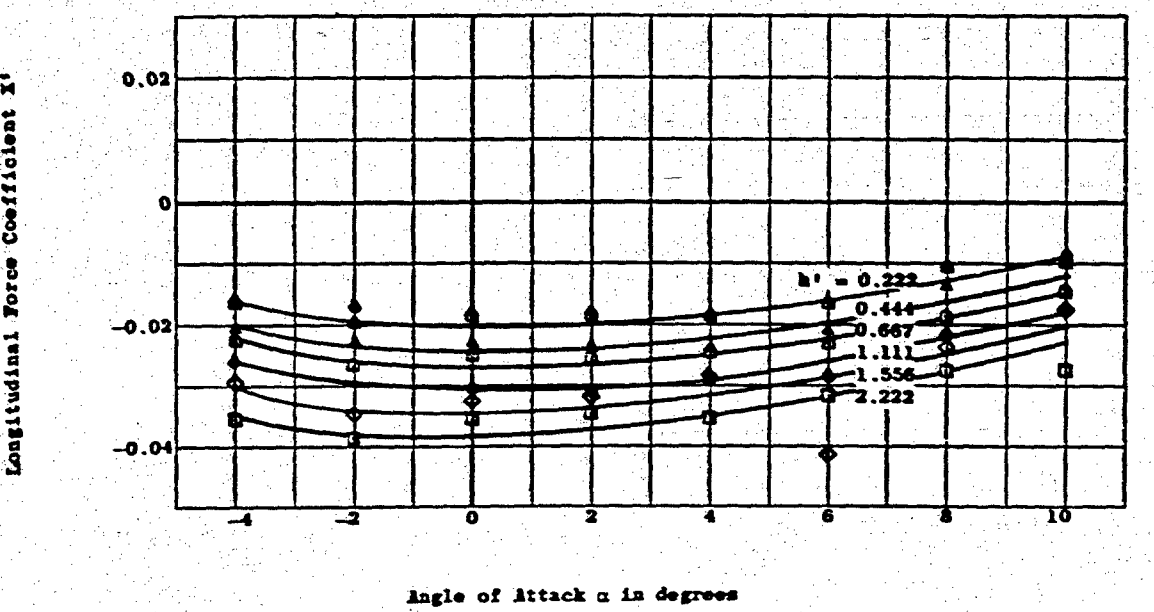

Figure 53 - Foil with Aspect Ratio of 1 Supported by Single Strut

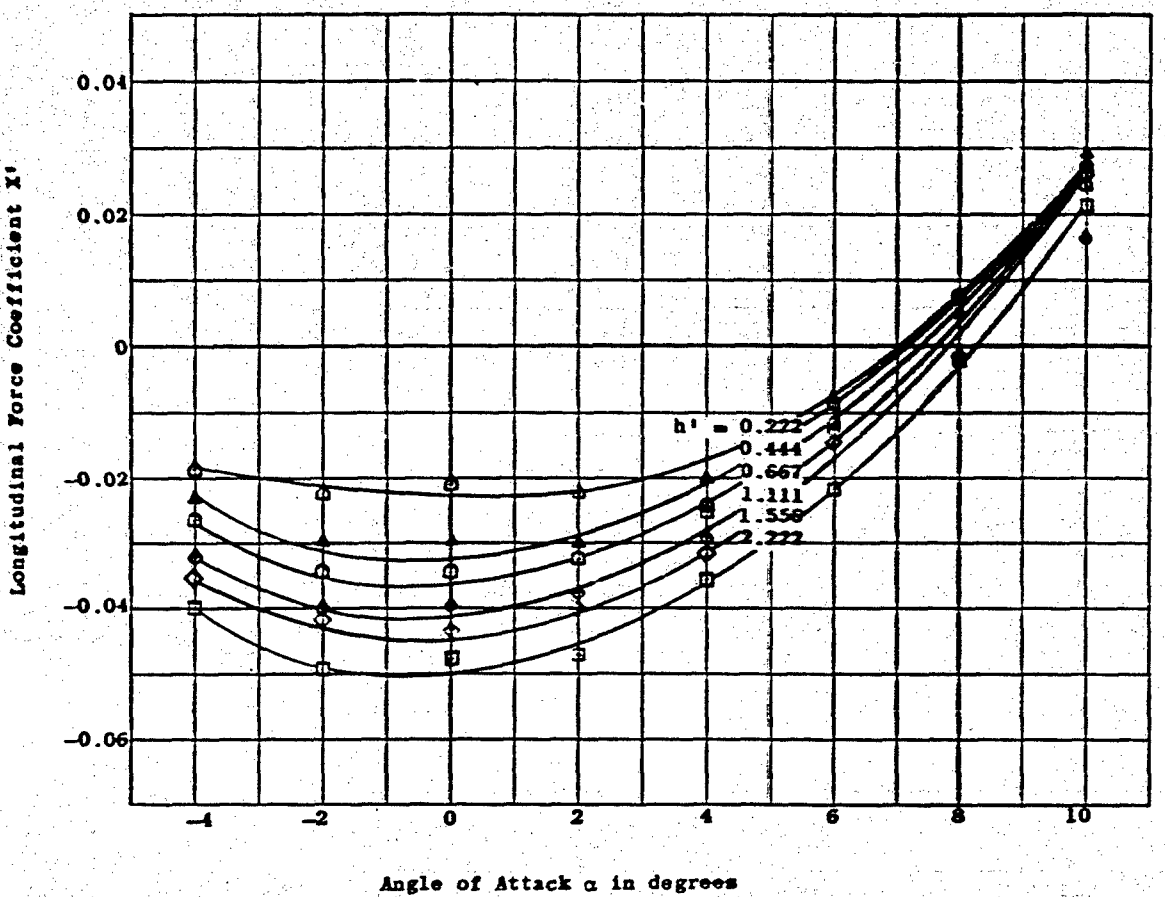

Figure 54 - Foil with Aspect Ratio of 2 Supported by Single Strut

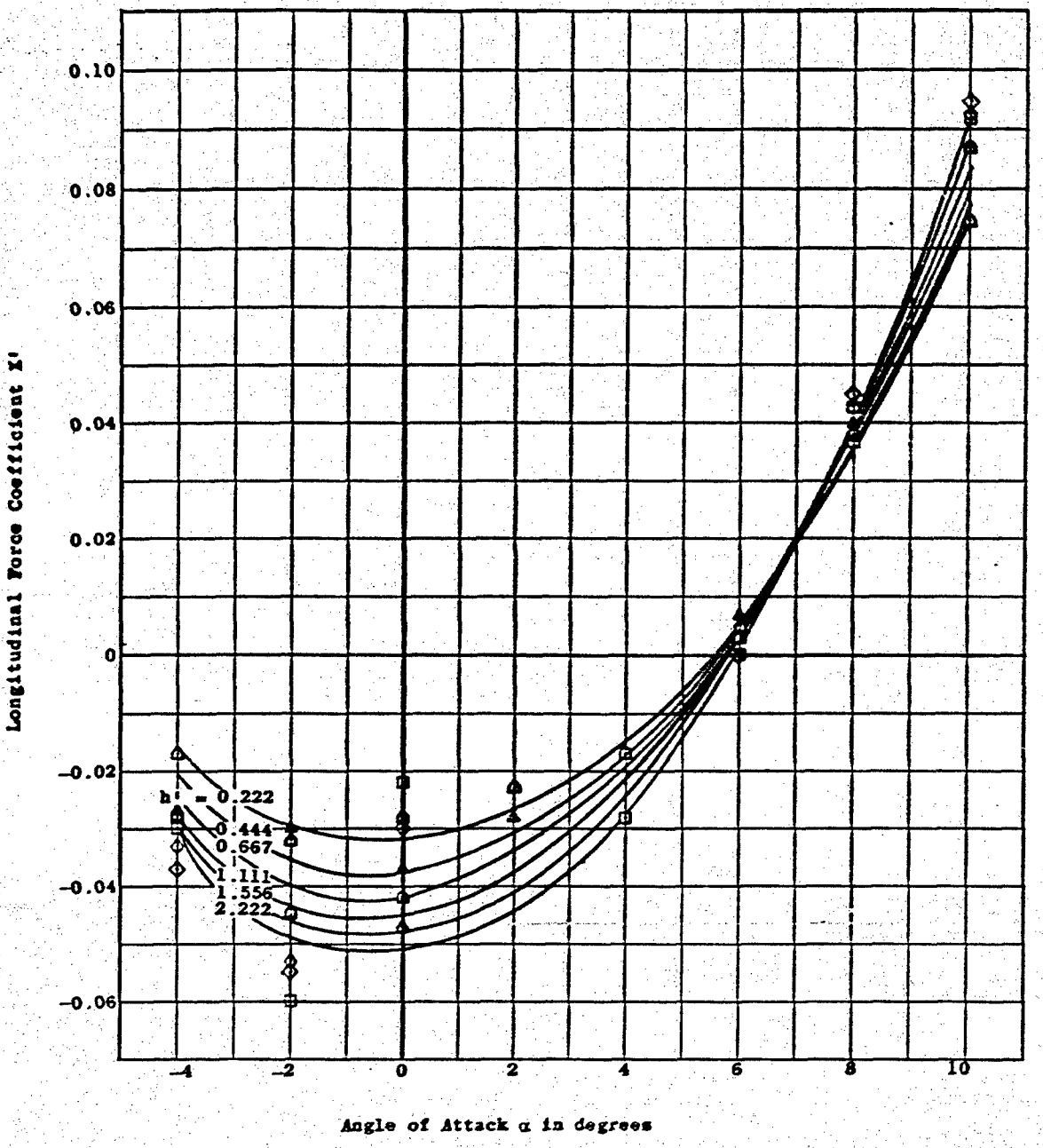

Figure 55 - Foil with Aspect Ratio of 3 Supported by Single Strut

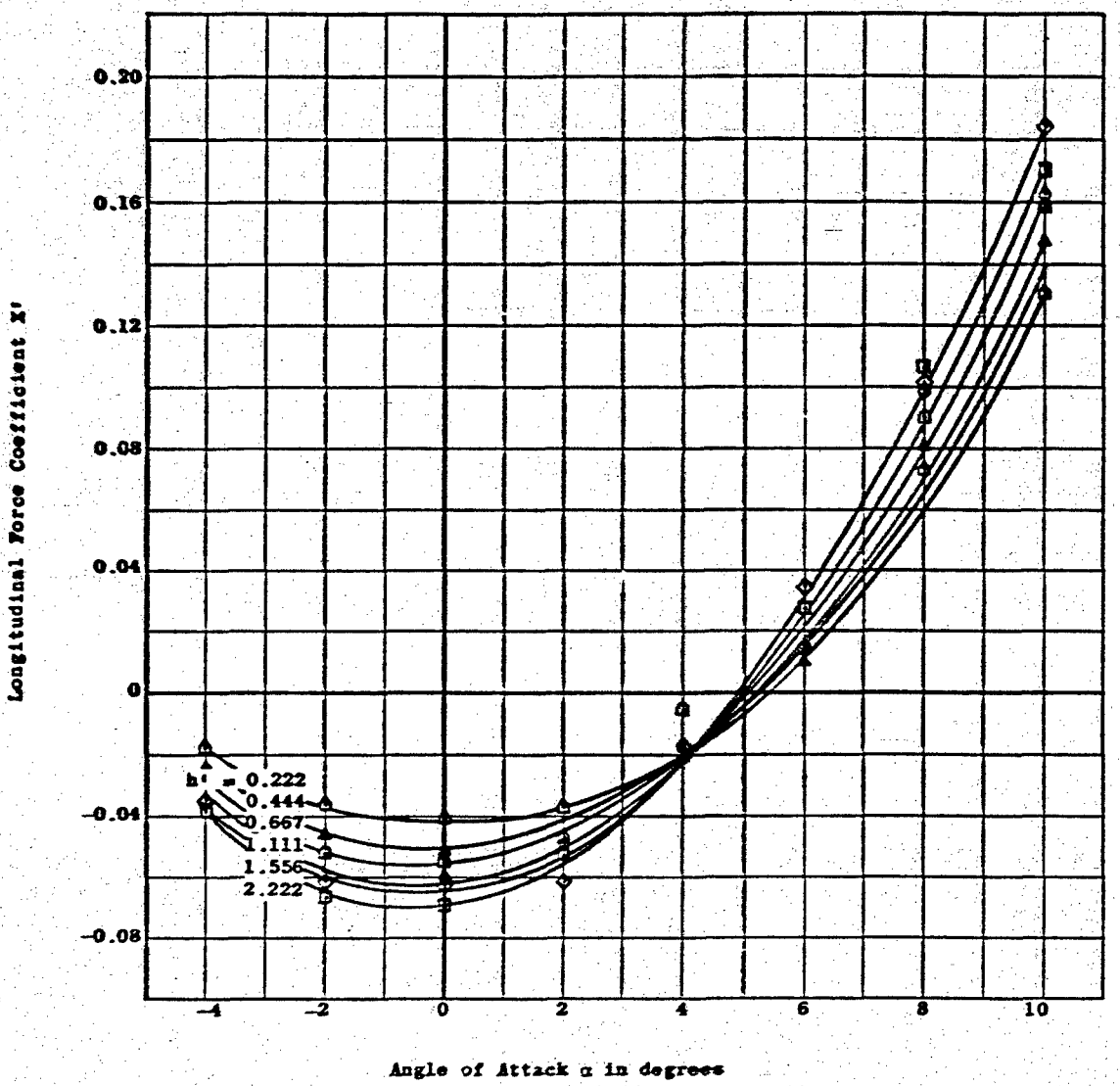

Figure 56 - Foil with Aspect Ratio of 4 Supported by Single Strut

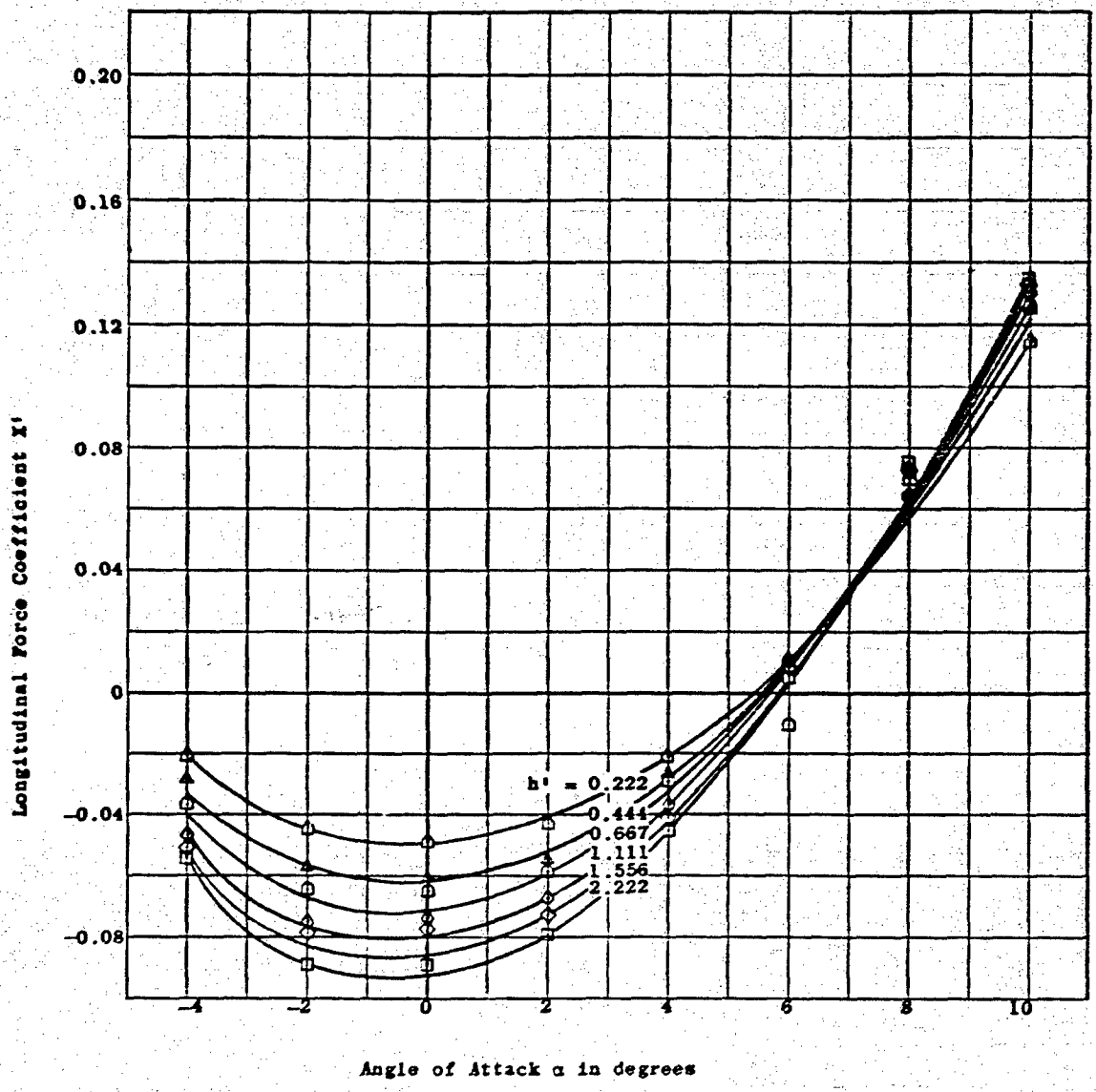

Figure 57 - Foil with Aspect Ratio of 4 Supported by Double Strut

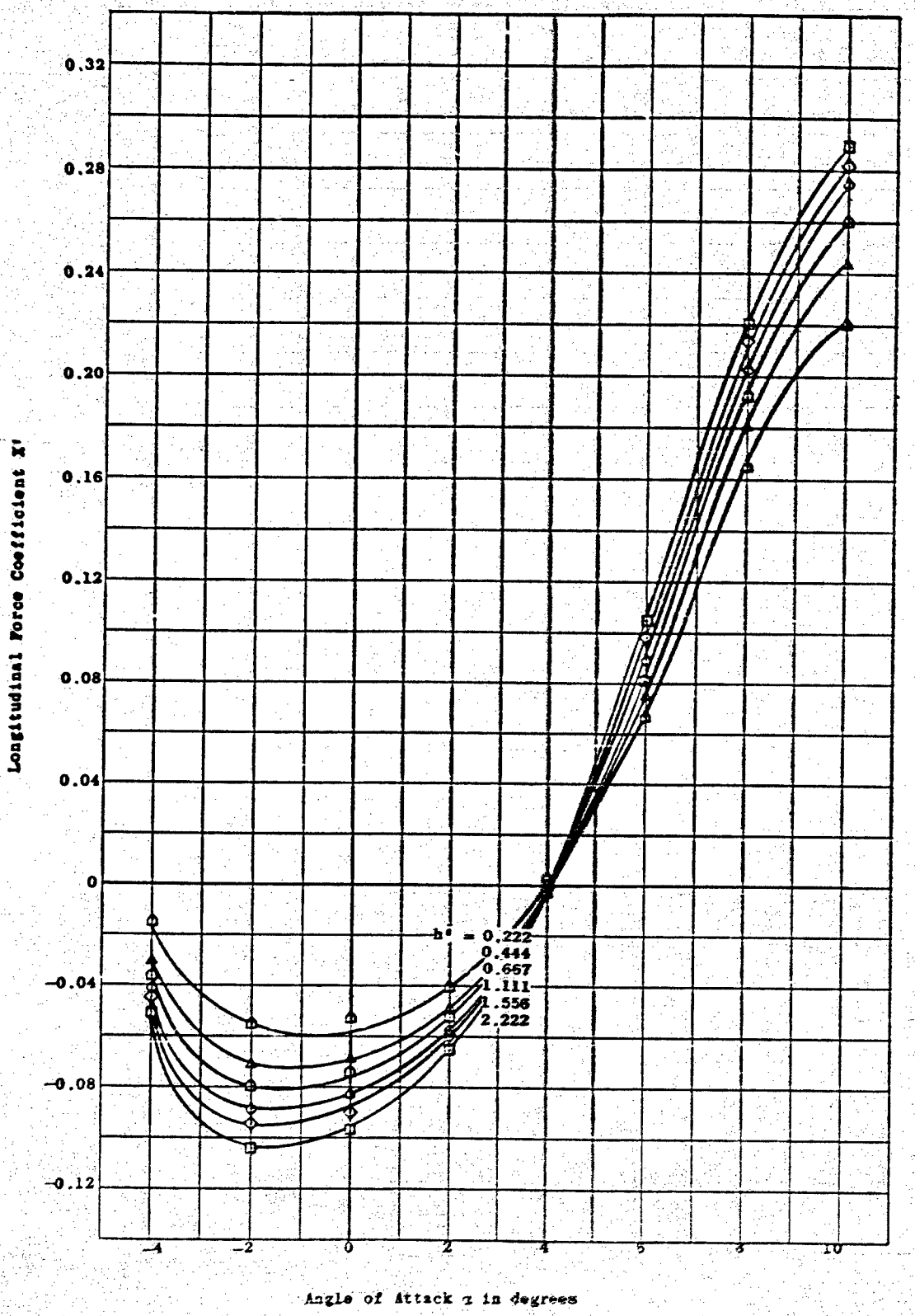

Figure 58 - Foil with Aspect Ratio of 6 Supported by Double Strut

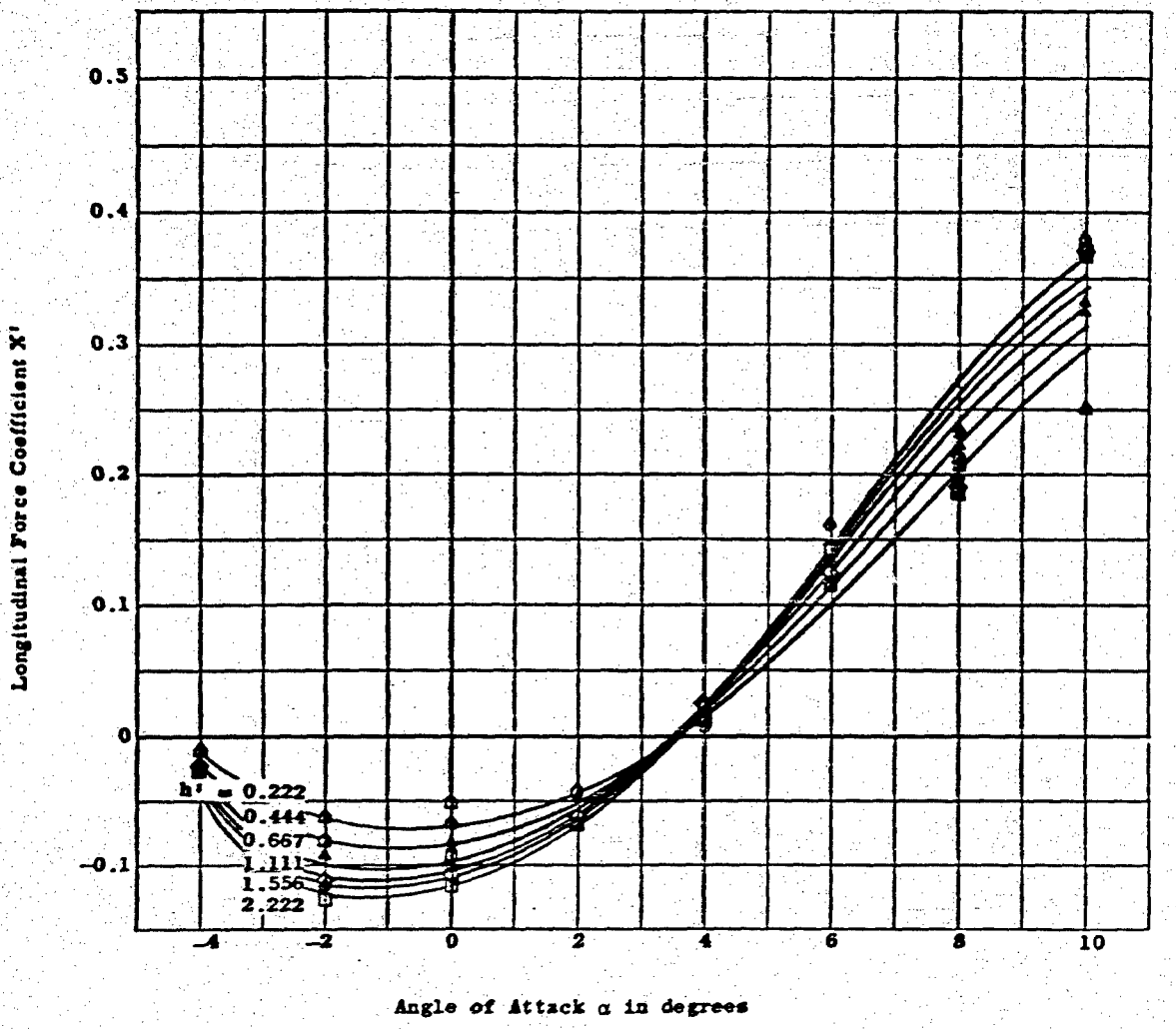

Figure 59 - Foil with Aspect Ratio of 3 Supported by Double Strut

APPENDIX F

LONGITUDINAL FORCE COEFFICIENTS FOR INDIVIDUAL CONFIGURATIONS OF TMB SERIES HF-1 AT A FROUDE NUMBER OF 5.50 AS A FUNCTION OF SUBMERGENCE

The coefficients in this appendix apply strictly to a Reynolds Number of 1.87×10^6 and a Froude Number of 5.50 but can be amended for higher values of these parameters using the method outlined in the text.

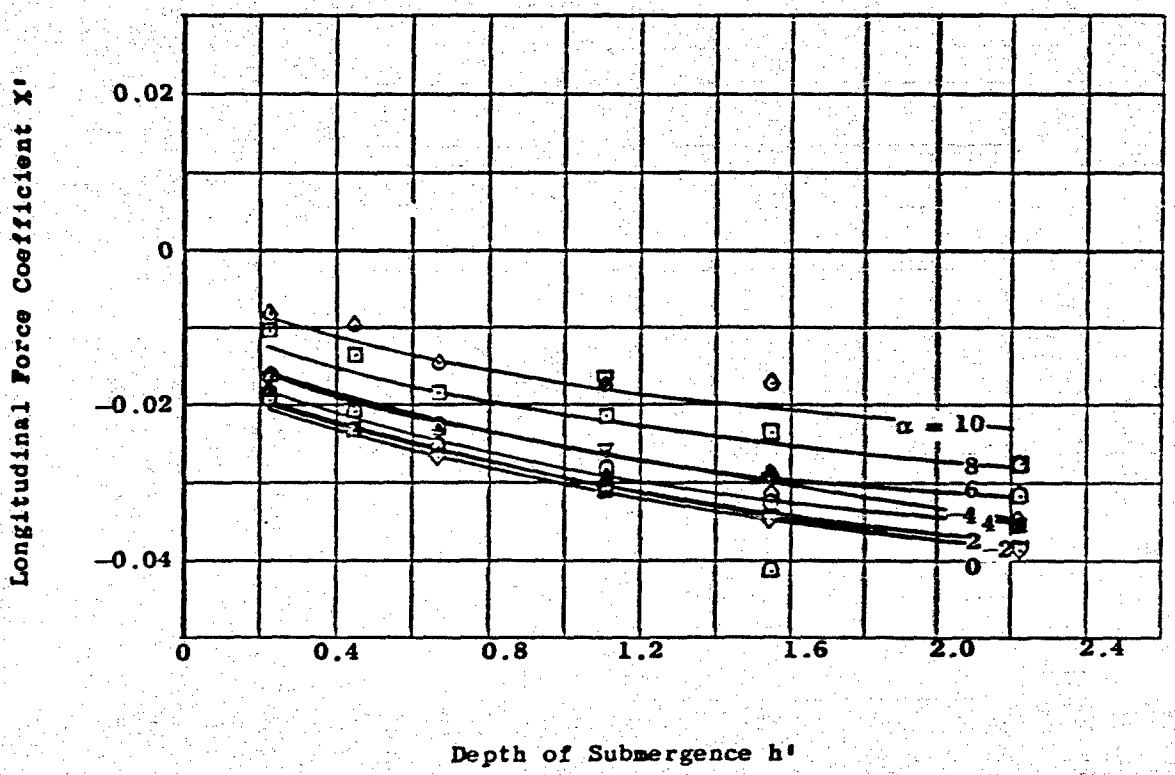

Figure 60 - Foil with Aspect Ratio of 1 Supported by Single Strut

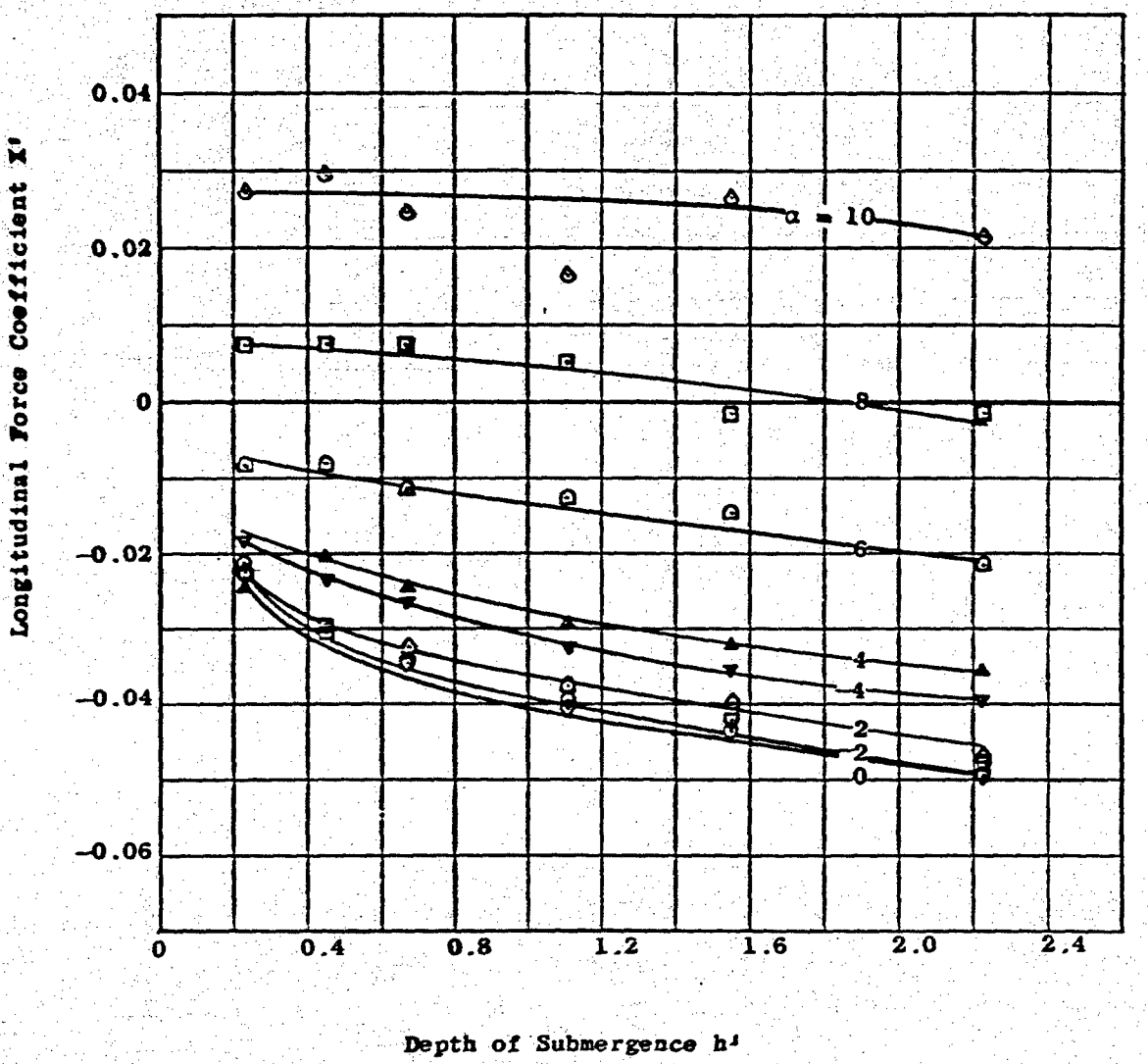

Figure 61 - Foil with Aspect Ratio of 2 Supported by Single Strut

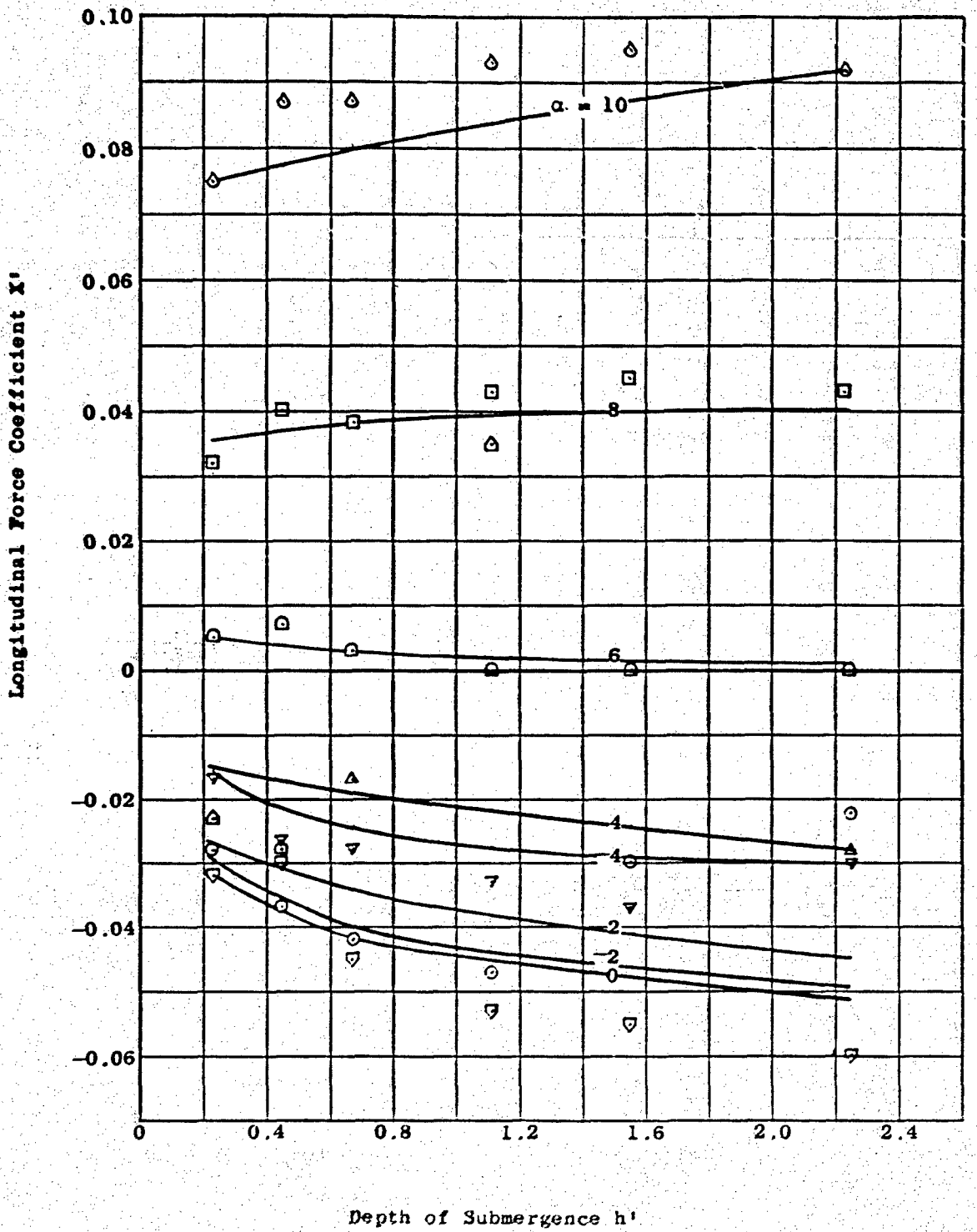

Figure 62 - Foil with Aspect Ratio of 3 Supported by Single Strut

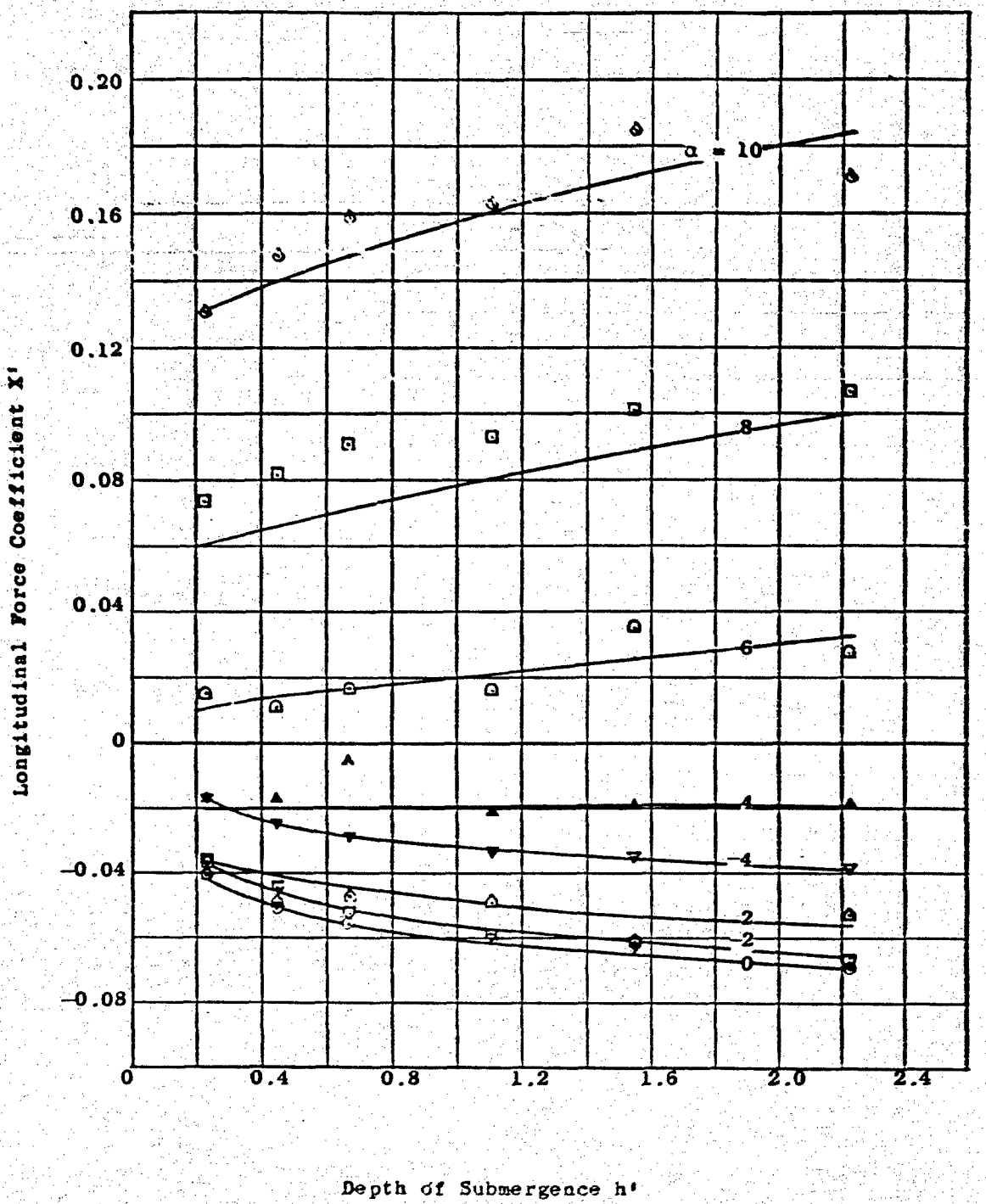

Figure 63 - Foil with Aspect Ratio of 4 Supported by Single Strut

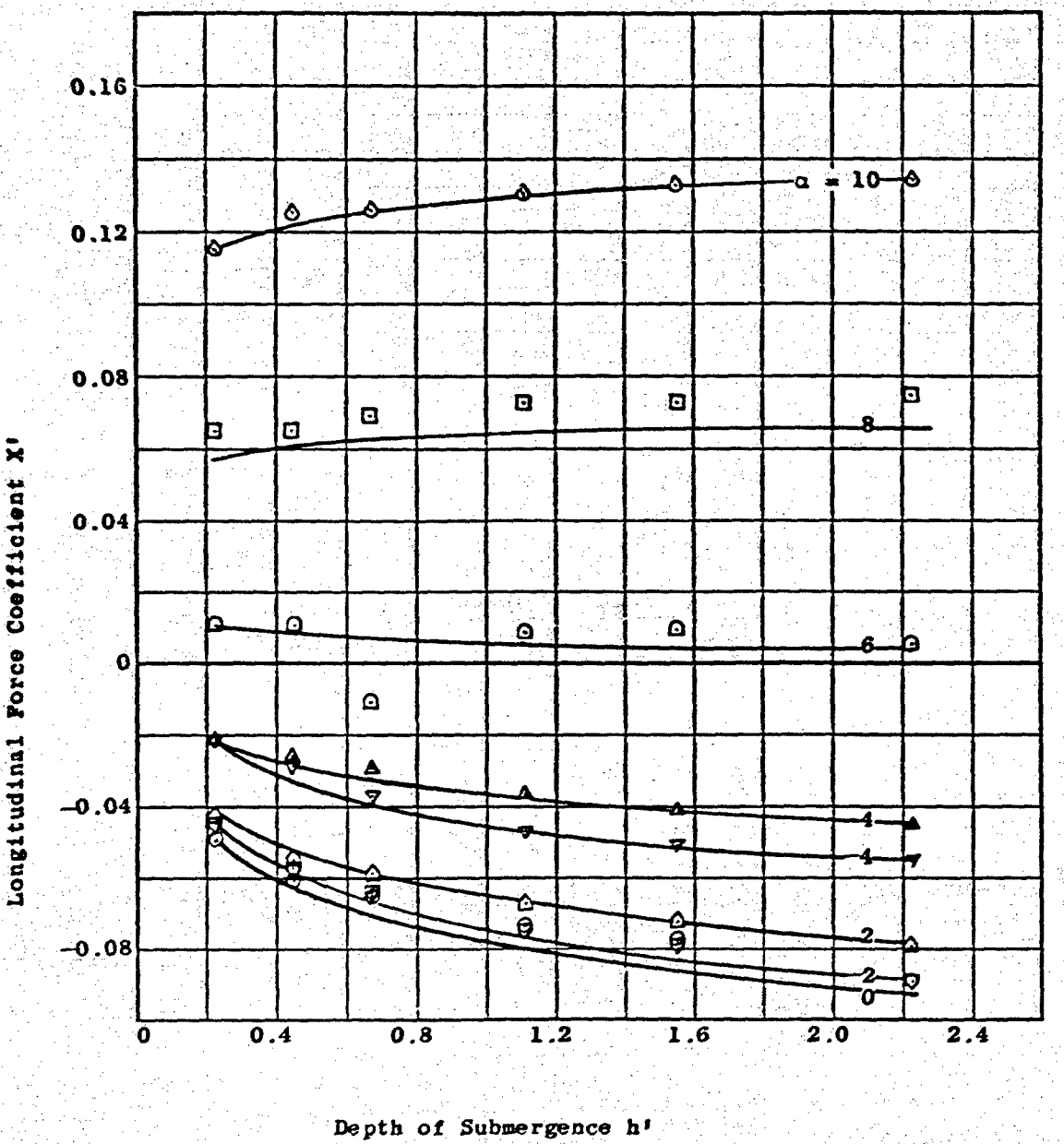

Figure 64 - Foil with Aspect Ratio of 4 Supported by Double Strut

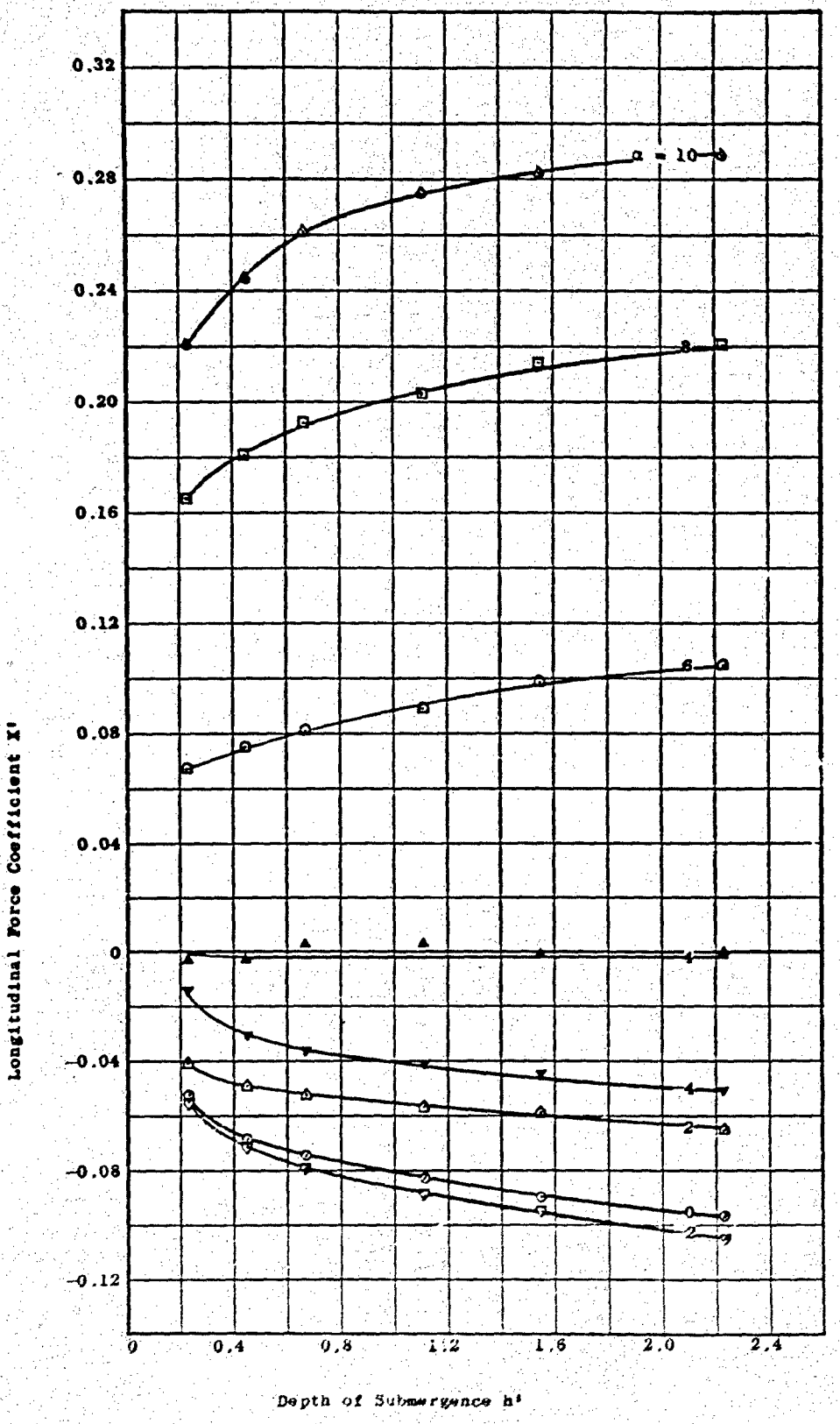

Figure 65 - Foil with Aspect Ratio of 6 Supported by Double Strut

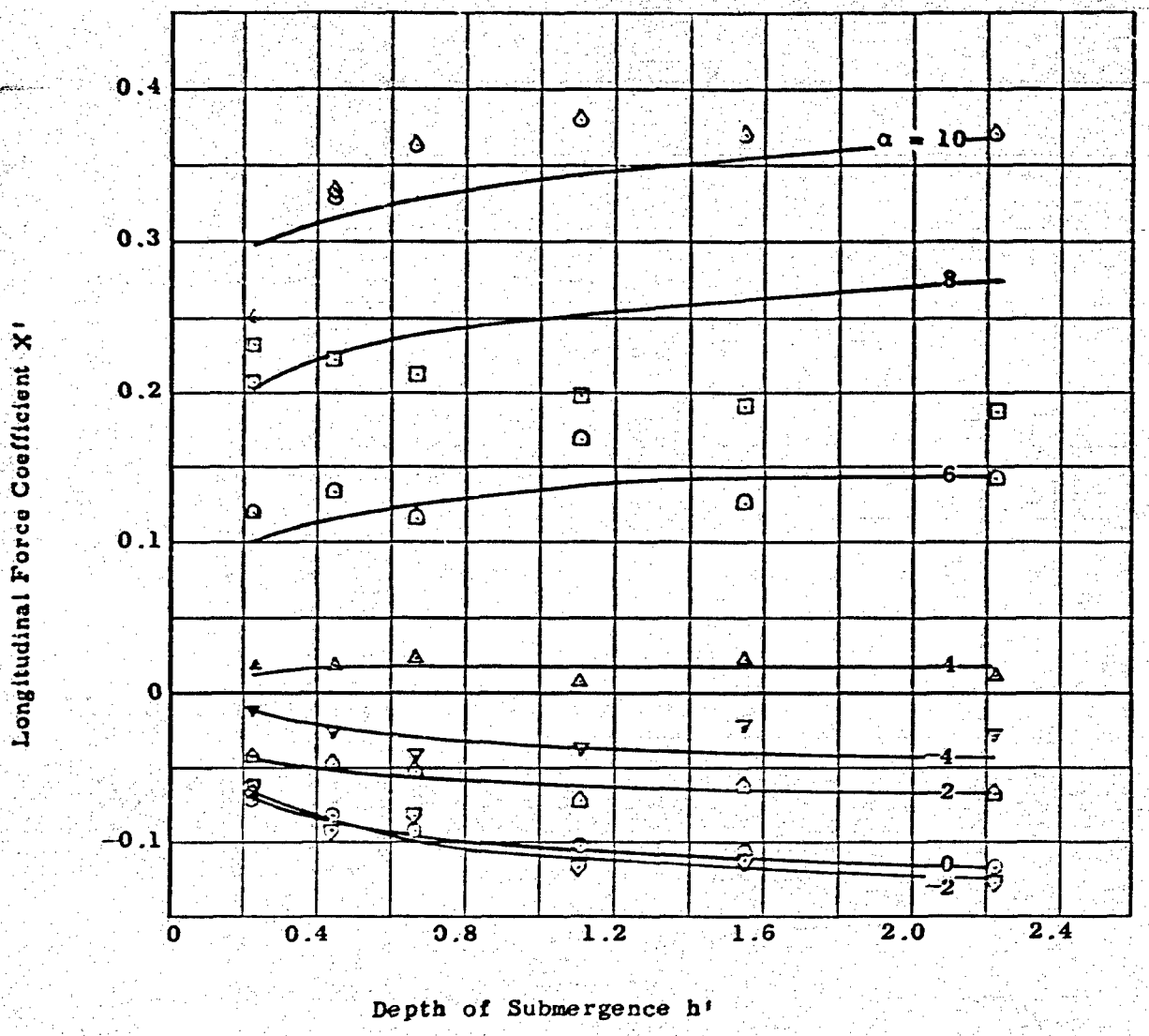

Figure 66 - Foil with Aspect Ratio of 3 Supported by Double Strut

REFERENCES

1. Stability and Control Division Memorandum to Technical Director, Hydromechanics Laboratory, David Taylor Model Basin of 25 July 1960, "High-Speed Hydrofoil Craft-Hydrodynamic Research Program of the Stability and Control Division."

2. Gertler, Morton, "The DTMB Planar-Motion-Mechanism System," Prepared for the Symposium on the Towing Tank Facilities on the occasion of the official opening of the Shipbuilding Research Institute, Zagreb, September 1960.

3. Wolff, John H., "Model Investigation of the Stability and Control Characteristics of PC(H)," David Taylor Model Basin Report C-1258 (March 1961) CONFIDENTIAL.

4. Goodman, Alex, "Experimental Techniques and Methods of Analysis used in the Submerged Body Research," Paper Presented before the Third Symposium on Naval Hydrodynamics, Scheveningen, Holland, 19 to 21 September 1960.

5. Wu, Y.T., "A Theory for Hydrofoils of Finite Span," Journal of Mathematics and Physics, Volume XXXIII (1954).

6. Wadlin, Kenneth L., and Christopher, Kenneth W., "A Method for Calculation of Hydrodynamic Lift for Submerged and Planing Rectangular Lifting Surfaces," NASA TR R-14 (1959).

7. Imlay, F.H., "Theoretical Motions of Hydrofoil Systems," NACA Report 918 (1948).

8. Gertler, M., "The Prediction of the Effective Horsepower of Ships By Methods In Use at the David Taylor Model Basin," David Taylor Model Basin Report 576, December 1947.

9. Martin, M., "The Stability Derivatives of a Hydrofoil Boat-Part I," Hydronautics, Incorporated Technical Report 001-10(I), January 1963.

INITIAL DISTRIBUTION

Copies

10 CHBUSHIPS,
3 Tech Library (Code 210L)
1 Hydromechanics, Logistics & Special Craft (Code 341B)
1 Ship Silencing Branch (Code 345)
2 Preliminary Design Branch (Code 420)
1 Hull Design Branch (Code 442)
1 Hull Design Branch (Code 449)
1 Hull & Seamanship Branch (Code 632)

2 Chief, Office of Naval Research
Navy Department
Washington 25, D.C.
Code (438)

2 Chief, Bureau of Naval Weapons
Navy Department
Washington 25, D.C.
Attn: Code RAAD-334 (1)
Code RRSY-1

1 Mr. John B. Parkinson
Langley Aeronautical Laboratory
National Aeronautics & Space Administration
Langley Field, Virginia

1 Chief of Naval Operations
Navy Department
Washington 25, D.C.
Attn: LCDR W. Norris (Op-725)

1 State University of Iowa
Iowa Institute of Hydraulic Research
Iowa City, Iowa

1 Southwest Research Institute
8500 Culebra Road
San Antonio 6, Texas
Attn: N.N. Abramson, Director of Mechanical Science

1 Oceanics, Inc.
114 East 40 Street
New York 16, New York
Attn: Dr. Paul Kaplan

1 Stanford University
Stanford, California
Attn: Dr. B. Perry

1 Boeing Airplane Company
Aero-Space Division
Box 3707
Seattle, Washington

1 California Institute of Technology
Pasadena, California
Attn: Hydrodynamics Laboratory

1 Director, Stevens Institute of Technology
Davidson Laboratory
Castle Point Station
Hoboken, New Jersey

1 Hydronautics, Incorporated
Pindell School Road
Howard County
Laurel, Maryland

1 Massachusetts Institute of Technology
Department of Naval Architecture & Marine Engineering
Cambridge 38, Massachusetts

1 Director, University of Minnesota
St. Anthony Falls Hydraulic Laboratory
Hennepin Island,
Minneapolis 14, Minnesota

1 Technical Research Group, Inc.
2 Aerial Way
Syosset, New York

1 Aerojet General Corporation
Azusa, California
Attn: Mr. J. Lovy

1 U.S. Navy Ordnance Test Station
Oceanic Research Group
3202 E. Foothill Blvd.
Pasadena, California

1 Lockheed Aircraft Corporation
Hydrodynamic Group
Sunnyvale, California
Attn: Mr. R. W. Kermeen

1 Grumman Aircraft Engineering Corporation
Marine Engineering Section
Bethpage, Long Island, New York

1 University of California
Institute of Engineering Research
Berkeley, California
Attn: Professor R. Paulling

1 General Dynamics/Convair
P. O. Box 1950
San Diego 12, California
Attn: Mr. R. Oversmith

David Taylor Model Basin. Report 1801.
EXPERIMENTAL INVESTIGATION OF NEAR-SURFACE HYDRODYNAMIC FORCE COEFFICIENTS FOR A SYSTEMATIC SERIES OF TEE HYDROFOILS, DTMB SERIES HF-1, by Jerome Feldman. Dec 1963. xii, 88p. diagrs., graphs, tables, refs.
UNCLASSIFIED

Experiments were conducted with the DTMB Planar-Motion-Mechanism System to determine the normal and longitudinal components of force for DTMB Series HF-1, a systematic series of Tee foils designed to operate in the subcavitating regime. The resulting data are represented in a form applicable to the hydrodynamic design of high-speed hydrofoil craft from the standpoint of stability and control. The data are further analyzed to establish the effects of parameters such as Froude Number, depth of submergence, and aspect ratio. Comparisons are made to determine the extent to which existing theories produce agreement with the experimental data.

1. Hydrofoils--Force components--Model tests
2. Hydrofoil boats--Stability
3. Hydrofoil boats--Control
4. Hydrofoil boats--Design
5. HF-1 (DTMB hydrofoil series)
I. Feldman, Jerome
II. S-F013 02 01, Task 1703.

David Taylor Model Basin. Report 1801.
EXPERIMENTAL INVESTIGATION OF NEAR-SURFACE HYDRODYNAMIC FORCE COEFFICIENTS FOR A SYSTEMATIC SERIES OF TEE HYDROFOILS, DTMB SERIES HF-1, by Jerome Feldman. Dec 1963. xii, 88p. diagrs., graphs, tables, refs.
UNCLASSIFIED

Experiments were conducted with the DTMB Planar-Motion-Mechanism System to determine the normal and longitudinal components of force for DTMB Series HF-1, a systematic series of Tee foils designed to operate in the subcavitating regime. The resulting data are represented in a form applicable to the hydrodynamic design of high-speed hydrofoil craft from the standpoint of stability and control. The data are further analyzed to establish the effects of parameters such as Froude Number, depth of submergence, and aspect ratio. Comparisons are made to determine the extent to which existing theories produce agreement with the experimental data.

1. Hydrofoils--Force components--Model tests
2. Hydrofoil boats--Stability
3. Hydrofoil boats--Control
4. Hydrofoil boats--Design
5. HF-1 (DTMB hydrofoil series)
I. Feldman, Jerome
II. S-F013 02 01, Task 1702.

David Taylor Model Basin. Report 1801.
EXPERIMENTAL INVESTIGATION OF NEAR-SURFACE HYDRODYNAMIC FORCE COEFFICIENTS FOR A SYSTEMATIC SERIES OF TEE HYDROFOILS, DTMB SERIES HF-1, by Jerome Feldman. Dec 1963. xii, 88p. diagrs., graphs, tables, refs.
UNCLASSIFIED

Experiments were conducted with the DTMB Planar-Motion-Mechanism System to determine the normal and longitudinal components of force for DTMB Series HF-1, a systematic series of Tee foils designed to operate in the subcavitating regime. The resulting data are represented in a form applicable to the hydrodynamic design of high-speed hydrofoil craft from the standpoint of stability and control. The data are further analyzed to establish the effects of parameters such as Froude Number, depth of submergence, and aspect ratio. Comparisons are made to determine the extent to which existing theories produce agreement with the experimental data.

1. Hydrofoils--Force components--Model tests
2. Hydrofoil boats--Stability
3. Hydrofoil boats--Control
4. Hydrofoil boats--Design
5. HF-1 (DTMB hydrofoil series)
I. Feldman, Jerome
II. S-F013 02 01, Task 1703.

David Taylor Model Basin. Report 1801.
EXPERIMENTAL INVESTIGATION OF NEAR-SURFACE HYDRODYNAMIC FORCE COEFFICIENTS FOR A SYSTEMATIC SERIES OF TEE HYDROFOILS, DTMB SERIES HF-1, by Jerome Feldman. Dec 1963. xii, 88p. diagrs., graphs, tables, refs.
UNCLASSIFIED

Experiments were conducted with the DTMB Planar-Motion-Mechanism System to determine the normal and longitudinal components of force for DTMB Series HF-1, a systematic series of Tee foils designed to operate in the subcavitating regime. The resulting data are represented in a form applicable to the hydrodynamic design of high-speed hydrofoil craft from the standpoint of stability and control. The data are further analyzed to establish the effects of parameters such as Froude Number, depth of submergence, and aspect ratio. Comparisons are made to determine the extent to which existing theories produce agreement with the experimental data.

1. Hydrofoils--Force components--Model tests
2. Hydrofoil boats--Stability
3. Hydrofoil boats--Control
4. Hydrofoil boats--Design
5. HF-1 (DTMB hydrofoil series)
I. Feldman, Jerome
II. S-F013 02 01, Task 1702.